EXAMINATION OF *Klebsiella pneumoniae* 5'-METHYLTHIOADENOSINE/ S-ADENOSYLHOMOCYSTEINE NUCLEOSIDASE AND 5-METHYLTHIORIBOSE KINASE

by

Jason Alan Stonick

A thesis

submitted in partial fulfillment

of the requirements for the degree of

Master of Science in Chemistry

Boise State University

May 2016

BOISE STATE UNIVERSITY GRADUATE COLLEGE

DEFENSE COMMITTEE AND FINAL READING APPROVALS

of the thesis submitted by

Jason Alan Stonick

Thesis Title: Examination of *Klebsiella pneumoniae* 5'-Methylthioadenosine/S-adenosylhomocysteine Nucleosidase and 5-Methylthioribose Kinase

Date of Final Oral Examination: 10 March 2016

The following individuals read and discussed the thesis submitted by student Jason Alan Stonick, and they evaluated his presentation and response to questions during the final oral examination. They found that the student passed the final oral examination.

Kenneth A. Cornell, Ph.D.	Chair, Supervisory Committee
Juliette Tinker, Ph.D.	Member, Supervisory Committee
Henry Charlier, Ph.D.	Member, Supervisory Committee

The final reading approval of the thesis was granted by Kenneth A. Cornell, Ph.D., Chair of the Supervisory Committee. The thesis was approved for the Graduate College by John R. Pelton, Ph.D., Dean of the Graduate College.

DEDICATION

This thesis is dedicated to my parents for supporting my education and taking the statement “I’m moving to Boise next week” in due stride.

ACKNOWLEDGEMENTS

I would like to first acknowledge Dr. Ken Cornell as my mentor and primary resource during my research. I would also like to thank Dr. Juliette Tinker and Dr. Henry Charlier for serving as my committee members. Additional thanks go to Dr. Steven Clegg and Dr. Virginia Miller for kindly providing the *K. pneumoniae* strains I utilized in my assays. I would also like to give my thanks to the Biomolecular Research Center and its staff for funding me as a student and also being my laboratory home-away-from-home when I needed a quiet place to get my work done. Dr. Danny Xu and Patrick Erstad both contributed significantly to my research by performing molecular modeling of the MTRK enzyme and small molecule screening for novel MTN inhibitors. Finally, I would like to express my appreciation for the hard work of my fellow lab members, especially Kat Dunlevy and Ally Isnor, for contributing their time and effort to the work included in this thesis, and Necia Hunter for her laudable efforts to keep the lab space clean and functional.

The project described was supported by the Idaho Beef Council and the Institutional Development Awards (IDeA) from the National Institute of General Medical Sciences of the National Institutes of Health under Grants #P20GM103408 and #P20GM109095. We also acknowledge support from The Biomolecular Research Center at Boise State with funding from the National Science Foundation, Grants #0619793 and #0923535; the MJ Murdock Charitable Trust; and the Idaho State Board of Education.

ABSTRACT

Klebsiella pneumoniae is an opportunistic bacterial pathogen that is emerging as a major global threat as an infectious agent. This organism, along with many other pathogens, possesses a broad suite of antibiotic resistances that can make treatment exceedingly difficult. As such, the impetus for creating novel antibiotics is at an all-time high despite the fact that pharmaceutical investment into drug development is at an all-time low. S-adenosylmethionine (SAM) is a universally utilized metabolite involved in a wide array of biosynthetic processes, and whose products are catabolized by a different set of enzymes in mammals than used by many bacteria, protozoa, and plants. This divergence provides two specific targets for enzymatic inhibition in *K. pneumoniae*: 5'-Methylthioadenosine/S-adenosylhomocysteine Nucleosidase (MTN) and 5-Methylthioribose Kinase (MTRK). In order to examine the potential effects of drugs targeting these enzymes, recombinant proteins from *K. pneumoniae* were isolated and purified, and a profile of their respective kinetic activities were determined. The MTRK enzyme was identified as using an ordered sequential mechanism, and shows preferential binding towards substrate analogs with hydrophobic 5-alkylthio substitutions. In addition, binding affinities of transition state-analogs and novel non-nucleoside small molecule inhibitors of MTN were quantified. Finally, the effects of MTN inhibitors on *K. pneumoniae* whole-cell growth, and gene expression were assessed. A number of the inhibitors demonstrated strong affinities for the MTN enzyme and induced alterations in

cellular growth, autoinducer response, and the expression of genes associated with virulence.

TABLE OF CONTENTS

LIST OF TABLES

LIST OF FIGURES

LIST OF ABBREVIATIONS

5'dADO	5'-Deoxyadenosine
5-dRIB	5-Deoxy-D-ribose
5FMTR	5-Fluoro-methylthioribose
AI	Autoinducer
ACP	Acyl carrier protein
AdoMet	S-adenosylmethionine
ADP	Adenosine diphosphate
ATCC	American Type Culture Collection
ATP	Adenosine triphosphate
BSA	Bovine serum albumin
bp	Base pair
c-di-GMP	3,5-Cyclic diguanylic acid
CoA	Coenzyme A
CPS	Capsular polysaccharide
CRE	Carbapenem-resistant Enterobactericeae
dAdoMet	Decarboxy-S-adenosylmethionine
dcSAM	Decarboxy-S-adenosylmethionine
DHK-MTPene	1,2-dihydroxy-3-keto-5-methylthiopentene
DK-MTP-1-P	2,3-diketo-5-methylthiopentyl-l-phosphate
DMSO	Dimethylsulfoxide

DNA	Deoxyribonucleic acid
DPD	4,5-dihydroxy-2,3-pentanedione
DTT	Dithiothreitol
ELISA	Enzyme-linked immunosorbent assay
Esp	*Escherichia* secretion protein
eDNA	Extracellular deoxyribonucleic acid
ESBL	Extended-spectrum β-lactamases
ETR	5-Ethylthioribose
HIV	Human immunodeficiency virus
HRP	Horseradish peroxidase
IPTG	Isopropyl β-D-1-thiogalactopyranoside
kD	Kilo dalton
KI	Knock-in
KMTB	2-Keto-4-methylthiobutyrate
KO	Knock-out
KPC	*Klebsiella pneumoniae* carbapenemase
LB	Luria Bertani
LDH	Lactate dehydrogenase
Leu	Leucine
LPS	Lipopolysaccharide
mRNA	Messenger ribonucleic acid
MTA	5'-Methylthioadenosine
MTAP	5'-Methylthioadenosine phosphorylase

MTN	5’-Methylthioadenosine/S-adenosylhomocysteine nucleosidase
MTR	5-Methylthioribose
MTRK	5-Methylthioribose kinase
MTR-1P	5-Methylthioribose-1-phosphate
MTRu-1P	5-Methylthioribulose-1-phosphate
NAD	Nicotinamide adenine dinucleotide
NADH	Nicotinamide adenine dinucleotide hydride
OD	Optical density
PBS	Phosphate buffered saline
PBST	Phosphate buffered saline tween
PCR	Polymerase chain reaction
PEP	Phosphoenolpyruvate
PGA	Polyglucosamine
PK	Pyruvate kinase
pro-AI-2	1-deoxy-3-dehydro-D-ribulose
PVDF	Polyvinylidene fluoride
RNA	Ribonucleic acid
rRNA	Ribosomal ribonucleic acid
SAH	S-Adenosylhomocysteine
SAHH	S-adenosylhomocysteine hydrolase
SAM	S-Adenosylmethionine
SDS-PAGE	Sodium dodecyl sulfate polyacrylamide gel electrophoresis
SRH	S-ribosylhomocysteine

Stx	Shiga toxin
TFMTR	5-trifluoro-methylthioribose
Tir	Translocated intimin receptor
tRNA	Transfer ribonucleic acid
Trp	Tryptophan
TSA	Transition state analog
UV	Ultraviolet
WHO	World Health Organization
WT	Wildtype

CHAPTER ONE: INTRODUCTION

Infectious Diseases

Microbial infections have been responsible for some of the most devastating events in human history. The bubonic plague, smallpox, cholera, tuberculosis and innumerable other infectious agents will forever be remembered because of the immense impact they have had on human lives. It is no wonder, then, that the advent of antibiotic drugs in the mid-20th century stands among the greatest of human achievements. However, the efficacy of drug treatments have universally waned from the moment of their introduction. Resistance mechanisms towards new antibiotics have inevitably sprung forth after their use in the market, often in the span of just a few short years (Figure 1.1).

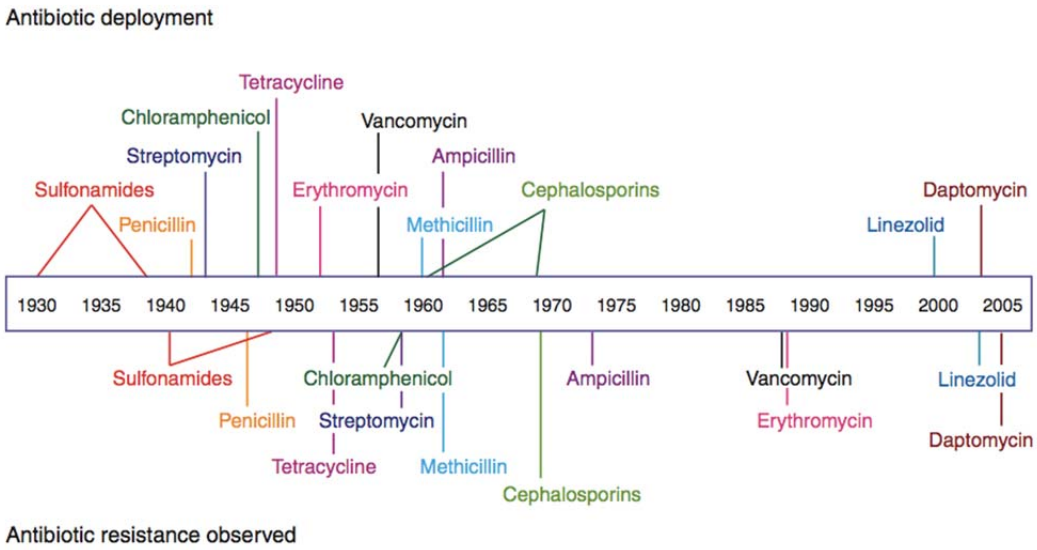

Figure 1.1. Timeline of antibiotic use and appearance of drug resistance. Adapted from Clatworthy, et al., 2007.

The short efficacious lifespan of new antimicrobials has disincentivized pharmaceutical companies from investing resources in further antibiotic research and development. This has led to a critical decline in the number of new treatments available, while the prevalence of antibiotic-resistant organisms steadily rises (Spellberg, et al., 2004). Current trends suggest we are moving towards the emergence of a so-called "post-antibiotic" era, in which we will once again lack the means to medically treat infections (WHO, 2015). The implications of this are drastic considering approximately 720,000 nosocomial infections and 75,000 resultant deaths occur every year in the United States alone (Magill, et al., 2014). Globally, 90 million people contracted malaria and 2.6 million contracted pneumonia in 2014 (WHO, 2014). In fact, mortality from infectious and parasitic diseases accounts for 19.1% of global deaths, even in our current pre-"post-antibiotic" world (WHO, 2004).

As such, a new class of antimicrobial drugs would be more valuable now than at any time since prior to the discovery of penicillin. However, in view of the rate of evolutionary acquisition of resistance, it is critical that efforts be made to limit the ability for pathogens to quickly develop a means of subverting a drug's mode of action. Modern thinking asserts that molecules that interfere with microbial pathogenicity rather than survival will reduce the selective pressure that leads to antibiotic resistance, and allow natural immunity to fight off an infection. Therefore, drugs that are designed with these precepts should be capable of preventing or delaying the emergence of drug resistance.

Klebsiella pneumoniae

Classification and Threat

Klebsiella pneumoniae is a Gram-negative rod shaped bacteria in the Enterobactericeae family. While part of the normal flora of the human body, various strains possess high pathogenic capacity, especially while acting as a nosocomial agent and towards people with pre-existing conditions resulting in compromised immune systems (e.g. diabetes, alcoholism, HIV, etc.). Its modes of pathogenicity allow it to clinically manifest as urinary tract infections, pneumonia, septicemia and soft tissue infections. *Klebsiella pneumoniae* accounts for 3-7% of hospital-associated bacterial infections (Podschun, et al., 1998), placing it among the eight most prevalent infectious pathogens. However, the greatest concern towards *K. pneumoniae* is due to the drug resistance profile of many clinical isolates. Pathogenic strains often carry plasmid-born resistances, and *K. pneumoniae* was among the first organisms found to possess genes for aminoglycoside resistance and extended-spectrum β-lactamase (ESBL) activity, which confers resistance to cephalosporins and aztreonam (Arnold, et al., 2011).

In the early 1990's, a novel β-lactamase was found in *Klebsiella*, termed "*Klebsiella pneumoniae* carbapenemase" (KPC). KPC confers resistance to virtually all β-lactam drugs, including penicillins, cephalosporins, monobactams, and carbapenems (Arnold, et al., 2011). This was a critical development as carbapenems are a class of drug with regulated medical use as a "last resort" treatment for Gram-negative bacterial infections in order to preserve their efficacy and longevity. The KPC gene proved to be highly mobile and spread rapidly among other Gram-negative species, creating a class of

organisms known as "carbapenem-resistant Enterobactericeae" (CRE). The KPC gene is now the most commonly found carbapenemase gene worldwide (Nordmann, et al., 2009).

In 2009, a new carbapenemase gene with a novel mode of action was isolated from *K. pneumoniae* (Yong, et al., 2009). Named the "New Delhi metallo-β-lactamase", this gene is also rapidly spreading across the globe and among other Gram-negative bacteria such as *E. coli, Enterobacter cloacae, and Salmonella enterica*. A survey of New Delhi carbapenemase-bearing clinical isolates in the U.S. showed that all of them also possessed resistance to additional antibiotics including aminoglycosides and fluoroquinolones, and also possessed one or more alternate β–lactamases (Rasheed, et al., 2013). Due to difficulty of treatment, CRE organisms are significantly more virulent, with mortality rates for septic patients at 71.9% vs. 21.9% for non-CRE infections (Borer, et al., 2009). The rate of occurrence is also increasing, with the proportion of CRE infections accelerating from 0.6% to 5.6% during 2004-2008 (Gupta, et al., 2011). *K. pneumoniae* currently poses a major threat to the medical community and is poised to become an even greater danger in the near future.

Pathogenic strains of *K. pneumoniae* possesses a suite of traits that help to enable their capacity for infection and morbidity, which include: mucoviscosity, cellular adhesion, biofilms, and siderophores.

Mucoviscosity

High mucoviscosity, often referred to as hypermucoviscosity, is a common characteristic of many infectious strains of *K. pneumoniae*. Manifesting as an extraordinarily thick accumulation of extracellular capsular polysaccharide (CPS) surrounding the cells. Positive strains can be readily identified by a "stringiness" of the

colonies (Figure 1.2). The capsule serves as a physical buffer that helps exaggerate bacterial defense mechanisms.

Figure 1.2. Hypermucoviscous *Klebsiella pneumoniae*. This positive stretch test of a hypermucoviscous strain shows the characteristic stretch of a mucoid colony. (Shon, et al., 2013).

The hypermucoviscosity trait strengthens defense against host immune responses and contributes significantly to host mortality during infection. *K. pneumoniae* strains of the K1 and K2 serotypes most highly associated with hypermucoviscosity express an estimated 15-17 genes implicated in upregulation of CPS synthesis (Wu, et al., 2009; Arakawa, et al., 1995). Of these, the *magA* gene (K1 strains), confers complete resistance to bactericidal human serum and a greater than 10^5-fold decrease to the lethal dose in mice (Fang, et al., 2004). High capsule production in both serotypes are reported to confer resistance to opsonin-dependent phagocytosis by human neutrophils (Domenico, et al., 1994). Non-capsule forming *K. pneumoniae* mutants showed drastically reduced virulence in mouse pulmonary infections (Chhibber, et al., 2003). These findings

highlight the importance of capsule production as a virulence factor in *K. pneumoniae* infections.

Cellular Adhesion

Many pathogenic strains of *K. pneumoniae* possess the ability to bind to the surface biomolecules of mammalian cells. This is achieved largely through the action of extracellular structures referred to as pili or fimbriae. These long, thin columnar structures protrude from the cell membrane through the capsular layer and facilitate binding to extracellular matrix proteins and cell surface markers (Proft, et al., 2009). Pathogenic *K. pneumoniae* genomes encode two distinct adhesive fimbriae, designated as type 1 and type 3. Type 1 fimbriae are characterized by their capacity to agglutinate guinea pig erythrocytes (Figure 1.3). They are also responsible for adhesion to human bladder and tracheal cells (Fader, et al., 1979; Fader, et al., 1988). In contrast, type 3

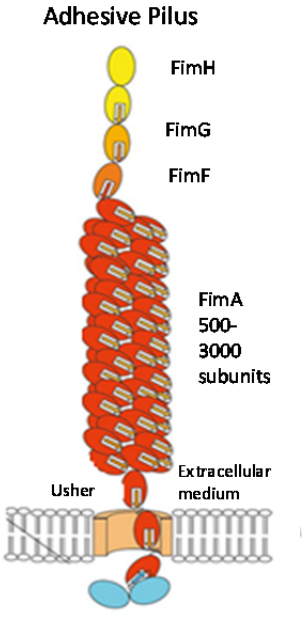

Figure 1.3. Structure of a type 1 fimbriae. The main body is comprised of a helix of repeating subunits and is capped by a single adhesive subunit. Fimbriae can range in length from 1 to 2 μm. (Adapted from Bodelon, et al., 2013.)

fimbriae are characterized by their ability to only agglutinate tannin-treated erythrocytes, and enable adhesion to respiratory tissues (Hornick, et al., 1992). These fimbriae also confer bacterial adherence towards plastic surfaces (Jagnow, et al., 2003) and the ubiquitously expressed extracellular matrix proteins (collagen, fibrinogen, and fibronectin) found in epithelial tissues (Hennequin, et al., 2007).

Multiple plasmid-borne adhesive factors also exist in *K. pneumoniae*. The adhesive factor CF29K was acquired from other enteropathogens, and mediates binding to gastrointestinal tissues (Martino, et al., 1995). Interestingly, high capsule production antagonizes tissue adherence. This is proposed to occur by blocking adhesive factor accessibility due to excess capsule (Schembri, et al., 2005). Tissue specific downregulation of capsule production may act as an early adaptive response that facilitates bacterial adherence at the site of infection (Vartivarian, et al., 1993). Subsequent upregulation of capsule production may later improve virulence by protecting the pathogen from host immune responses.

Biofilms

Recent studies indicate that the many decades of research examining *in vitro* bacterial cultures may have focused on a mostly irrelevant planktonic growth phase. Under natural growth conditions, bacteria more often form complex microbial communities called biofilms. These colonies are formed from extracellular secretions of carbohydrates, proteins and DNA that form a dense connective network that enmeshes the cells together (Figure 1.4). Bacterial behavior within these structures is highly modified, displaying functions that are not observed in free planktonic growth. Cells

growing within biofilms are known to undergo an alteration in their expression of surface markers, nutrient metabolism, and in their virulence profiles (Schembri, et al., 2003).

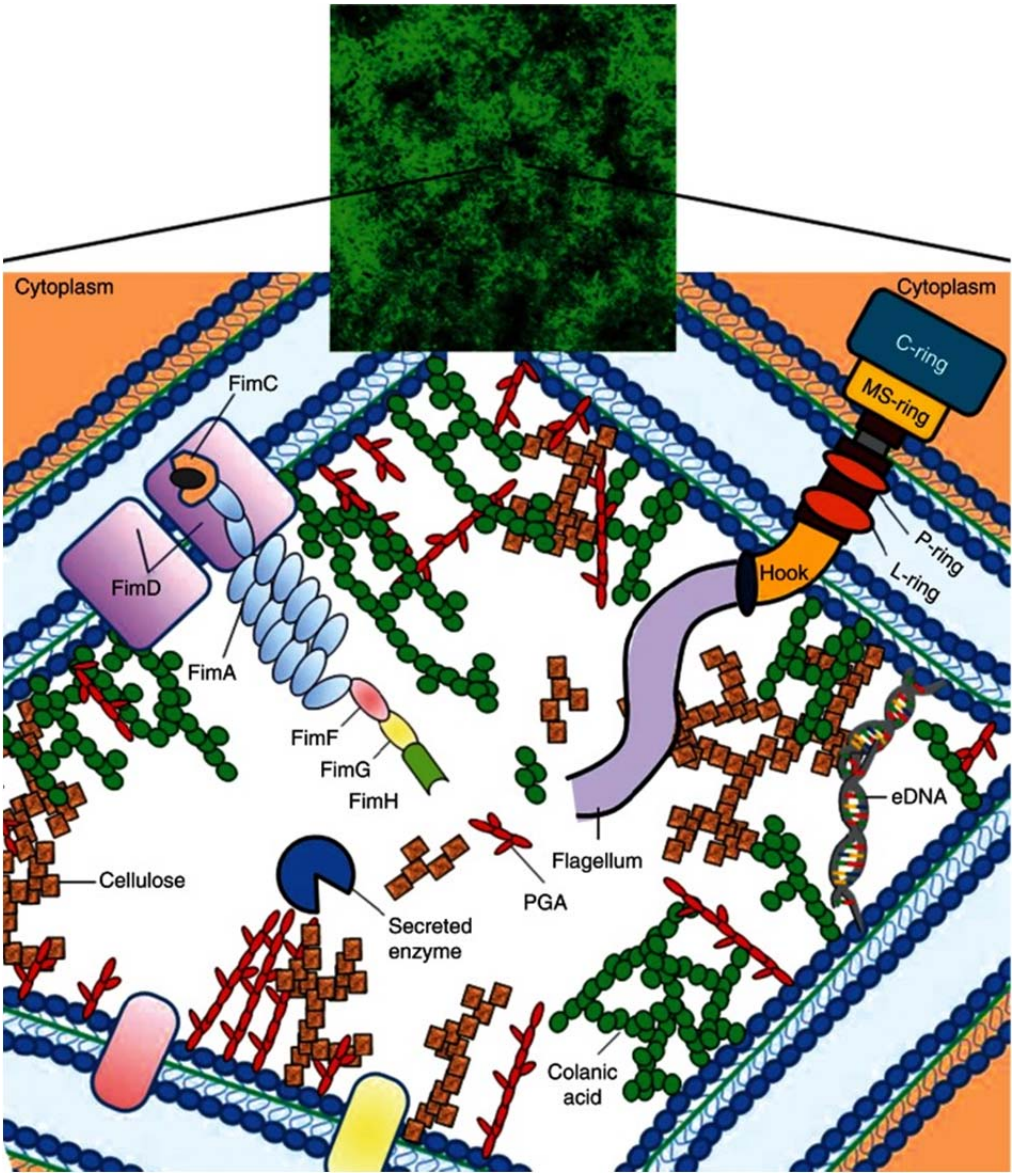

Figure 1.4. Extracellular components of biofilms. Biofilm deposition is facilitated by bacterial adhesins and flagella. The polymeric matrix is composed mostly of structural polymers like colonic acid, cellulose, polyglucosamine (PGA), and extracellular DNA (eDNA) (Kostakioti, et al., 2013).

Biofilm formation is initiated by cellular adhesion to either living tissue or abiotic surfaces, especially in response to adhesion by type 1 fimbriae (Pratt et al., 1998). Plastics are particularly prone to biofilm formation, contributing heavily to the incidence

of catheter-related urinary tract infections (Trautner & Darouiche, 2004). Following initial bacterial adhesion, various extracellular biofilm constituents are secreted. The composition of these secreted molecules are dictated heavily by environmental factors (Harmsen, et al., 2010). Biofilm formation is found to be highly dependent on expression of the type-3 fimbriae subunit MrkA in *K. pneumoniae* (Schroll, et al., 2010). Biofilms permit the accumulation of Autoinducer (AI) signaling molecules and the second messenger, 3,5-cyclic diguanylic acid (c-di-GMP), which induce alterations in gene expression to promote biofilm maturation and expansion (Kostakioti, et al., 2013).

Compared to free-living organisms, microbes within biofilms possess traits that enable environmental survival and are therefore more likely to cause clinical disease. The inherent hydrophilicity of polysaccharides produces a "slime" that helps prevent cell desiccation, and the physical nature of biofilms results in resistance to removal from surfaces by shear forces. Cells cloistered within biofilms are also physically protected from human immune responses (Jesaitis, et al., 2003). Poor diffusional properties within these biomaterials, combined with metabolic changes that are not fully characterized result in an upwards of 500-fold increase in antibiotic resistances (Costerton, et al., 1995).

Even more pernicious is the existence of internal "persister" cells. These deeply embedded cells experience an environment of nutrient and oxygen deprivation that induces a state of metabolic stasis. The cessation of nearly all molecular activity grants inherent insensitivity towards many antibiotics. However, persister cell activity can be resumed following the death of nearby non-persister cells in response to antibiotic treatment (Lewis, 2005). As a result, biofilm-associated infections often require surgical

removal of affected tissues to prevent chronic recurrence. The co-localization and concentration of cell populations in biofilms have also been found to expedite lateral gene transfer, facilitating the spread of plasmid-borne drug resistances and virulence factors (Flemming, & Wingender, 2010).

Siderophores

Siderophores comprise a class of secreted small molecules that act as metal ion chelators and are used primarily to scavenge iron from the environment and import it into the cell. Iron is a vital component of enzymes involved in many cellular processes, including respiration and DNA synthesis. The vast majority of iron in humans is sequestered within hemoglobin, ferritin, and transferrin, leaving a free Fe^{3+} ion concentration of approximately 10^{-24} M (Vasil, & Ochsner, 1999). However, optimal growth conditions for microorganisms require roughly 1 μM of iron, requiring a means of extracting host iron to enable efficient proliferation by pathogens (Miethke, et al., 2008). There are dozens of physically distinct siderophores produced by Gram-negative bacteria, with no discernable conservation of type utilized, even by closely related species. A survey of 475 *K. pneumoniae* strains showed 98.8% produced siderophores (Podschun, et al., 1992) with aerobactin being the most relevant form utilized during infection (Russo, et al., 2015). Previous research has shown that genetic knock-outs of siderophore genes in *K. pneumoniae* produce avirulent strains (Hsieh, et al., 2008), thus identifying siderophores as a requisite component of pathogenicity. The *rmpA* gene, one of the most widely shared enhancers of CPS among *K. pneumoniae* strains, has been reported to be downregulated at high iron concentrations (Cheng, et al., 2010). Potentially, siderophore-

mediated loss of capsule synthesis may improve the ability of the organism to establish new sites of colonization during a septic infection.

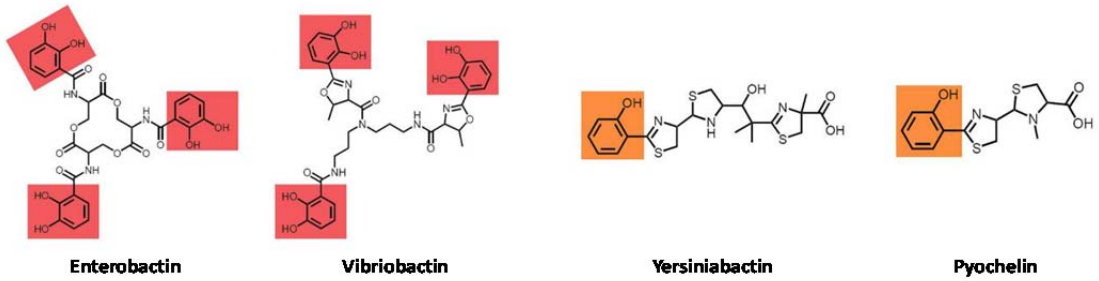

Figure 1.5. Structural diversity of bacterial siderophores. Iron chelating groups are highlighted and color coded by common structure. (Adapted from Miethke & Marahiel, 2007.)

5'-Methylthioadenosine/S-adenosylhomocysteine Nucleosidase

Function and Prevalence

S-adenosylmethionine (SAM or AdoMet) is one of the most widely used molecules in biochemical pathways and is the second most utilized enzymatic substrate after ATP (Fontecave, et al., 2004). Four of the most critical SAM functions are

Figure 1.6. Depiction of substrate-bound *E. coli* MTN. Ribbon diagram of the MTN enzyme co-crystallized as a native homodimer with two bound non-hydrolyzable MTA analog molecules in the active sites (Lee, at al., 2001; PDB: 1NC1).

transmethylation reactions, bacterial autoinducer production, polyamine synthesis, and radical SAM reactions. The enzyme 5'-methylthioadenosine/S-adenosylhomocysteine nucleosidase (known as MTN, mtnN, or MTAN) is responsible for the irreversible depurination of several metabolic products of SAM-dependent reactions by addition of a water molecule. MTN is a functional homodimer with each unit mutually forming part of two symmetric binding sites (Figure 1.6). Bacterial MTN catalyzes the breakdown of three known substrates: 5'-methylthioadenosine (MTA), S-adenosylhomocysteine (SAH), and 5'-deoxyadenosine (5'dADO). The products of MTN reactions are recycled via purine and methionine salvage pathways (Figure 1.7). In mammals, the analogous enzyme activities are performed by two different enzymes: 5'-methylthioadenosine phosphorylase (MTAP) and S-adenosylhomocysteine hydrolase (SAHH). MTAP is a homotrimer with similar but not identical binding site properties to MTN, and catalyzes the reversible phosphorylytic depurination of MTA. SAHH is evolutionarily distinct and does not deadenylate the substrate SAH. Instead it resembles an enzymatic class of NAD-dependent hydrogenases and cleaves the 5' carbon-sulfur bond of SAH to yield adenosine and homocysteine using an NADH cofactor (Turner, et al., 2000).

The buildup of MTA and SAH are both toxic to cells (Christa, et al., 1988) and strong product inhibitors of the pathways that form them (Parveen & Cornell, 2011). As a result of the expansive number of enzymes involved in radical SAM reactions there is still an incomplete profile of the consequences of 5'dADO buildup. However, it also has been characterized as a product inhibitor for some of its dependent enzymes, such as biotin and lipoyl synthases (Choi-Rhee & Cronan, 2005).

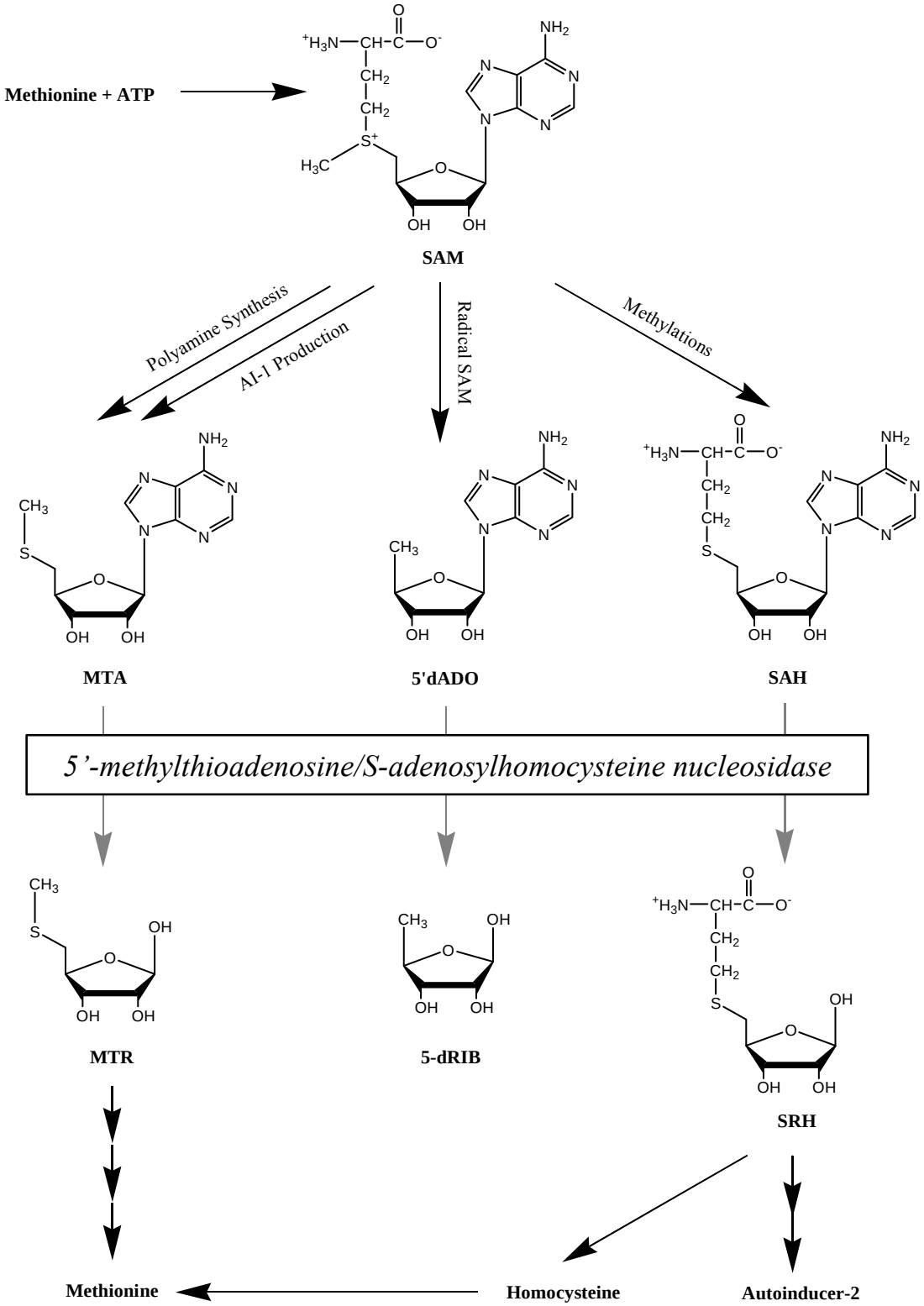

Figure 1.7. Central role of MTN on SAM-dependent metabolic pathways. Bacterial MTN facilitates the deadenylation of three distinct products of S-adenosylmethionine (SAM) dependent reactions.

The accumulation of these three nucleosides as a result of MTN inhibition is therefore expected to act as a powerful means of debilitating a multitude of biochemical pathways. Despite the central role of MTN in these diverse metabolic functions, it is not strictly required for cellular survival. MTN gene knock-out strains (MTN KOs) of *Staphylococcus aureus* and *Neisseria meningitides* grew normally in nutrient replete media, but showed reduced virulence (Bao, et al., 2013; Heurlier, et al., 2009). MTN KO strains of *E. coli* (RK4353, O157:H7) showed reduced growth rates, altered metabolism, and decreased toxin production (Knippel, 2013). This supports a role for MTN in the promotion of organismal growth and the expression of virulence factors instead of cell survival. As a result, targeting MTN with chemotherapeutics should enable the host immune system to more effectively cope with infection, placing the drugs themselves under less selective pressure for the development of antibiotic resistance (Clatworthy, et al., 2007). The MTN enzyme is relatively well conserved among bacteria, being found in 51 of 138 bacterial species examined (Parveen & Cornell, 2011) and is also utilized by various parasites, such as *Entamoeba histolytica* (Larson, et al., 2010) and *Giardia lamblia* (Riscoe, et al., 1988). MTN is also found in most plant species, where it plays a role in synthesis of the hormone ethylene (Kushad, et al., 1985). The broad organismal utilization of MTN could allow a potent MTN inhibitor to act as a broad-spectrum antimicrobial against a diverse array of organisms.

Previous efforts at designing inhibitors for MTN have largely consisted of attempts to create molecules that act as either early or late-stage transition state analogs (TSAs). The underlying principle is that enzymes function by stabilizing an energetically unfavorable intermediate transition between the reactants and products. Thus, the affinity

of the enzyme towards molecules resembling that intermediate state are theorized to exceed that of the natural substrates by a factor equal to the rate of catalytic acceleration (Wolfenden, et al., 2001). The mechanism of MTN during catalysis is initiated by the protonation of N7 of the adenyl group, followed by a donation of electron density from the ribose ring oxygen and S_N1-type dissociation of the purine from the ribose. Afterwards, a localized water molecule attaches to the resultant highly reactive ribooxacarbenium ion (Figure 1.8). Efforts have thus centered around modifying electron density and bond length properties on the 1' carbon, examining the influence of 5' alkylthio substitutions, and utilizing a non-hydrolyzable glycosidic bond to prevent the drugs from enzymatic degradation.

Efforts to create TSA inhibitors of bacterial MTN have been remarkably successful. Dissociation constants for some late-stage TSA inhibitors have been as low as 47 femtomolar against *E. coli* MTN, which represents a 91 million-fold greater binding affinity than for the substrate SAH (Singh, et al., 2005). These inhibitors represent some of the tightest binding non-covalent inhibitors for any known enzyme. Unfortunately, their observed effects on cellular behavior have typically been less dramatic. *V. cholerae* growth in media supplemented with a TSA inhibitor at a million-fold concentration greater than the K_i failed to affect growth (Schramm, et al., 2008).

However, TSA drugs applied even at picomolar concentrations were found to disrupt autoinducer-2 and biofilm formation in both *V. cholerae* and *E. coli* (Gutierrez, et al., 2009). More recently, ten different MTN inhibitors were discovered to significantly reduce growth in *Helicobacter pylori* and are being examined as species-specific

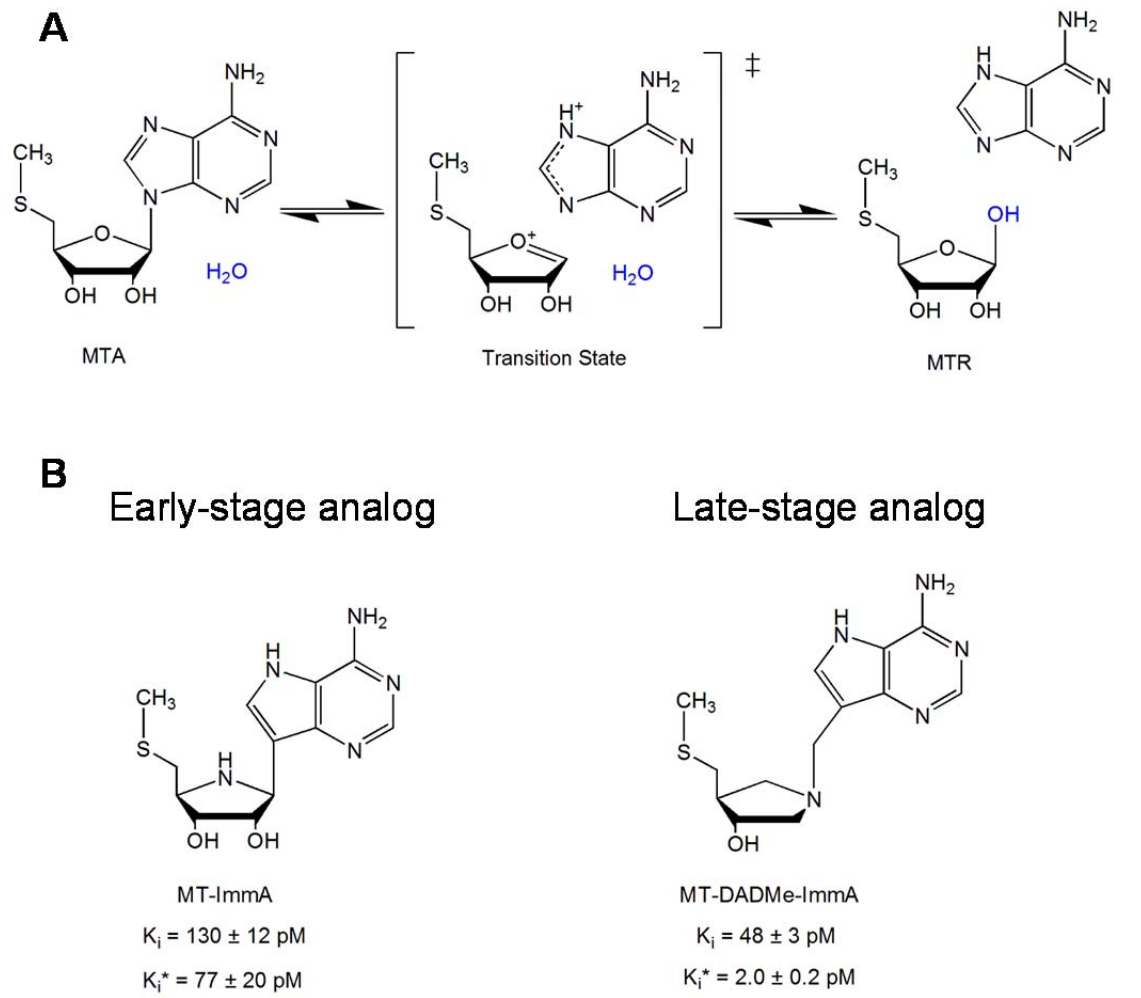

Figure 1.8. Rationale for MTN transition-state analog design. A) Representation of MTN catalysis of 5'-methylthioadenosine to 5-methylthioribose and adenine. **B)** Examples of both early and late-stage transition state inhibitors. Both possess non-hydrolyzable bonds on the equivalent of the 1' carbon, with bond elongation in the late-stage analog. Early onset (unmarked) inhibition values were derived from initial enzyme velocities. Delayed-onset (*) inhibition values are derived from the kinetic rates following thermodynamic equilibrium of the drug-enzyme complex (data from Singh, et al., 2005).

antibiotics (Wang, et al., 2015). To date, no data regarding MTN inhibitor effects on *K. pneumoniae* growth have been published.

In order to be useful as chemotherapeutic agents, MTN inhibitors should demonstrate little to no effect on human cells. MTAP is the mammalian enzyme with greatest homology to MTN, and thus with the greatest concern for unintended inhibition.

While MTAP also acts on the substrate MTA, it uses a different nucleophile (phosphate) to effect a reversible cleavage of the glycosidic bond to generate adenine and MTR-1-phosphate. Though similar to MTN in function, the differences in active sites are drastic enough to allow the design of molecules that preferentially inhibit MTN without significantly affecting MTAP (Longshaw, et al., 2010). In particular, the clustering of positively charged amino acids near the ribosyl 2' carbon for MTAP, and its more occluded binding site near the 5' carbon have been proposed as exploitable differences for drug design (Lee, et al., 2003). An extensive analysis of TSA inhibitors have shown up to a 1300-fold binding discrimination favoring MTN over MTAP (Longshaw, et al., 2010).

A broad variety of extremely powerful transition state analog inhibitors of the MTN enzyme have been identified. Due to MTN's diverse role in multiple metabolic pathways, enzymatic inhibition of this enzyme is expected to induce changes the metabolic processes involved in transmethylations, the production of autoinducers and polyamines, radical SAM reactions contributing to vitamin and cofactor synthesis, and methionine salvage.

Activated Methyl Cycle

Transmethylations are a ubiquitously utilized biological process. Methyl recipients include most main classes of biomolecules: phospholipids, proteins, nucleic acids, carbohydrates, and some small molecules like catechol and glycine. More than twenty distinct SAM-dependent methyltransferases have been identified (Chiang, et al., 1996). DNA methylation is the most studied function of methyltransferases, where the cytosine residues in CpG motifs are methylated to regulate histone association and mark

cell cycle progression (Cheng, et al., 2001). Additional methyl recipients include rRNA (Vester & Long, 2009), tRNA (Urbonavicius, et al., 2005), proteins that affect enzymatic activity and influence signal transduction, and L-rhamnose sugars, which are methylated before incorporation into the glycan chains in bacterial cell walls (Steiner, et al., 2008). While the complete role of phospholipid methylation is still debated, it is known to function as an alternate synthetic method for creating phosphatidylcholine (Chiang, et al., 1996). A summary of known methyl recipient molecules and the processes that are affected are shown in Table 1.1.

Table 1.1. Effects of molecular methylation, by acceptor type.

DNA	*Gene repression, genome imprinting, replication timing, development, DNA repair*
Protein	*Protein function (via charge, orientation, hydrophobicity, etc.), signal transduction, chemotaxis, growth phase regulation*
Lipids	*Phosphatidylcholine synthesis, calcium transport, adenylate cyclase activation, signal transduction*
Carbohydrates	*Glycan formation*
Small molecules	*Neurotransmitter degradation, amino acid synthesis*

SAM is the most common methyl group donor, and the product of these reactions is SAH (Figure 1.9). Transmethylation reactions are subject to product inhibition by SAH at low micromolar concentrations (Caudill, et al., 2001).

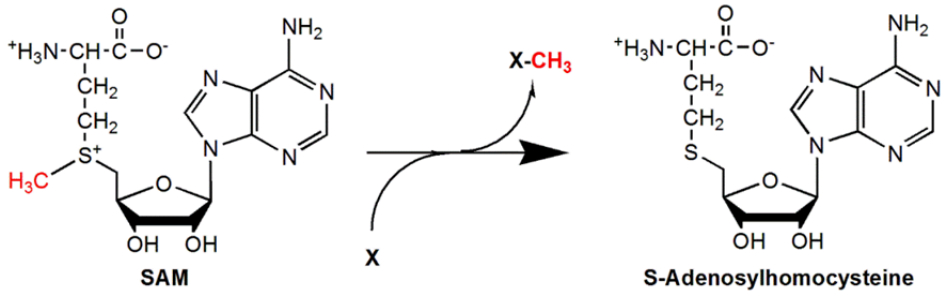

Figure 1.9. Mechanism of general SAM-dependent methyltransferase activity. SAM represents the most widely utilized source of methyl donor groups.

Autoinducer Production

Autoinducers (AIs) are a class of small molecules utilized by single-celled organisms as a means of coordinating group behavior in a process known as “quorum sensing”. First discovered in *V. fischeri* and *V. harveyi*, autoinducer signaling was responsible for stimulating bioluminescence in response to high cellular concentration (Kaplan & Greenberg, 1985). Later studies discovered quorum sensing was a mechanism utilized by a large number of Gram-positive and Gram-negative bacteria. Processes influenced by quorum sensing include bioluminescence, spore formation, biofilm development, and virulence factor secretion (Rutherford, et al., 2012). Most Gram-negative bacteria are capable of producing two distinct forms of autoinducers, AI-1 and AI-2.

AI-1 is formed from the methionyl group of SAM that spontaneously cyclizes upon addition of a hydrocarbon chain from acyl-carrier protein (ACP). The acyl chain length varies between bacteria and is thereby considered to be a form of species-specific communication. AI-2 is formed by isomerization of the ribose moiety of S-ribosylhomocysteine (SRH) to 4,5-dihydroxy-2,3-pentanedione (DPD). In aqueous environments, DPD cyclizes and forms a complex with aqueous boric acid (Figure 1.10). AI-2 is invariant among species and thought to act as a universal quorum sensing molecule. As AI-2 synthesis is dependent on a product of MTN metabolism and AI-1 is subject to feedback inhibition by MTA, both signaling pathways are highly dependent on nucleosidase activity.

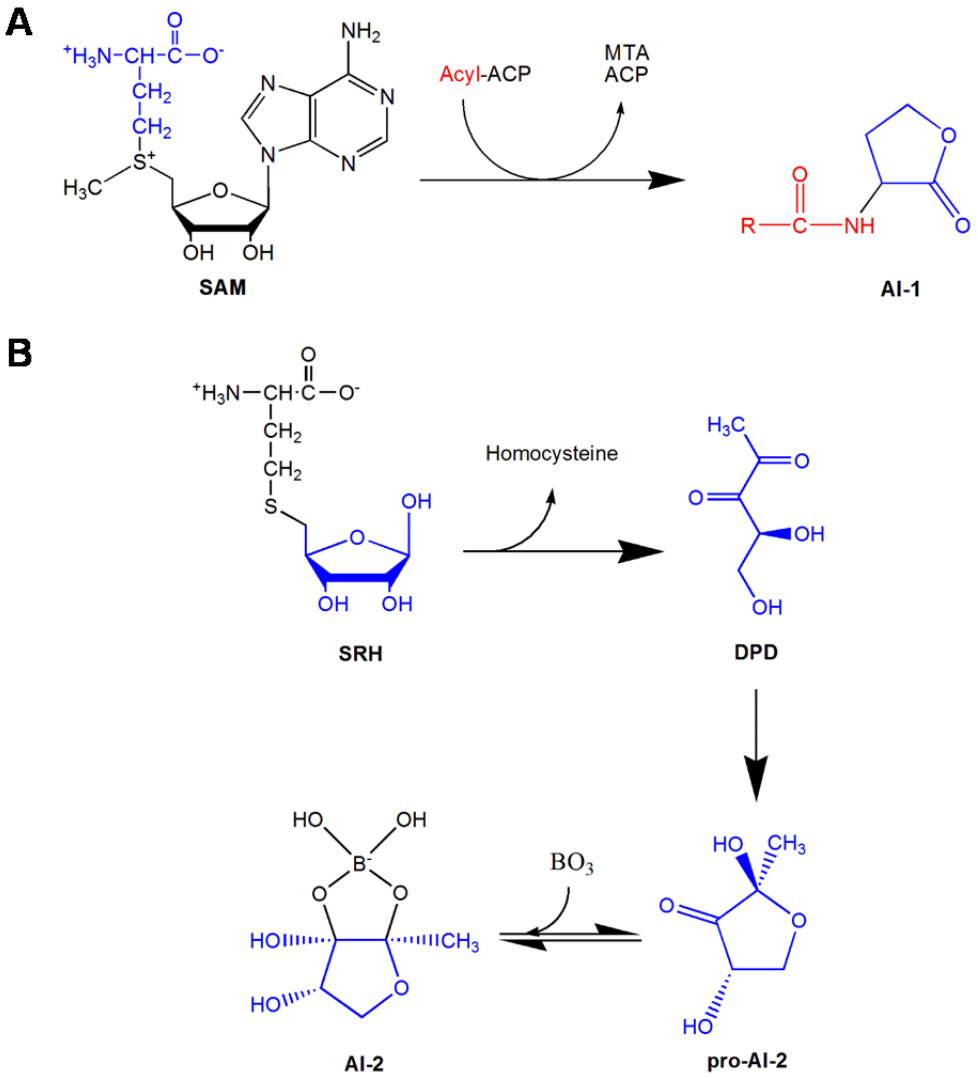

Figure 1.10. Synthetic pathways of Autoinducers 1 and 2. A) Production of AI-1 from SAM and acyl carrier-protein. The reaction is mediated by LasI and creates an acyl homo-serine lactone with a hydrocarbon chain length that varies depending upon the species. **B)** Synthesis of AI-2 from S-ribosylhomocysteine, as mediated by LuxS. This reaction creates 4,5-dihydroxy-2,3-pentadione (DPD). DPD spontaneously cyclizes to the precursor molecule 1-deoxy-3-dehydro-D-ribulose (pro-AI-2), which exists in equilibrium with an active borate diester form (AI-2).

K. pneumoniae lacks the AHL synthase enzymes required to create AI-1 and relies solely on AI-2. AI-2 deficient mutants of the *LuxS* gene in *K. pneumoniae* displayed structural impairments in early biofilm formation (Balestrino, et al., 2005). *K.*

pneumoniae knock-out strains for AI-2 transport proteins were also shown to have an increase in the production of extracellular lipopolysaccharides (Araujo, et al., 2010).

Polyamine synthesis

Polyamines are small organic polycations utilized by all forms of life and are considered as an element of the minimal metabolome of cells (Lee, et al., 2009). The positive charges enable interactions with negatively charged molecules like DNA, proteins, and cell wall components. In bacteria, polyamines are known to play a role in DNA replication, transcription, translation, cellular growth, siderophore synthesis, swarming, and biofilm formation (Lee, et al., 2009). Regulation of apoptosis is also known to be under partial control by polyamines (Seiler & Raul, 2005). There are four major polyamines synthesized in most organisms: putrescine, spermidine, spermine and cadaverine. Among bacteria, spermine and cadaverine are often synthesized only in trace amounts. Many bacteria, including *K. pneumoniae*, are incapable of synthesizing spermine. In contrast, putrescine and spermidine are heavily utilized, with intracellular concentrations typically in the low millimolar range (Shah & Swiatlo, 2008). The biosynthetic pathway for polyamines is initiated by the formation of putrescine from either L-ornithine or L-arginine. Both spermidine and spermine are synthesized by the addition of a propylamine group from decarboxylated SAM to putrescine and spermidine, respectively (Figure 1.11). These events are catalyzed by spermidine and spermine synthases and form MTA as a byproduct. Cadaverine is synthesized through an independent mechanism, in which L-lysine is converted to cadaverine directly by lysine decarboxylase. MTA acts as a product inhibitor of both spermidine and spermine synthases (Pajula & Raina, 1979; Evans, et al., 2004).

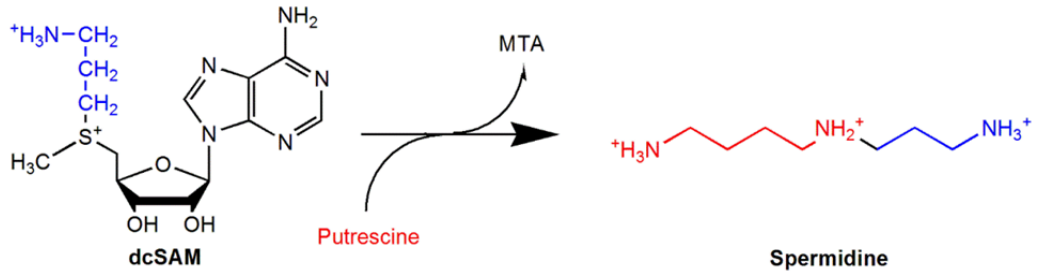

Figure 1.11. Spermidine synthesis. Formation of spermidine from putrescine and decarboxylated S-adenosylmethionine (dcSAM) via the spermidine synthase enzyme. The addition of a second aminopropyl group from dcSAM to spermidine by spermine synthase produces the polyamine spermine. Spermine is not usually synthesized *de novo* in bacteria, but can be formed in the presence of exogenous spermidine (Shaw & Swiatlo, 2008).

Radical SAM syntheses

Radical SAM enzymes constitute a recently discovered superfamily whose function is dependent on a conserved CxxxCxxC amino acid domain, with a non-conserved fourth cysteine contributing to a catalytic [4Fe-4S] cluster (Challand, et al., 2009). Radical SAM functions encompass more than 40 distinct synthetic processes with a conserved mechanism by which the iron-sulfur cluster facilitates the removal of methionine from SAM to produce a 5'-deoxyadenosine radical (Figure 1.12). The radical is quickly transferred to either another substrate or onto the SAM radical enzyme by the abstraction of a hydrogen atom. Some functions of SAM radical enzymes include: DNA

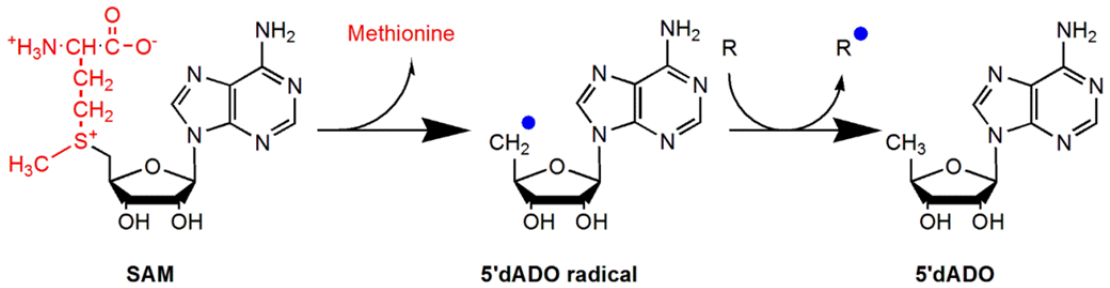

Figure 1.12. The general mechanism of radical formation and transfer by SAM radical enzymes. The 5'-deoxyadenosine radical species transfers the radical electron by the abstraction of a hydride group from the target small molecule or enzyme.

repair, anaerobic DNA metabolism, lipoyl production, and the synthesis of the cofactors pyrroloquinoline quinone, biotin, and thiamine (Frey, et al., 2008). Thiamine (vitamin B_1) is an essential cofactor in the central carbon metabolism of both glucose and pentose sugars (Figure 1.13). Thiamine deficiency is known to cause significant defects in cellular proliferation (Gigliobianco, et al., 2010). The radical SAM enzymes biotin synthase, lipoyl synthase, thiamine synthase, and tyrosine lyase are all subject to product inhibition by a combination of 5'dADO and methionine (Challand, et al., 2009).

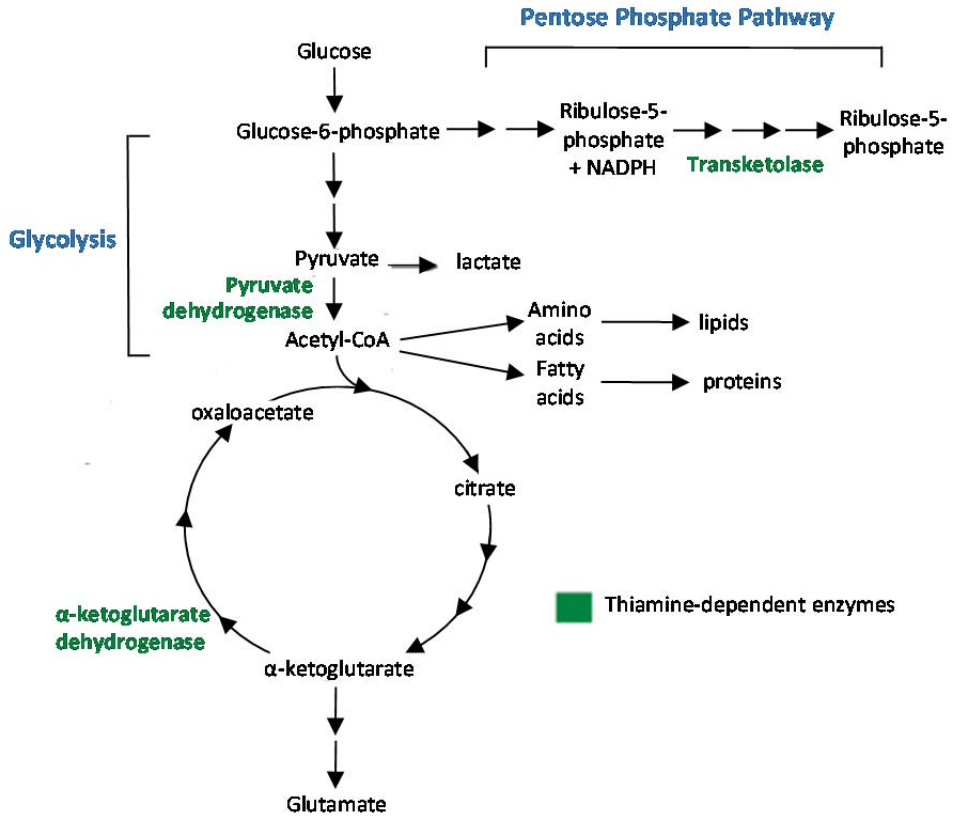

Figure 1.13. The role of thiamine as a cofactor in central carbon metabolism. Thiamine is crucial for the function of enzymes involved in glycolysis, the citric acid cycle, and the pentose phosphate pathway. (Adapted from Harrigan, et al., 2008.)

Methionine salvage pathway enzymes – 5-methylthioribose kinase (MTRK)

5-Methylthioribose Kinase

Methionine recycling is intertwined with all three MTN substrates. MTRK is the enzyme responsible for initiating methionine salvage from 5-methylthioribose (MTR), the product of MTA depurination by MTN. MTRK facilitates the phosphate transfer from ATP to carbon-1 of MTR (Figure 1.14). Unlike MTN, the MTRK enzyme is utilized by a much more restricted group of bacteria (*Klebsiella, Bacillus, Rhizobium,* etc.). MTRK is also broadly present in plants but is absent in mammals, suggesting it could be a good target for species-specific antibiotic or herbicide development.

The methionine salvage pathway (Figure 1.14) begins with MTA produced from SAM-dependent polyamine or AI-1 synthesis. MTN depurinates MTA to produce adenine and MTR. MTRK then catalyzes the phosphotransfer reaction from ATP to MTR to produce 5-methylthioribose-1-phosphate (MTR-1P). In *K. pneumoniae,* the remainder of the pathway is as follows: MTR-1P undergoes isomerization to methylthioribulose-1-phosphate, and is subsequently dehydrogenated to 2,3-diketo-methylthiopentane-1-phosphate. This is then dephosphorylated to 1,2-dihydroxy-3-keto-5-methylthiopentene, which is then oxidatively decarboxylated to 2-keto-4-methylthiobutyrate (KMTB). KMTB is then selectively transaminated to reform methionine.

This process is adhered to by many organisms, with slight variations among species. Methionine is also a product of radical SAM reactions and can be recycled from homocysteine, a product of SAH breakdown. The recycling of methionine is an important function, as the molecule is energetically costly to synthesize *de novo*. Many

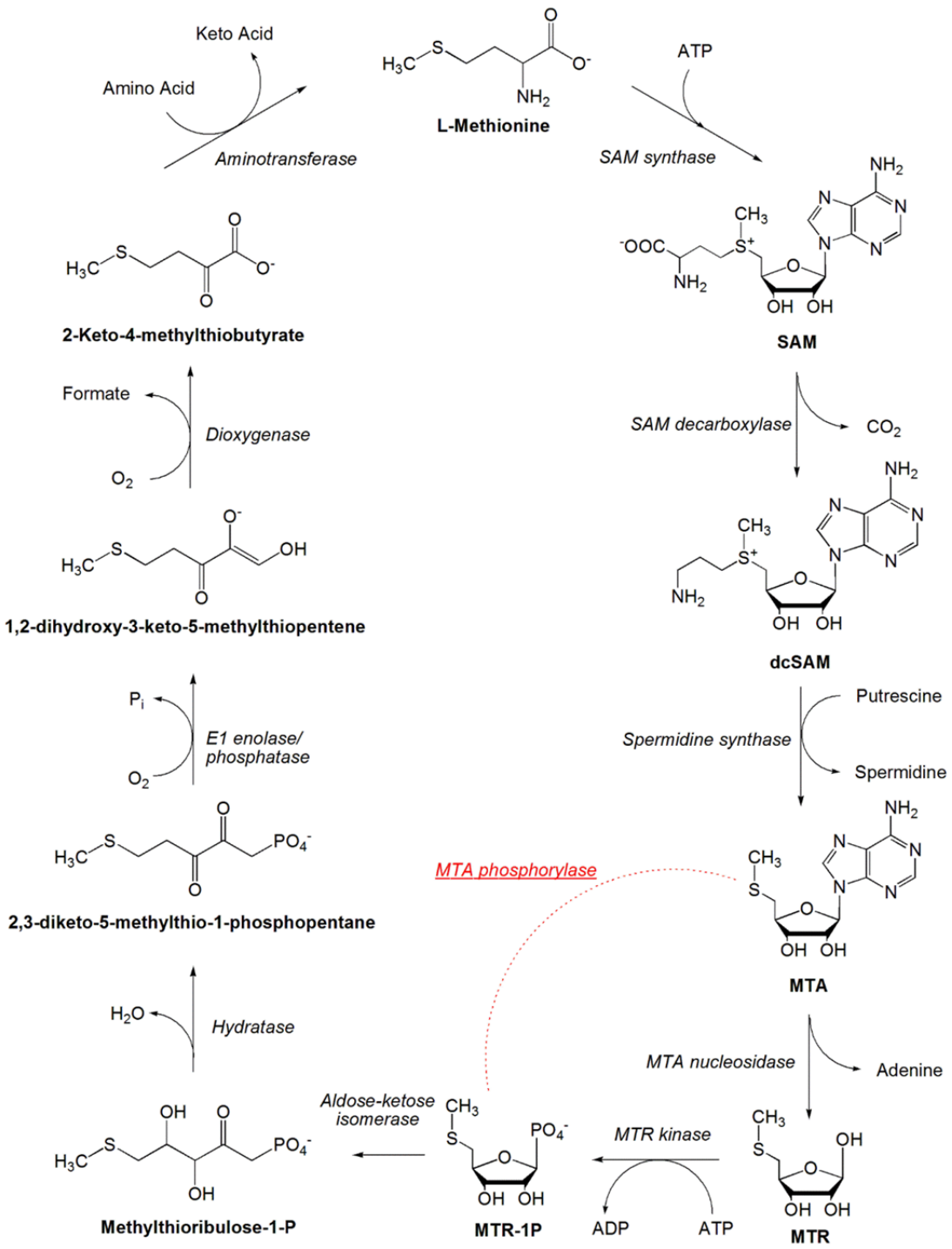

Figure 1.14. Methionine salvage cycle in *Klebsiella pneumoniae*. The activity of the alternative mammalian MTAP pathway is denoted by a dashed line.

organisms lack synthetic enzymes to create methionine, and rely upon the salvage pathways to conserve this amino acid (Albers, 2009). As MTRK is not utilized by

mammals, it has undergone investigation as a potential target of antibiotic development. A large number of MTR analogs with substitutions of the 5-alkylthio moiety have proved successful in inhibiting MTRK activity. Substituted 5-phenylthioribose analogs in particular have demonstrated strong effects on *K. pneumoniae* growth, the most potent of which displayed an IC_{50} value of 2.5 picomolar (Winter, et al., 1993). The analogs 5-trifluoromethylthioribose (TFMTR) and 5-ethylthioribose (ETR) have been demonstrated to act as catalyzable substrates and continue through downstream metabolism to produce the toxic molecules of carbonothioic difluoride (thiophosgene gas) and ethionine, respectively (Gianotti, et al., 1990; Tower, et al., 1991; Winter, et al., 1993). The broad acceptance of MTR analogs as either functional inhibitors or accepted substrates shows an high degree of substrate promiscuity which may provide opportunities for exploitation in future drug designs.

Summary

The bacterial organism *Klebsiella pneumoniae* acts as an important nosocomial pathogen and is poised to become an even greater threat in the near future. *K. pneumoniae* possesses two enzymes, 5'-methylthioadenosine nucleosidase (MTN) and 5-methylthioribose kinase (MTRK), which are not found in humans. These enzymes contribute to many important metabolic functions, which include: transmethylations, autoinducer synthesis, polyamine production, radical SAM reactions, and the salvage of methionine. As a result, MTN and MTRK have been identified as targets for the development of novel antimicrobial therapeutics. The research presented here consists largely of efforts following the purification of these two enzymes from genes cloned and expressed from the *K. pneumoniae* genome. Chapter 2 (pg. 27) presents a manuscript

derived from the characterization of the kinetic properties, substrate affinity, and kinetic mechanism of the MTRK enzyme. Chapter 3 (pg. 46) reports a manuscript based on investigations into MTN regarding kinetics towards the three unique substrates, and the determination of inhibition constants for several transition state analog and novel non-nucleoside small molecule inhibitors. Chapter 4 (pg. 61) contains research towards a third publication that investigates the *in vitro* effects of MTN inhibitors against *K. pneumoniae* regarding growth, biofilm formation, autoinducer-2 secretion, and the transcriptional expression of multiple virulence factors.

CHAPTER 2: PAPER #1 – CHARACTERIZATION OF *Klebsiella pneumoniae* 5-METHYLTHIORIBOSE KINASE

Abstract

5-Methylthioribose kinase (MTRK) is an enzyme unique to the methionine salvage pathway of plants and some microbes. The MTRK enzyme catalyzes the phosphorylation of 5-methylthioribose (MTR), a product of the synthesis of polyamines, autoinducer-1, and ethylene, in order to initiate the methionine salvage pathway. The absence of MTRK in mammals has established this enzyme as a potential target for the development of novel antibiotics. Analysis of genomic data for MTRK reveals a high degree of sequence homology between diverse organisms, and suggests the presence of both methionine and purine-dependent regulatory elements for MTRK gene expression in the nosocomial pathogen *Klebsiella pneumoniae*. A *K. pneumoniae* recombinant MTRK enzyme was cloned and purified and the K_m values for MTR and ATP were found to be 21 ± 2 and 70 ± 10 μM respectively, with a specific activity of 6.2 ± 0.2 μmol/min per mg. Investigation into substrate acceptance of MTR analogs with substitutions at the 5-carbon position demonstrated a high affinity towards groups with hydrophobic properties. Product inhibition studies using MTR-1-phosphate (MTR-1P) suggest an ordered sequential reaction mechanism with ATP binding first and MTR-1P being the first product released.

Introduction

Methionine salvage is important for the recycling of methionine utilized in S-adenosylmethionine (SAM) dependent methylation reactions, polyamine synthesis, and the radical SAM reactions involved in vitamin biosynthesis [8, 21, 26]. Recovery of methionine from MTA is a highly conserved function [26], as the *de novo* synthesis of methionine is considered to be energetically "costly". Indeed, many organisms lack *de novo* methionine synthetic pathways entirely and instead rely solely on exogenous sources and salvage methods. The utilization of the MTRK enzyme is common among plants but highly unusual among bacterial species. Of note among these are the genus *Serratia*, *Enterobacter,* and *Klebsiella*. These organisms act as common nosocomial agents with significant clinical impacts. The absence of MTRK in mammals and the majority of bacterial species provides an opportunity for the development of targeted antibiotics that would not disturb the human microbiome.

The MTRK enzyme is a functional homodimer with a structural homology to the choline/ethanolamine kinase enzyme family [17]. It is responsible for committing the waste product 5-methylthioribose (MTR) to the salvage pathway by phosphorylation at the 1-carbon position, at the expense of ATP. The methionine salvage pathway itself (Figure 2.1) is initiated following the addition of methionine to ATP, which produces S-adenosylmethionine (SAM or AdoMet). SAM is utilized in an array of biochemical processes that produce three major products: S-adenosylhomocysteine (SAH), 5'-deoxyadenosine (5'dADO), and 5'-methylthioadenosine (MTA). The majority of SAM is consumed in transmethylation reactions [31], producing SAH, while 5'dADO is the

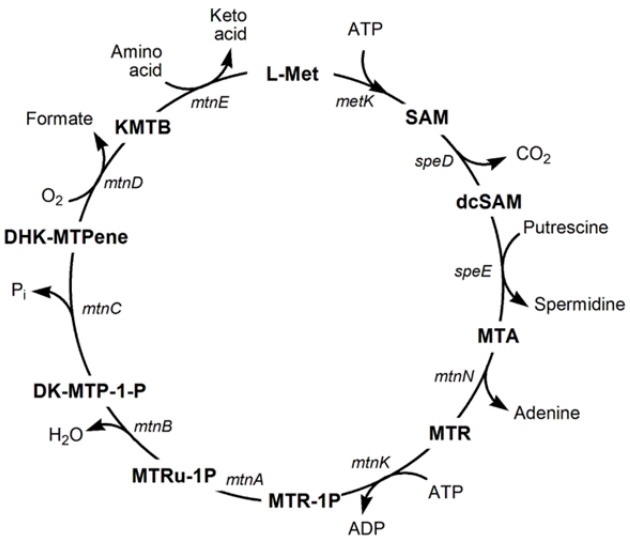

Figure 2.1. Methionine salvage pathway in *Klebsiella pneumoniae*. Following the utilization of methionine in the production of polyamines via S-adenosylmethionine (AdoMet), 5-methylthioribose is progressively restructured into methionine by a suite of dedicated enzymes (metK; speD, E; mtnN, K, A, B, C, D, E) [35].

product of radical-SAM reactions for vitamin biosynthesis. In the third process, SAM is decarboxylated and subsequently loses a propylamine group to produce 5'-methylthioadenosine (MTA) and the polyamines spermidine or spermine. MTA is also a by-product of the synthesis of the signaling hormone ethylene in plants [8], and of the quorum sensing molecule autoinducer-1 among Gram-negative bacteria [7]. In mammals, MTA is directly converted to 5-methylthioribose-1-phosphate (MTR-1P) by the enzyme 5'-methylthioadenosine phosphorylase, whereas in plants and certain bacteria, this process requires the concerted effort of both the 5'-methylthioadenosine/S-adenosylhomocysteine nucleosidase (MTN) and MTRK enzymes.

The pathways for the recovery of methionine following the production of MTR-1P are highly similar among all organisms. Initially, MTR-1P undergoes an isomerization to methylthioribulose-1-phosphate (MTRu-1P), and a successive dehydrogenation and dephosphorylation to 1,2-dihydroxy-3-keto-5-methylthiopentene (DHK-MTPene). A dioxygenase converts this to 2-keto-4-methylthiobutyrate (KMTB), which is then

selectively transaminated to reform methionine. Many organisms catalyze these reactions using multifunctional enzymes, with *K. pneumoniae* utilizing a bi-domain enolase/phosphatase and plants such as *A. thaliana* possessing a dehydratase/enolase/phosphatase [26].

This work presents a kinetic characterization of the *K. pneumoniae* MTRK enzyme as well as an examination of the kinetic mechanism and MTRK substrate analog utilization.

Materials and Methods

Bacterial strains and culture conditions. *K. pneumoniae* ATCC strain 43816 was used for gene amplification. Protein induction and purification were performed in *E. coli* BL21 (Invitrogen) cells. All growth was performed in Luria-Bertani media at 37°C with shaking at 225 rpm.

Chemicals and substrates. 5'-deoxy-5'-methylthioadenosine (MTA), S-ribosylhomocysteine (SRH), 5-deoxyribose (5-dRIB), phosphoenolpyruvate (PEP), dithiothreitol (DTT), and lactate dehydrogenase/ pyruvate kinase were purchased from Sigma. Nicotinamide adenine dinucleotide (NADH) was purchased from Acros Organics, and magnesium chloride was acquired through J.T. Baker Chemical Co. MTR and MTR analogs were provided by Dr. Michael Riscoe (OHSU). MTR-1P was prepared in lab through enzymatic reactions. In short, to a 2mL solution of 1mM MTA and 0.3M sodium phosphate of pH=7, 7μg recombinant human MTA phosphorylase (previously purified in lab) was added and allowed to react at room temperature over 1.5 hours. The solution was then centrifuged through a Merck Millipore 3000 NMWL centrifuge filter, and the

flow-through collected. Complete conversion of reactant was verified by the loss of activity as a substrate for MTN enzyme (previously purified in lab).

Gene cloning. The MTRK gene sequence was amplified by whole-cell PCR using the primer pair MTRKF (5'- GAATTCATGTCGCAATACCATACCTT – 3') and MTRKR (5' – GCGGCCGCTCAGCTGTACTGGCGTACCC - 3'), and the PCR product was digested and ligated into poly-His-encoding pPROEX HTA plasmid (Invitrogen) at the EcoR1/Not1 digest sites. The plasmid was transformed into chemically competent *E. coli* One Shot® TOP10 cells and purified using the GeneJET Plasmid Miniprep Kit (ThermoFisher). Insert orientation was confirmed by PCR and sequencing (VA DNA Sequencing Core Facility) and the plasmid was transformed into *E. coli* BL21 cells (Invitrogen) and subsequently grown under ampicillin selection.

Protein purification. 500mL LB were inoculated with the plasmid-bearing strain and grown to an OD_{600} of 0.4. Protein expression was induced with 0.5mM IPTG and the cells were then grown overnight. Cells were centrifuged at 5000xG for 15 minutes, washed once in 50mL PBS, centrifuged again and the pellet was lysed with 3mL BPER® reagent over 15 minutes at room temperature with frequent vortexing. Lysate was then centrifuged again and the supernatant was added to 3mL cobalt HisPur™ resin and set to agitate at 4°C overnight. Column elutions were performed by centrifugation at 700xG for 2 minutes, and consisted of a flow-through, three washes with 3mL wash buffer (10mM imidazole, 50mM $NaPO_4$, 300mM NaCl, pH= 7.4), and three elutions with 1.5mL 500mM elution buffer (250mM imidazole, 50mM $NaPO_4$, 300mM NaCl, pH= 7.4). Protein identity and purity was confirmed by 15% polyacrylamide SDS-PAGE assessed by PageRuler Plus Prestained Protein Standard (ThermoFisher), stained with Coomassie

Blue. The enzyme concentration was quantified by A_{280} (ε_{280} = 1.04 mg/mL). The final elution from the purification procedure was used for kinetic analyses, due to highest apparent purity, and was quantified at 500ng/µL (data not shown) before being diluted to 100ng/µL at 20% glycerol for long-term storage and use in spectrophotometric assays.

MTR kinase enzyme assay. Reaction conditions were based on a linked spectrophotometric assay wherein ADP production is stoichiometrically linked in a one-to-one relationship with NADH oxidation [44]. In brief, assays were performed at 25°C in 1mL total volume with 1mM PEP, 0.3mM NADH, 2mM $MgCl_2$, 5mM DTT, 0.1M sodium phosphate pH 7, and 14U lactate dehydrogenase (LDH)/ 11U pyruvate kinase (PK) (purchased combined from Sigma). Reaction scheme is as follows:

1) ATP + MTR → MTR-1P + ADP Scheme 1
2) ADP + PEP → ATP + pyruvate
3) Pyruvate + NADH → lactate + NAD^+

For kinetic activity determinations, the non-varied substrate was used at a concentration approximately ten times the derived K_m (200 µM for MTR, 1mM for ATP). MTR was examined at concentrations between 1 and 200 µM and ATP between 10 and 200 µM. After addition of LDH/PK enzymes to substrates, the reaction mixture was given 5 minutes to reach equilibrium before addition of 1 µg MTRK and enzymatic activity was continually monitored at 340 nm on Varian Cary 50 spectrophotometer (ε_{340} = 6.22 mM^{-1} cm^{-1}). Data was analyzed using GraphPad Prism 6.0 software and fit to the Michaelis-Menten equation, where:

$$v_o = v_{max}[S]/(K_m + [S]) \quad \text{Eqn. 1}$$

Alternate substrate assays were performed with 1mM ATP and the MTR analog used in lieu of MTR at a concentration of 20 μM.

Homology modeling. The crystal structure of *Bacillus subtilis* 2PUP (GI: 37999472) was obtained from Protein Data Bank (PDB: 4L0M). Homology modeling of the *Klebsiella pneumoniae* sequence (GI: 11846464) was carried out using Maestro and Prime (ver. 4.2) of Schrodinger Suite 2015-4 [40]. Sequence alignment of 2PUP and *K. pneumoniae* was conducted using the BLAST algorithm in the structure prediction wizard in Prime. The three-dimensional *K. pneumoniae* structure was modeled using the *Bacillus subtilis* MTRK crystal structure (PDB: 2PUP) as the template. Using the energy-based approach in Prime, Bgp and MtnN homology models were constructed as homo-dimers with no ligands in the active sites. The homology model was then aligned with the *Bacillus subtilis* structure (PDB: 2PUP) using Schrodinger. The coordinates of ADP and PO_4^{2-} were copied into the active sites of the *K. pneumoniae* homology model.

Molecular docking. Grid generation and ligand docking was performed using the Glide (ver. 6.9) [41] algorithm in Schrodinger. Grid generation using the default parameters was performed on both of the MTRK structures, with the grid centered in the active site and a search radius of 17 Å. Molecular docking of MTR was conducted using the standard precision (SP) method and default parameters in Glide. Results were visualized in Maestro and images were rendered using Pymol (ver. 1.8) [42].

Results and Discussion

Genomic analysis – Examination of the genomic region surrounding MTRK in *K. pneumoniae* reveals some unexpected structural organization, as well as several putative regulatory elements (Figure 2.2). The MTRK gene in *B. subtilis* has been identified as

part of a region containing independent regulons that encode the genes for every enzyme of the methionine salvage pathway [24]. In contrast, the *K. pneumoniae* MTRK gene is adjacent only to MTR-1P isomerase (Figure 2.2). These genes are separated by a 101 base pair region and are encoded on complimentary strands. Present in the promoter region separating MTR-1P isomerase and MTRK are multiple consensus sequences for *metR* and *metJ* regulatory domains. These regulatory mechanisms allow differential expression dependent on intracellular methionine availability. The palindromic nature of these sequences allows them to potentially operate as shared regulators for the two enzymes, though the advantage of separating these genes is hard to surmise, as they fulfill a shared metabolic role. These met-regulatory domains account for the observed moderation of MTRK activity following growth in methionine-rich environments [16], as well as the increased MTRK expression noted under sulfur-starved conditions [17]. The regulatory method stands in contrast to that used by *B. subtilis*, which utilizes the S-box sequence found in Gram-positive bacteria, an element common to genes involved in sulfur metabolism [35]. The sequence upstream of MTRK also contains a *purR* regulatory sequence, establishing a link to purine metabolism. This is most likely due the relationship of MTRK with the enzyme preceding it in the salvage pathway, MTN, which acts as a purine nucleosidase.

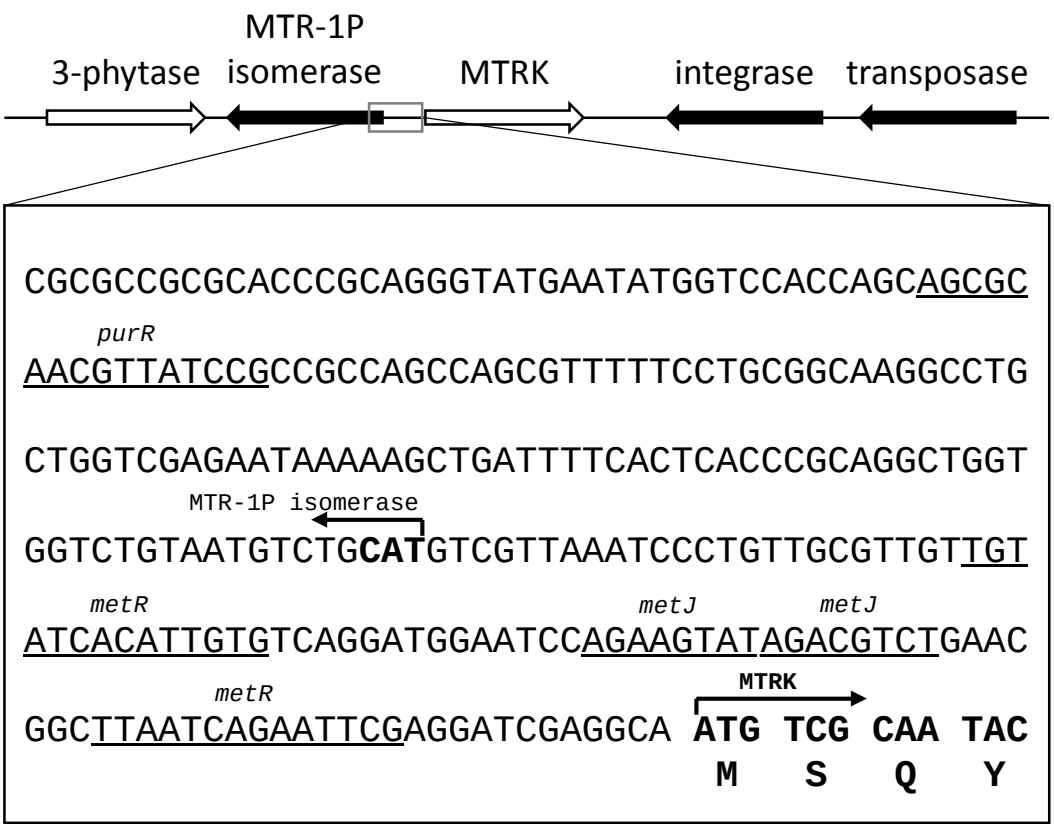

Figure 2.2. Upstream sequence for *K. pneumoniae* MTRK. The MTRK and MTR-1P genes are adjacent but not members of an operon. Predicted regulatory sequences determined from the consensus sequences for: *metJ* – AGACGTCT, *metR* – TGAANNATNNTTCA and *purR* – ACGCAAACGTTTTCNT [36][37][38].

A multiple sequence alignment between a set of bacterial and plant MTRK genes showed high degrees of homology, with *K. pneumoniae* possessing a 30-40% residue identity to each examined sequence (Figure 2.3). Critically, the residues identified as

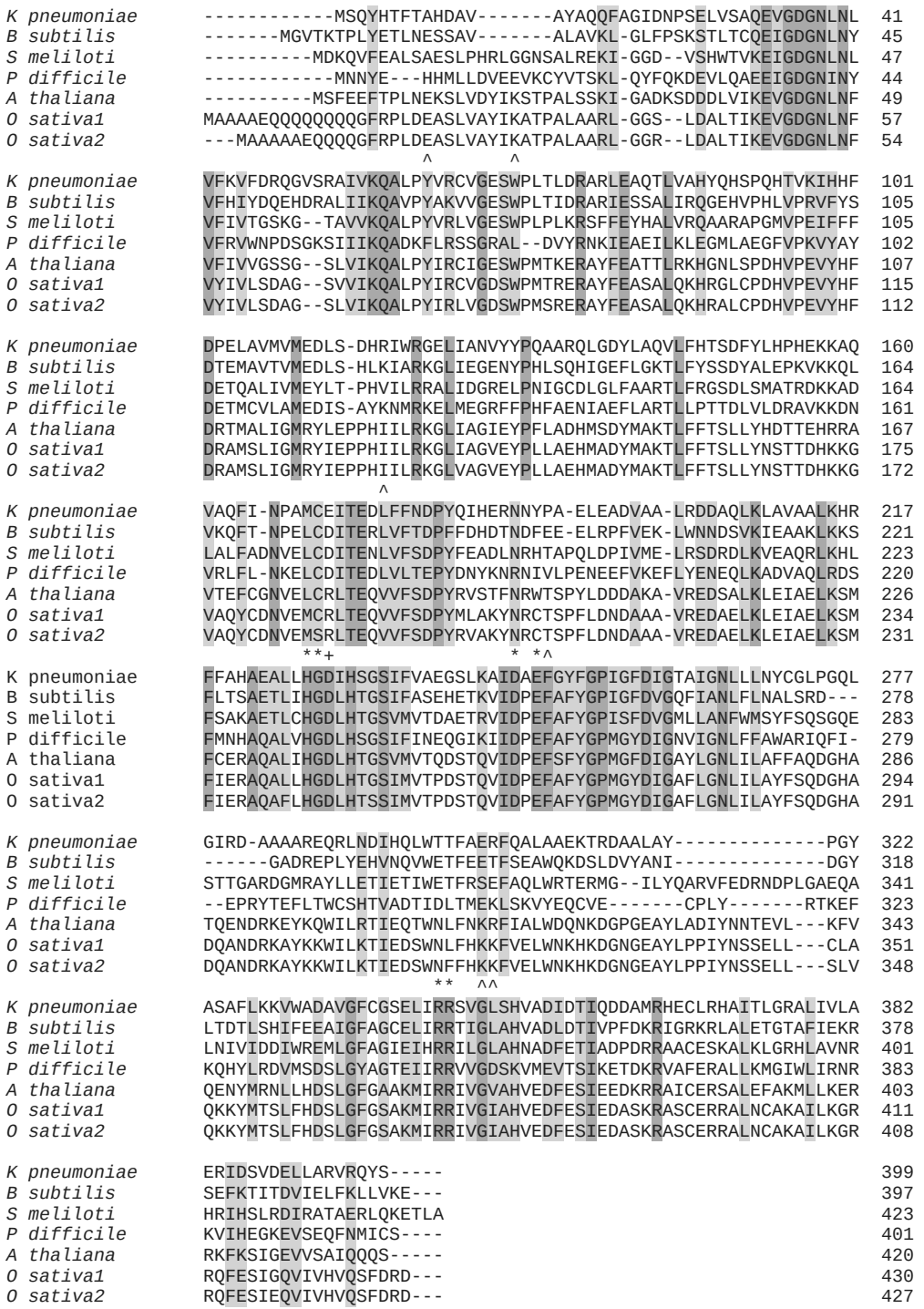

Figure 2.3. Bacterial and plant MTRK sequence alignment. Represented are diverse sequences from *K. pneumoniae, B. subtilis, R. meliloti, C. difficile, A. thaliana* and both *O. sativa* isotypes. Residues involved in MTR substrate specificity, ATP/Mg^{2+} coordination, and with catalysis are marked above with ^, *, and +, respectively. Alignment was performed with ClustalOmega software [33].

comprising the binding pocket and those that participate in substrate/cofactor binding and orientation are highly homologous [20]. This suggests a strong evolutionary conservation of enzyme in form and function between highly disparate organisms.

Protein purification – Addition of the N-terminal poly-His selection marker resulted in a calculated molecular weight of 48.3 kD, matching the observed weight and holding consistent with that previously reported for the native enzyme [2]. The recombinant protein was identified by size and the apparent purity was confirmed as >95% by SDS-PAGE (Figure 2.4).

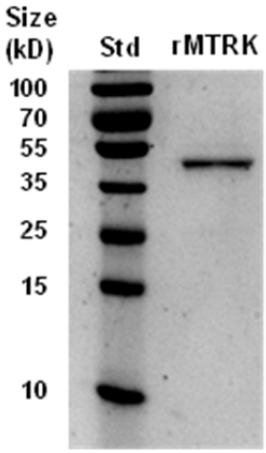

Figure 2.4. SDS-PAGE of purified recombinant MTRK. Lane 1: Protein molecular weight standard. Lane 2: 2µg recombinant MTRK. The calculated molecular weight for purified rMTRK was 48.3 kD.

Substrate kinetics assays – Results of both MTR and ATP substrate-specific data were indicative of typical Michaelis-Menten kinetics (Figure 2.5). The enzymatic rate fell within expected parameters, showing a specific activity of 6.2 µmol/min/mg. The apparent K_m values for both substrates were determined at near-saturating conditions for the non-varied substrates. The K_m values were demonstrated to be at physiologically relevant concentrations of 21 and 70 µM for MTR and ATP, respectively. MTR as a

substrate demonstrated a higher catalytic efficiency than ATP by a factor of 3.3 (Table 2.1).

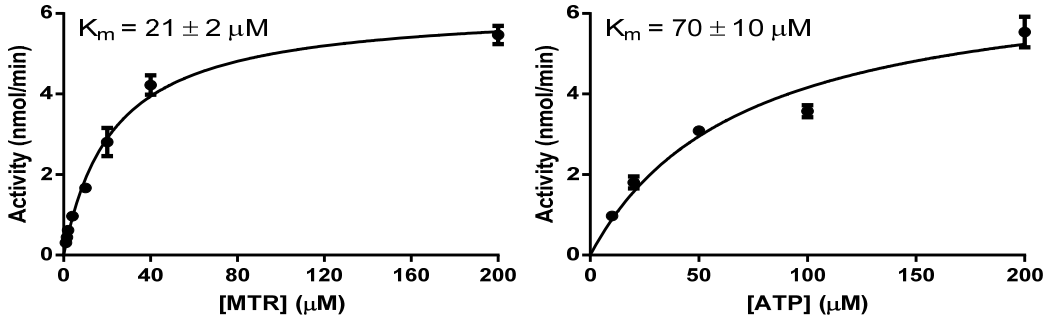

Figure 2.5. Substrate velocity plots of MTRK. The substrate kinetics for MTR (left) and ATP (right) were determined using a coupled spectrophotometric assay. The data was fit to the Michaelis-Menten equation using GraphPad Prism 6.0 software.

The K_m for MTR was in close accord with that previously reported from enzyme purified from *K. pneumoniae* cellular extracts at 12.2 μM [2]. K_m values from *Enterobacter aerogenes* for MTR and ATP were also placed at 8.1 and 74 μM [15]. A K_m for ATP had additionally been assigned for the OsMTK1 enzyme from *Oryza sativa* at 184 μM [19]. The *O. sativa* enzyme was also reported to display a significantly slower activity than for *K. pneumoniae* as well as evidence of cooperative binding, which was not observed for the *K. pneumoniae* MTRK. Despite the high degree of homology between bacterial and plant MTRK sequences, large discrepancies in activity and binding may be possible, though this may simply be an apparent difference as only one of the two *O. sativa* MTRK enzymes was kinetically profiled.

Alternate Substrate kinetics – Assays were performed under conditions identical to prior MTR substrate kinetics assays, with MTR analogs used in lieu of MTR at 20μM

Table 2.1. Summary of MTRK kinetic constants

	Specific Activity	k_{cat}	K_m	k_{cat}/K_m
MTR	6.2 ± 0.2 μmol/min/mg	300 ± 8 min^{-1}	21 ± 2 μM	14.2 $\mu M^{-1}min^{-1}$
ATP	…	…	70 ± 10 μM	4.3 $\mu M^{-1}min^{-1}$

K_m values represent the "apparent" K_m measured at conditions with the non-varied substrate held at near-saturating concentration

concentration and standardized to the activity of MTR. Activity was observed for many of the substrates examined, and that of n-propylthioribose exceeded that of MTR by a significant margin (Table 2.2). The previously identified substrate of 5-trifluoromethylthioribose showed approximately two-thirds the activity of the native substrate, while the singly-halogenated 5-fluoromethylthioribose showed one-fifth activity. Analogs with bulkier 5-carbon substitutions showed drastically limited activities. β-hydroxy-5-butylthioribose had one-twentieth the native catalytic rate and *para*-nitro-5-phenylthioribose showed no catalysis. As MTR is one of three structurally similar products of the MTN enzyme, we examined both alternate products of MTN metabolism, S-ribosylhomocysteine and 5-deoxyribose. Neither substrate produced any observable catalytic activity.

Table 2.2. Summary of the relative specific activities of MTR analogs.

Substrate	% Activity	Specific Activity (μmol/min/mg)
5-methylthioribose (MTR)	100	6.2
n-propylthioribose	168	10.4
5-trifluoromethylthioribose	66	4.1
5-fluoromethylthioribose	20	1.2
β-hydroxy-5-butylthioribose	5	0.3
p-nitro-5-phenylthioribose	0	0
S-ribosylhomocysteine	0	0
5-deoxyribose	0	0

The capacity of *n*-propylthioribose as a substrate is not entirely unexpected, as 5-ethylthioribose (not tested) has been shown to be an inhibitor of microbial growth owing to its conversion by MTRK towards the toxic molecule ethionine [27]. The rationale for its increased activity is difficult to ascertain, as the conserved Trp^{74}, Leu^{345}, and Leu^{180} residues in the *B. subtilis* crystal structure were proposed to gate the 5-carbon end of the ribose molecule in order to restrict the hydrocarbon chain length [20].

5-trifluoromethylthioribose is a previously identified substrate that is ultimately catalyzed to toxic carbonothioic difluoride [10], and exhibited two-thirds the activity of MTR whereas the singly halogenated 5-fluoromethylthioribose showed less activity despite it more closely resembling the native 5-methylthio group in size. This is most likely on account of the hydrophobic nature of saturated fluorocarbons (e.g. Teflon) discriminating binding in favor of the trifluoro-substituted analog. Examination of *β*-hydroxy-5-butylthioribose displayed an extremely limited degree of enzymatic activity, most likely due to the presence of the polar hydroxyl group. Additionally, *p*-nitro-5-phenylthioribose exhibited no catalytic activity, despite the fact that a large number of phenyl-substituted ribose analogs have been identified as highly potent inhibitors of MTRK and organismal growth [27]. Accordingly, it seems that MTRK possesses a certain degree of promiscuity for substitutions at the 5' position, with a high discrimination towards hydrophobic groups, and with group size potentially being of lesser importance towards binding. In addition, a computational model of the *K. pneumoniae* active site incorporating MTR into the binding pocket implicates a large degree of freedom regarding rotation of the 5-carbon groups. Though Leu^{345} in the *B. subtilis* crystallographic structure (Leu^{349} for *Klebsiella* MTRK) was proposed to act as a

hydrophobic component of the binding pocket, its carbonyl group presents itself towards the binding pocket at a distance of approximately 6Å from the sulfur component of MTR (Figure 2.6). This may help in recognition of MTR by the coordination of a water molecule between the enzyme and substrate and serve to explain why 5-deoxyribose was not able to be utilized as a substrate.

Kinetic mechanism determination – In order to determine the substrate reaction order, product inhibition studies were performed with MTR-1P. The analogous assay with ADP could not be performed due to constraints of the linked enzymatic assay.

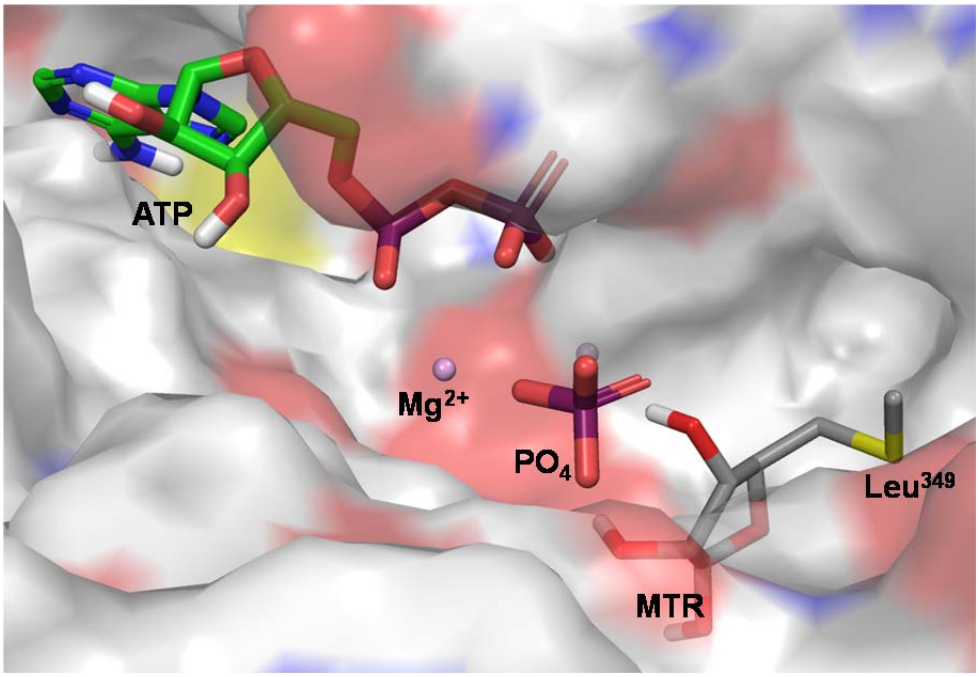

Figure 2.6. Modeled binding site of *K. pneumoniae* MTRK. The region incorporating the 5-carbon region of MTR permits a high degree of freedom regarding group size and orientation. The carbonyl moiety of Leu^{349}, may coordinate with the sulfur atom of the substrate.

Double reciprocal plots of MTR-1P against both MTR and ATP substrates are presented in Figure 2.7. The results are consistent with an ordered sequential binding

order based on Cleland's rules, where MTR-1P appears to be the first product released [43].

Due to constraints of the linked-enzymatic assay utilized, the substrate binding order could not be directly examined, however, we herein propose a binding order based on our data's conformity to mechanistic indications derived from protein structure and homology. In X-ray crystallographic studies of *B. subtilis* MTRK [20], structures were solved exclusively with ATP derivatives and in its unbound form. No equivalent structures containing bound MTR could be obtained, suggesting ATP as the catalytic initiator. Additionally, structural analysis of MTRK identified the two most closely related proteins as being choline kinase and aminoglycoside phosphotransferase type IIIa [20]. Both have been identified as functioning via a sequential binding mechanism with ATP being the first substrate bound [1][32]. Structurally similar mammalian kinases such as casein kinase and cAMP-dependent protein kinase also exhibit a sequential ordered

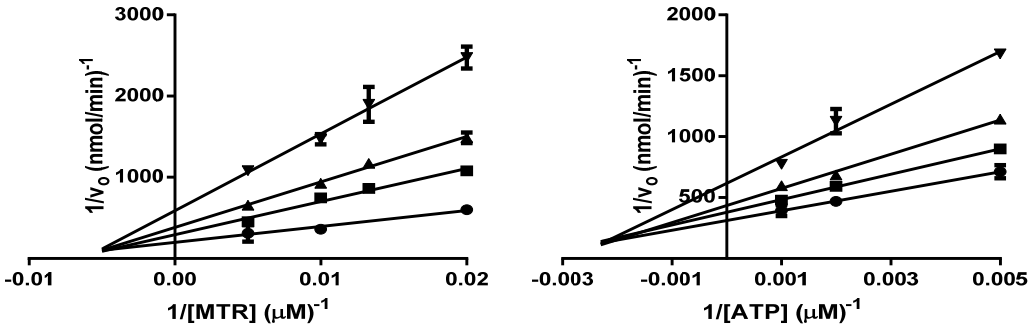

Figure 2.7. Double reciprocal plots of MTR-1P product inhibition. Left panel shows MTR-1P product inhibition against MTR substrate, ● = 0, ■ = 50, ▲ = 100, ▼ = 200 μM MTR-1P. Right panel shows MTR-1P product inhibition against ATP substrate, ● = 0, ■ = 20, ▲ = 50, ▼ = 100 μM MTR-1P. Both inhibition profiles are indicative of a mixed mode of inhibition.

mechanism with ATP binding first [29]. Examination of the enzyme binding site would corroborate this conclusion, as ATP appears to be placed in an occluded cleft within the binding pocket where the clearest route to the ATP-binding pocket is through the site of MTR binding (Figure 2.6). This would seem to necessitate an ordered sequential mechanism with the binding of ATP occurring prior to MTR. This organization of substrates would seem to necessitate a sequential binding mechanism in order to allow catalysis.

Our product inhibition data is consistent with these alternate data and accordingly, we suggest an identical mechanism for MTRK, wherein ATP binds first, followed by MTR with MTR-1P and ADP products being released, in order (shown in Figure 2.8).

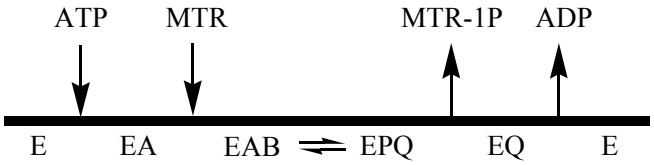

Figure 2.8. Cleland line describing MTRK binding. A sequential binding order with ATP binding first and methylthioribose-1-phosphate as the first product released.

Conclusion

MTRK is essential component of the methionine salvage pathway in the pathogenic bacteria *K. pneumoniae*. The gene does not form an operon with other genes responsible for methionine recycling, and appears to be under the regulatory control of elements involved in both purine and methionine metabolism. The purified enzyme displayed a specific activity of 6.2 μmol/min/mg, and the substrates MTR and ATP had apparent K_m values of 21 and 70 μM. Enzyme activity towards analogs of MTR revealed the enzyme to favor molecules with short, hydrophobic 5-carbon substitutions, and product inhibition studies implicate an ordered sequential reaction order. We expect this

data can be used to design inhibitors with characteristics to perform as more potent antibiotics against target organisms.

Acknowledgements

Special thanks to Dr. Danny Xu, and Patrick Erstad for providing the molecular modeling of the *K. pneumoniae* MTRK enzyme.

Bibliography

1. Thompson, Paul R.; Boehr, David D.; Berghuis, Albert M.; Wright, Gerard D. Mechanism of aminoglycoside antibiotic kinase APH(3')-IIIa: role of the nucleotide positioning loop. *Biochemistry*, **2002**. 41 7001-7007.
2. Cornell, Kenneth A.; Winter, R.W.; Tower, Paula A.; Riscoe, Michael K. Affinity purification of 5-methylthioribose kinase and 5-methylthioadenosine/S-adenosylhomocysteine nucleosidase from *Klebsiella pneumoniae*. *Biochemical Journal*, **1996**, 317 285-290.
3. Sekowska, Agnieszka; Robin, Stephane; Daudin, Jean-Jacques; Henaut, Alain; Danchin, Antoine. Extracting biological information from DNA arrays: an unexpected link between arginine and methionine metabolism in *Bacillus subtilis*. *Genome Biology*, **2001**. 2(6): research0019.1-0019.12.
4. Grundy, Frank J.; Henkin, Tina M. Synthesis of serine, glycine, cysteine, and methionine, p 245-254. In Sonenshein, A.; Losick, R.; Hoch, J (ed). *Bacillus subtilis and its closest relatives*, **2002**. ASM Press, Washington, DC. doi: 10.1128/9781555817992.ch18
5. Murphy, Brooke A.; Grundy, Frank J.; Henkin, Tina M. Prediction of gene function in methylthioadenosine recycling from regulatory signals. *Journal of Bacteriology*, **2002**. 2314-2318.
6. Riscoe, Michael K.; Ferro, Adolph J. 5-Methylthioribose its effects and function in mammalian cells. *Journal of Biological Chemistry*, **1984**. 259, 5465-5471.
7. Lee, Jeffrey E.; Smith, G. David; Horvatin, Cathy; Huang, David J.T.; Cornell, Kenneth A.; Riscoe, Michael K.; Howell, P. Lynne. Structural snapshots of MTA/AdoHcy nucleosidase along the reaction coordinate provide insights into enzyme and nucleosidase flexibility during catalysis. *Journal of Molecular Biology*, **2005**. 352; 559-574.
8. Waduwara-Jayabahu, Ishari; Oppermann, Yasmin; Wirtz, Markus; Hull, Zachary T.; Schoor, Sarah; Plotnikov, Alexander N.; Hell, Rudiger; Sauter, Margret; Moffatt, Barbara

A. Recycling of methylthioadenosine is essential for Normal vascular development and reproduction in *Arabidopsis*. *Plant Physiology*, **2012**. 158, 1728-1744.

9. Shapiro, Stanley K.; Almenas, Aldona; Thomson, John F. Biosynthesis of methionine in *Saccharomyces cerevisiae*. *Journal of Biological Chemistry*, **1965**. 240, 2512-2518.

10. Gianotti, Alan J.; Tower, Paula A.; Sheley, John H.; Conte, Paul A.; Spiro, Craig; Ferro, Adolph J.; Fitchen, John H.; Riscoe, Michael K. Selective Killing of *Klebsiella pneumoniae* by 5-Trifluoromethylthioribose: chemotherapeutic exploitation of the enzyme 5-methylthioribose kinase. *Journal of Biological Chemistry*, **1990**. 265, 831-837.

11. Kushad, M.M.; Orvos, A.; Ferro, Adolph. 5'-Methylthioadenosine nucleosidase and 5-methylthioribose kinase activities in relation to stress-induced ethylene biosynthesis. *Physiologia Plantarum*, **1992**. 86, 532-538.

12. Pfeffer, Morris; Shapiro, Stanley K. Biosynthesis of methionine from S-adenosylmethionine in *Escherichia coli*. *Biochemical and Biophysical Research Communications*, **1962**. 9, 405-409.

13. Shapiro, Stanley K.; Schlenk, Fritz. Conversion of 5-methylthioadenosine into S-adenosylmethionine by yeast cells. *Biochimica et Biophysica Acta*, **1980**. 633, 176-180.

14. Balish, Edward; Shapiro, Stanley K. Methionine biosynthesis in *Escherichia coli*: induction and repression of methylmethionine (or adenosylmethionine): homocysteine methyltransferase. *Archives of Biochemistry and Biophysics*, **1967**. 119, 62-68.

15. Ferro, Adolph J.; Barrett, Annabella; Shapiro, Stanley K. 5-Methylthioribose Kinase: A new enzyme involved in the formation of methionine from 5-methylthioribose. *Journal of Biological Chemistry*, **1978**. 253, 6021-6025.

16. Tower, Paula A.; Alexander, David B.; Johnson, Linda L.; Riscoe, Michael K. Regulation of methylthioribose kinase by methionine in *Klebsiella pneumoniae*. *Journal of General Microbiology*, **1993**. 139, 1027-1031.

17. Sekowska, Agnieszka; Mulard, Laurence; Krogh, Susanne; Tse, Jane KS; Danchin, Antoine. MtnK, methylthioribose kinase, is a starvation-induced protein in *Bacillus subtilis*. *BMC Microbiology*, **2001**. 1:15.

18. Ku, Shao-Yang; Cornell, Kenneth A.; Howell, P. Lynne. Structure of *Arabidopsis thaliana* 5-methylthioribose kinase reveals a more occluded active site than its bacterial homolog. *BMC Structural Biology*, **2007**. 7(1):70. doi:10.1186/1472-6807-7-70

19. Sauter, Margret; Cornell, Kenneth A.; Beszteri, Sara; Rzewuski, Guillaume. Functional analysis of methylthioribose kinase genes in plants. *Plant Physiology*, **2004**. 136, 4061-4071.

20. Ku, Shao-Yang; Yip, Patrick; Cornell, Kenneth A.; Riscoe, Michael K.; Behr, Jean-Bernard; Guillerm, Georges; Howell, P. Lynne. Structures of 5-methylthioribose kinase

reveal substrate specificity and unusual mode of nucleotide binding. *The Journal of Biological Chemistry*, **2007**. 282, 22195-22206.

21. Sekowska, Agnieszka; Kung, Hsiang-Fu; Danchin, Antoine. Sulfur metabolism in *Escherichia coli* and related bacteria: facts and fiction. *Journal of Molecular Microbiology and Biotechnology*, **2000**. 2(2), 145-177.

22. Sauter, Margret; Moffatt, Barbara; Saechao, Maye C.; Hell, Rudiger; Wirtz, Markus. Methionine salvage and S-adenosylmethionine: essential links between sulfur, ethylene, and polyamine biosynthesis. *Biochemical Journal*, **2013**. 451(2), 145-154.

23. Tower, Paula A.; Johnson, Linda L.; Ferro, Adolph J.; Fitchen, John H.; Riscoe, Michael K. Synergistic activity of 5-trifluoromethylthioribose and inhibitors of methionine synthesis against *Klebsiella pneumoniae*. *Antimicrobial Agents and Chemotherapy*, **1991**. 1557-1561.

24. Sekowska, Agnieszka; Danchin, Antoine. The methionine salvage pathway in *Bacillus subtilis*. *BMC Microbiology*, **2002**. 2:8.

25. Riscoe, Michael K.; Ferro, Adolph J.; Fitchen, John H. Analogs of 5-methylthioribose, a novel class of antiprotozoal agents. *Antimicrobial Agents and Chemotherapy*, **1988**. 1904-1906.

26. Albers, Eva. Metabolic characteristics and importance of the universal methionine salvage pathway recycling methionine from 5'-methylthioadenosine. *IUBMB Life*, **2009**. 61(12), 1132-1142.

27. Winter, R.W.; Cornell, Kenneth A.; Johnson, Linda L.; Riscoe, Michael K. Synthesis and testing of substituted phenylthioribose analogs against *Klebsiella pneumoniae*. *Bioorganic & Medicinal Chemistry Letters*, **1993**. 3:10, 2079-2082.

28. Cornell, Kenneth A.; Swarts, William E.; Barry, Ronald D.; Riscoe, Michael K. Characterization of recombinant *Escherichia coli* 5'-Methylthioadenosine/S-adenosylhomocysteine nucleosidase: analysis of enzymatic activity and substrate specificity. *Biochemical and Biophysical Research Communications*, **1996**. 228, 724-732.

29. Ubersax, Jeffrey A.; Ferrell, James E. Jr. Mechanisms of specificity in protein phosphorylation. *Nature Reviews Molecular Cell Biology*, **2007**. 8, 530-541.

30. Cornell, Kenneth A.; Primus, Shekerah; Martinez, Jorge A.; Parveen, Nikhat. Assessment of methylthioadenosine/S-adenosylhomocysteine nucleosidases of *Borrelia burgdorferi* as targets for novel antimicrobials using a novel high-throughput method. *Journal of Antimicrobial Chemotherapy*, **2009**. 63(6), 1163-72.

31. Parveen, Nikhat; Cornell, Kenneth A. Methylthioadenosine/S-adenosylhomocysteine nucleosidase, a critical enzyme for bacterial metabolism. *Molecular Microbiology*, **2012**. 79(1) 7-20.

32. Peisach, Daniel; Gee, Patricia; Kent, Claudia; Xu, Zhaohui. The crystal structure of choline kinase reveals a Eukaryotic protein kinase fold. *Structure*, **2003**. 11(6), 703-713.

33. Sievers, F; et al. Fast, scalable generation of high-quality protein multiple sequence alignments using Clustal Omega. *Molecular Systems Biology*, **2011**. 7:539 doi:10.1038/msb.2011.75

34. Trackman, Philip C.; Abeles, Robert H. Methionine synthesis from 5'-S-methylthioadenosine. *The Journal of Biological Chemistry*, **1983**. 258(11); 6717-6720.

35. Sekowska, Agnieszka; Denervaud, Valerie; Ashida, Hiroki; Michoud, Karine; Haas, Dieter; Yokota, Akiho; Danchin, Antoine. Bacterial variations on the methionine salvage pathway. *BMC Microbiology*, **2004**. 4;9.

36. Rolfes, Ronda J.; Zalkin, Howard. Purification of the *Escherichia coli* purine regulon repressor and identification of corepressors. *Journal of Bacteriology*, **1990**. 172(10); 5637-5642.

37. Augustus, Anne M.; Sage, Harvey; Spider, Leonard D. Binding of MetJ repressor to specific and non-specific DNA and the effects of SAM on these interactions. *Biochemistry*, **2010**. 29(15); 3289-3295.

38. Lorenz, Eva; Stauffer, George V. Characterization of the MetR binding sites for the glyA gene of *Escherichia coli*. *Journal of Bacteriology*, **1995**. 177(14); 4113-4120.

39. Oruganty, Krishnadev; Talevich, Eric E.; Neuwald, Andrew F.; Kannan, Nataraj. Identification and classification of small molecule kinases: insights into substrate recognition and specificity. *BMC Evolutionary Biology*, **2016**. 16:7.

40. Schrodinger Release 2015-4: Prime, version 4.2, Schrodinger, LLC, New York, NY, **2015**.

41. Small-Molecule Drug Discovery Suite 2015-4: Glide, version 6.9, Schrodinger, LLC, New York, NY, **2015**.

42. The PyMOL Molecular Graphics System, Version 1.8 Schrodinger, LLC.

43. Cleland, William W. The kinetics of enzyme-catalyzed reactions with two or more substrates or products: I. Nomenclature and rate equations. *Biochimica et Biophysica Acta*, **1963**. 67; 104-137.

44. Ku, Shao-Yang; Yip, Patrick; Cornell, Kenneth A.; Riscoe, Michael K.; Howell, P. Lynne. Crystallization and preliminary X-ray analysis of 5'-methylthioribose kinase from *Bacillus subtilis* and *Arabidopsis thaliana*. *Acta Crystallographica*, **2004**. 60(1); 116-119.

CHAPTER 3: PAPER #2 – DRUG INHIBITION of *Klebsiella pneumoniae* 5'-METHYLTHIOADENOSINE/S-ADENOSYLHOMOCYSTEINE NUCLEOSIDASE

Abstract

5'-Methylthioadenosine/S-adenosylhomocysteine nucleosidase (MTN) is an enzyme responsible for catabolism of the three downstream products of S-adenosylmethionine dependent reactions important for cellular fitness and proliferation. Here we present a kinetic examination of purified, recombinant MTN from the Gram-negative pathogen *Klebsiella pneumoniae.* For the three MTN substrates of 5'-methylthioadenosine, S-adenosylhomocysteine, and 5'-deoxyadenosine, we have established K_m values of 5.8 ± 0.8, 4.7 ± 0.2 and 7.0 ± 0.4 μM, and specific activities of 15.4, 5.9, and 11.3 μmol/min/mg, respectively. The enzyme inhibitory activities were determined for four previously described transition-state analogs and four novel non-nucleoside small molecules inhibitors. Transition-state inhibitors consistently possessed inhibition constants in the high picomolar range, and the small molecule inhibitor K_i values were grouped in the low micromolar range.

Introduction

S-adenosylmethionine (SAM) is a molecule with a central role in a broad array of metabolic processes. Created by the addition of methionine to ATP, SAM is utilized in a multitude of disparate pathways in *K. pneumoniae*. Predominantly, SAM is utilized as the most common methyl group donor for the transmethylation of biomolecules such as DNA, tRNA, proteins, carbohydrates, lipids, etc. [5]. In addition, SAM is the precursor

for the synthesis of polyamines, the production of quorum-sensing autoinducer molecules, and a substrate for radical-SAM enzymes responsible for the synthesis of vitamins and cofactors such as pyrroquinoline quinone (Figure 3.1) [24][23]. The MTN enzyme serves to deadenylate the three unique products of SAM metabolism, 5'-methylthioadenosine (MTA), S-adenosylhomocysteine (SAH), and 5'-deoxyadenosine (5'dADO). These three nucleosides all function as potent product inhibitors for their respective enzymes [5] and the buildup of MTA is known to be toxic at high physiological concentrations [20]. The products of MTN reactions, 5-methylthioribose (MTR) and S-ribosylhomocysteine (SRH), are recycled to methionine by subsequent enzyme reactions, while the fate 5-deoxyribose (5-dRIB) is still unknown.

A role for MTN in microbial virulence has been proposed in *Staphylococcus aureus* where MTN gene knock-out strains failed to cause infectious mortality in mice [3]. MTN gene knock-outs in pathogenic *E. coli* O157:H7 also demonstrated reduced growth rates, cellular adhesion, biofilm formation, and Shiga toxin production [20]. These effects were reversible by vitamin supplementation, suggesting that loss of MTN led to 5'dADO accumulation and behavioral changes due to product inhibition of SAM-dependent reactions involved in vitamin synthesis.

As antibiotic resistance becomes increasingly widespread, the need for novel treatments becomes increasingly urgent. This is of particular concern regarding the bacterial species *Klebsiella pneumoniae*, which is notorious for the frequency and expansiveness of its antibiotic resistance profile. This organism is the most common among the carbapenem-resistant Enterobactericeae, and clinical isolates typically bear

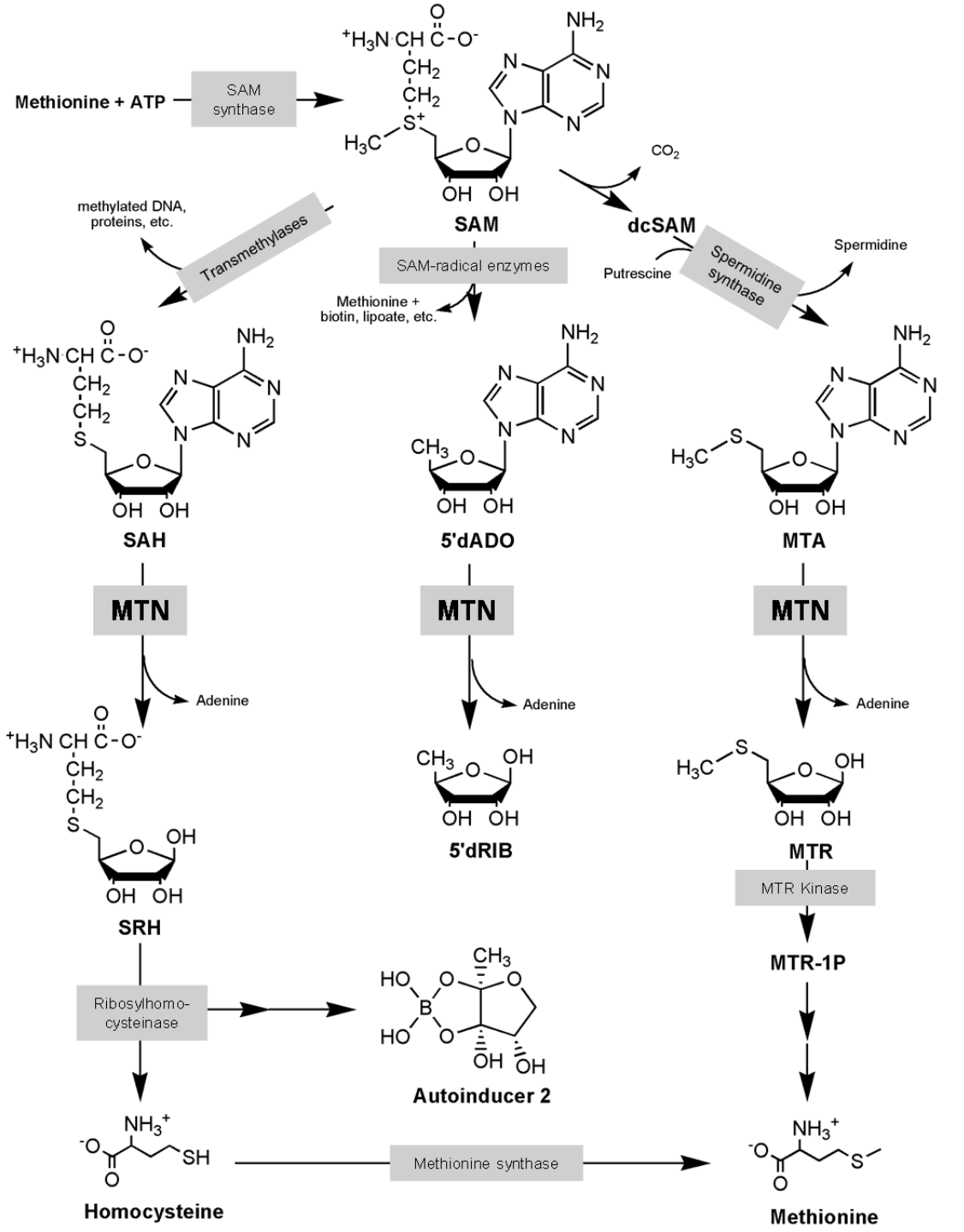

Figure 3.1. Central role of MTN in catabolism of the products of SAM-dependent reactions. MTN catabolizes three distinct products of SAM metabolism. All three substrates are product inhibitors of their formative transmethylation, SAM-radical, and polyamine syntheses.

multiple resistances [6][27]. The conserved utilization of MTN in many pathogenic bacteria and numerous protozoan parasites and its absence in mammals provides an opportunity for the development of a novel broad spectrum antimicrobial agents [5].

To date, investigations into inhibitors targeting MTN have yielded mixed results. Some bacterial species (*H. pylori, B. burgdorferi*) appear to be highly sensitive to MTN inhibitors [27][15]. Other organisms (*E. coli, S. aureus, V. cholera*) have their growth unaffected by inhibitors, but display reductions in autoinducer-2 secretion and biofilm formation [3][8][12]. Research on MTN inhibitors has largely focused on MTA analogs, and early and late-stage transition state analogs (TSAs) [28][12][13]. Both types of inhibitors exhibit strong binding towards *E. coli* MTN, with the late-stage transition state analogs in particular displaying among the tightest known non-covalent binding properties observed in biological systems, with some K_i values against *E. coli* MTN being placed in the low femtomolar range [12].

The *K. pneumoniae* and *E. coli* MTN amino acid sequences show a greater than 90% identity and complete conservation of catalytic residues (Figure 3.2). Despite this, previous reports have shown that the native *K. pneumoniae* MTN displayed a K_m for the MTA substrate that was more than 20-fold greater than that of the *E. coli* enzyme

```
E.coli            MKIGIIGAMEEEVTLLRDKIENRQTISLGGCEIYTGQLNGTEVALLKSGIGKVAAALGAT    60
K.pneumoniae      MKIGIIGAMEEEVTLLRDKIENRQTITIGGSEIYTGQLHGVDVALLKSGIGKVAAAMGAT    60

E.coli            LLLEHCKPDVIINTGSAGGLAPTLKVGDIVVSDEARYHDADVTAFGYEYGQLPGCPAGFK    120
K.pneumoniae      LLLERCQPDVIINTGSAGGLASTLKVGDIVVSDEARYHDADVTAFGYEYGQLPGCPAGFK    120

E.coli            ADDKLIAAAEACIAELNLNAVRGLIVSGDAFINGSVGLAKIRHNFPQAIAVEMEATAIAH    180
K.pneumoniae      ADEKLVAAAESCIKALDLNAVRGLIVSGDAFINGSVGLAKIRHNFPQAIAVEMEATAIAH    180

E.coli            VCHNFNVPFVVVRAISDVADQQSHLSFDEFLAVAAKQSSLMVESLVQKLAHG            232
K.pneumoniae      VCHNFKVPFVVVRAISDVADQQSHLSFEEFLAVAARQSTLMVENLVQNLARG            232
```

Figure 3.2. ClustalOmega alignment of *E. coli* and *K. pneumoniae* MTN sequences. The two sequences show an identity greater than 90%, with residues critical for substrate binding and catalysis strictly conserved and highlighted [21].

[17][22]. This apparent diversity of substrate recognition and catalysis poses a potential challenge for subsequent inhibitor development. In order to improve our understanding of the *K. pneumonia* MTN, we have cloned the MTN gene and characterized the specific activity and substrate kinetics of the recombinant enzyme. Finally, a series of MTN transition-state analogs and small molecule inhibitors were tested for enzyme inhibition to provide a framework for future drug design.

Materials and Methods

Chemicals and substrates: The transition state analogs **MTD** – (3R, 4S)-1-[(9-deazaadenin-9-yl)methyl]-3-hydroxy-4-(methylthiomethyl)pyrrolidine; **BTD** – (3R,4S)-4-(butylthiomethyl)-1-[(9-deazaadenin-9-yl)methyl]-3-hydroxypyrrolidine; **BCX** – (1S)-1-(9-deazaadenin-9-yl)-1,4-dideoxy-1,4-imino-5-methylthio-D-ribitol; **BCZ** - (1S)-1-(9-deazaadenin-9-yl)-1,4-dideoxy-1,4-imino-5-propyl-D-ribitol were kindly provided by Dr. Vern Schramm (Albert Einstein Medical College, Bronx, NY). The non-nucleoside small molecule inhibitors **5A** - (N-(2-furylmethyl)-N'-(4-nitrophenyl)urea); **8A** - 1-(4-nitrophenyl)-3-[4-[4[(4-nitrophenyl) carbamoylamimino] phenoxy]phenyl]-urea; **15A** - 2-[2-(5,6-dimethyl-1H-benzoimidazol-2-yl)vinyl]-5,6-dimethyl-1H-benzoimidazole; **27A** - 3-(1,3-benzothiazol-2-yl)-1-(5-{[(1,3-benzothiazol-2-yl)carbamoyl]amino}-2-methylphenyl)urea were obtained from the National Cancer Institute Developmental Therapeutics Program.

Identification of non-nucleoside inhibitors: The small molecule inhibitors tested here were identified based on the results of *in silico* screening of the NCI Diversity Set II small molecule library against the *E. coli* MTN structure performed by Dr. Danny Xu (Idaho State University, School of Pharmacy) and an enzyme analysis of the top thirty-

three compounds (unpublished results). The four most potent inhibitors against *E. coli* MTN (designated 5A, 8A, 15A, and 27A) were selected for assessment against *K. pneumoniae* MTN.

MTN plasmid creation and cell transformation: The MTN gene was amplified from *Klebsiella pneumoniae* (ATCC strain 43816) by whole-cell PCR using the primer pair KPMTNF (5'–ATGAAAATTGGCATTATTGGCG-3') and KPMTNR (5'–GCCACGTGCCAGGTTCTGTACC- 3'). The 696 base pair product was ligated into the C-terminal poly-His-encoding pTrcHis-TOPO plasmid (Invitrogen) according to manufacturer's instructions before being transformed into chemically competent *E. coli* One Shot™ TOP10 cells (Invitrogen) and purified using the GeneJET Plasmid Miniprep Kit (ThermoFisher). The purified plasmid was transformed into chemically competent *E. coli* OneShot™ BL21 (DE3) cells (Invitrogen). The insertion orientation was confirmed by PCR using the KPMTNF primer and a pTrcHis-TOPO manufacturer-provided external reverse primer. The plasmid sequence with the gene insertion was confirmed by sequencing services provided by GeneWIZ, Inc.

Protein expression and purification: Transformed BL21 cells were grown in 500mL LB broth at 30°C to an OD_{600} of 0.5, and induced with 0.5mM IPTG overnight. Cells were harvested by centrifugation (5000 x g, 15 min), and the pellets were washed once with PBS. The washed cell pellet was homogenized in 3mL B-PER® (ThermoFisher) reagent for 15 minutes at room temperature. Cell debris was removed by centrifugation (10000 x g, 25 min). The recombinant *Klebsiella* MTN was purified from the clarified supernatant using 3mL cobalt HisPur™ resin (ThermoFisher) according to manufacturer's instructions. Briefly, the recombinant enzyme was bound to the column

by an overnight incubation at 4ºC. Unbound material was removed by centrifugation at 700 x g for two minutes. The column was washed three times with 3mL wash buffer (10mM imidazole, 50mM $NaPO_4$, 300mM NaCl, pH= 7.4), and the recombinant protein eluted with three 1.5mL volumes of elution buffer (250mM imidazole, 50mM $NaPO_4$, 300mM NaCl, pH= 7.4). Protein quantity was assessed by Bio-Rad protein assay performed with a bovine serum albumin standard, and the purity was confirmed by SDS-PAGE using PageRuler Plus Prestained Protein Standard (ThermoFisher) and stained with Coomassie Blue. The concentration of pure enzyme was adjusted to 70 μg/mL in 20% glycerol, and stored at -80ºC before use in spectrophotometric enzyme assays.

Enzyme activity and kinetics: Nucleosidase assays were performed as previously described [12]. Briefly, 1mL reactions contained 100mM sodium phosphate buffer (pH 6.5), and 1-50 μM substrate (MTA, SAH, or 5'dADO) at 25°C. Reactions were initiated by the addition of 0.7 μg of enzyme. Reaction velocities were monitored at 275nm using a Varian Cary-50 spectrophotometer (ε_{275} = 1.60 $mM^{-1}cm^{-1}$) and the data was fit to the Michaelis-Menten equation with GraphPad Prism 6.0 software:

$$v_o = v_{max}[S]/(K_m + [S]) \qquad \text{Eqn. 1}$$

Inhibition assays: For assessment of TSA inhibition, reaction conditions were performed as with kinetics assays. Transition-state analog inhibition was measured at 2-500 nM in the presence of 50 μM MTA and fit to the modified equation for competitive inhibition as previously described [12].

$$v_o'/v_o = (K_m + [S])/[(K_m + [S]) + (K_m[I]/K_i)] \qquad \text{Eqn. 2}$$

For analysis of non-nucleoside small molecule inhibitors, concentrations of 0.1-10 μM were used. MTA substrate concentrations were varied between 5-50 μM. Data

was fit to the equations for competitive inhibition, noncompetitive inhibition, and mixed inhibition using GraphPad Prism 6.0 software. Data from all four small molecules (5A, 8A, 15A, 27A) fit best to the competitive inhibition model. Subsequently, the small molecule inhibitors were tested as described for the transition state analogs and the data fit to the modified equation for competitive inhibition (Eqn. 2).

Results and Discussion

Enzyme purification – SDS-PAGE analysis of the purified, recombinant MTN (with C-terminal poly-His purification sequence) showed a >95% purity and an apparent molecular weight of 30 kD (Figure 3.3). This is in close agreement with the ProtParam [29] calculated molecular weight of 29.7 kD, based on the amino acid sequence and prior reports for the 26.5 kD native enzyme [17].

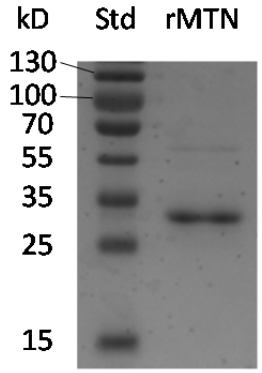

Figure 3.3. SDS-PAGE gel of recombinant *K. pneumoniae* MTN. Lane 1: Protein molecular weight standard. Lane 2: 2µg recombinant MTN. The estimated molecular weight for purified rMTN is 30 kD.

Substrate kinetics – All three substrates demonstrated typical Michaelis-Menten kinetics (Figure 3.4).

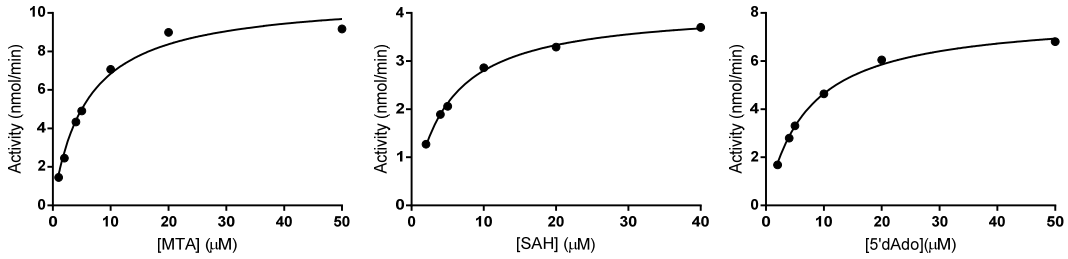

Figure 3.4. Substrate velocity plots. Data is shown for the substrates 5'-methylthioadenosine (left), S-adenosylhomocysteine (middle), and 5'-deoxyadenosine (right). All data was fit to Michaelis-Menten equation using GraphPad Prism 6.0 software.

Enzyme activity and kinetic constants for each native substrate are summarized in Table 3.1. Specific activities for the three substrates (measured at 50 μM) ranged from 5.3 to 13.8 μmol/min per mg of enzyme. MTA was the most efficiently catalyzed substrate, consistent with previous reports for numerous other bacterial enzymes [22][15][8][25]. The K_m values for MTA and SAH (5.8 and 4.7 μM, respectively) are in good agreement with previously reported values of 8.1 μM and 4.3 μM for native *K. pneumoniae* MTN purified from cellular extracts [17]. The K_m for 5'dADO was 7 μM. This is the first reported kinetic study for this substrate. MTN demonstrated the highest catalytic rate (460 min^{-1}) and efficiency (79 $\mu M^{-1}min^{-1}$) for MTA. The catalytic efficiencies for SAH and 5'dADO substrates were approximately half the values obtained for MTA.

Table 3.1. Summary of MTN Kinetic Constants

	Specific Activity (μmol/min/mg)	K_m (μM)	v_{max} (nmol/min)	k_{cat} (min^{-1})	k_{cat}/K_m ($\mu M^{-1}min^{-1}$)
MTA	13.8	5.8 ± 0.8	10.8	460 ± 20	79
SAH	5.3	4.7 ± 0.2	4.1	174 ± 3	37
5'dADO	9.8	7.0 ± 0.4	7.1	335 ± 7	48

The *K. pneumoniae* MTN substrate specific activities for MTA and SAH are approximately 30-fold lower than the corresponding specific activities reported for the *E. coli* enzyme (373 and 156 μmol/min per mg of enzyme, respectively) [22]. In addition, *K. pneumoniae* MTN displays a fourteen-fold increase in K_m for MTA relative to the *E. coli* enzyme (5.8μM vs. 0.4 μM), while the K_m for SAH is highly similar for the two enzymes (4.7μM to 4.3μM for *E. coli*) [22]. As *K. pneumoniae* possesses a complete enzyme pathway to recycle methionine from MTR while *E. coli* does not, the increased activity of the *E. coli* enzyme most likely represents an evolutionary adaptation in order to help maintain low intracellular concentrations of toxic MTA.

Inhibition values – Four transition-state analogs and four competitive inhibitors identified by *in silico* screening were tested against *K. pneumoniae* MTN. Fits of the inhibition data to the equation for competitive inhibition are provided in Appendix A. As previously described, the TSA molecules all show discrete early and late-onset inhibition profiles resulting from a latent conformational transition of the enzyme-inhibitor complex [12]. Representative graphs for the late-transition state analog MT-DADMe ImmA (MTD) are shown in Figure 3.5.

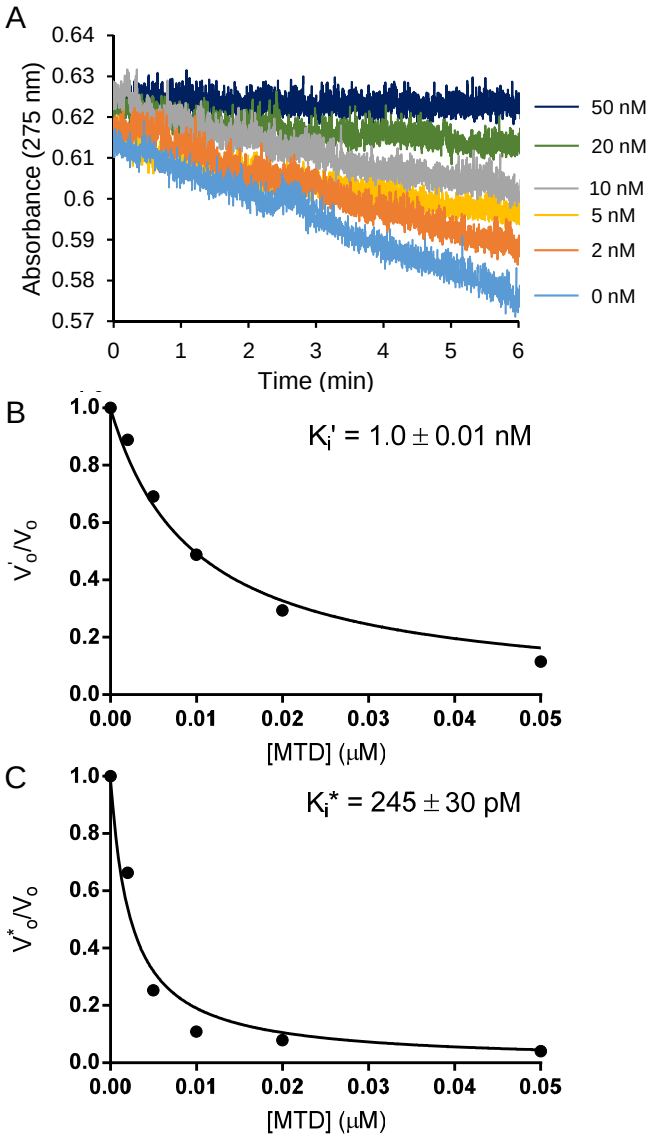

Figure 3.5. Inhibition of MTN activity by MTD. A) Kinetic activity profiles **B)** Early-onset inhibition graph C) Late-onset inhibition graph. Data was fit to the modified equation for competitive inhibition (Eqn. 2) [12].

As expected, TSAs showed binding interactions with the enzyme that were 3-4 orders of magnitude stronger than for than the non-nucleoside inhibitors (Figure 3.6).

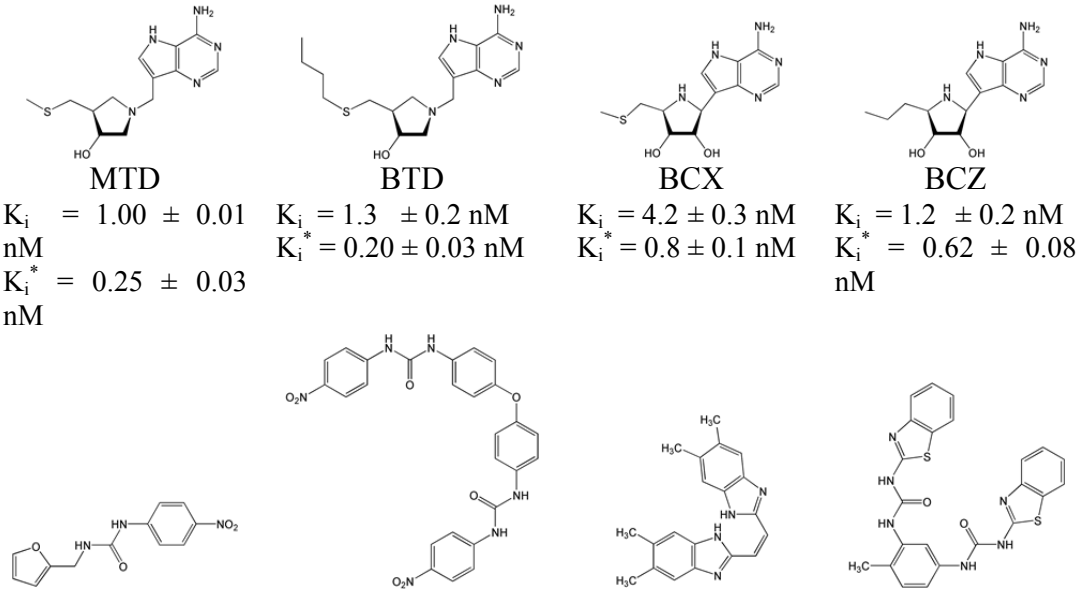

Figure 3.6. Summary of inhibition constants. Late-stage transition-state analogs are represented by MTD and BTD, and early-stage by BCX and BCZ. The four novel small molecule inhibitors are shown in the second row. All transition-state analogs demonstrated discrete early and late-onset inhibition profiles with picomolar to

Relative binding affinities of the inhibitors towards *K. pneumoniae* and *E. coli* enzymes reflected the observed discrepancies between MTA substrate activities. In general, the *E. coli* enzyme shows inhibition constants for the TSAs within the femtomolar to picomolar range in contrast to the inhibition constants for the *Klebsiella* MTN that are reported here. For the early stage (BCX, BCZ) and late stage (MTD, BTD) TSAs, the K_i values were 10-fold, and 125 to 675-fold higher, respectively, than the values determined against the *E. coli* enzyme [12]. Binding affinities of the four non-nucleoside inhibitors were also lower than the 20-600 nM K_i values observed against *E. coli* MTN (unpublished data).

Previously, Gutierrez, et al. compared the K_i values of BCX and MTD to classify MTN mediated catalysis according to early dissociative or late dissociative transition

state models [19]. High fold increases (>40) in binding affinity for the late-stage TSA MTD relative to the early-stage TSA BCX indicated a late dissociated transition state. Interestingly, the disparity in *K. pneumoniae* MTN affinities between early-stage and late-stage TSAs were less dramatic than previously reported [19]. Our studies show only a 3.4-fold improved affinity for MTD relative to BCX. This is largely due to a lower observed K_i value for BCX (0.84 nM) compared to the 45nM reported in the initial study [19]. Our data suggests that the *K. pneumoniae* MTN adheres more closely to an early dissociative transition state model that is more similar to *N. meningitides* and *H. pylori* MTNs than to the more evolutionarily related *E. coli* enzyme.

Conclusion

Klebsiella pneumoniae MTN possesses a highly similar sequence identity to that of *E. coli*, but demonstrates a 14-fold higher K_m value for MTA and a 30-fold reduction in specific activity relative to what is reported for the *E. coli* enzyme. Likewise, both transition-state analogs and non-nucleoside small molecule inhibitors were found to have lesser capacities for enzymatic inhibition. This highlights an unexpected degree of variability in activity among highly homologous enzymes, which could influence the direction of future drug design to exploit the differences between species. We also report the identification of a new set of non-nucleoside inhibitors of MTN, which will serve as a starting point for our goal to develop MTN inhibitors that will circumvent the inconsistent effects on cellular behavior observed for the otherwise potent transition state analog inhibitors.

Bibliography

1. Kim, Youngbae; Lew, Chih M.; Gralla, Jay D. *Escherichia coli* pfs transcription: regulation and proposed roles in autoinducer-2 synthesis and purine excretion. *Journal of Bacteriology*, **2006**. 7457-7463.

2. Silva, Anisia J.; Parker, William B.; Allan, Paula W.; Ayala, Julio C.; Benitez, Jorge A. Role of methylthioadenosine/ S-adenosylhomocysteine nucleosidase in *Vibrio cholera* cellular communication and biofilm development. *Biochemical and Biophysical Research Communications*, **2015**. 461; 65-69.

3. Bao, Yan; Li, Yajuan; Jiang, Qiu; Zhao, Liping; Xue, Ting; Hu, Bing; Sun, Baolin. Methylthioadenosine/S-adenosylhomocysteine nucleosidase (pfs) of *Staphylococcus aureus* is essential for the virulence independent of LuxS-AI-2 system. *International Journal of Medical Microbiology*, **2013**. 303; 190-200.

4. Wang, Shanzhi; Thomas, Keisha; Schramm, Vern L. Catalytic site cooperativity in dimeric methylthioadenosine nucleosidase. *Biochemistry*, **2014**. 53; 1527-1535.

5. Parveen, Nikhat; Cornell, Kenneth A. Methylthioadenosine/S-adenosylhomocysteine nucleosidase, a critical enzyme for bacterial metabolism. *Molecular Microbiology*, **2011**. 79(1); 7-20.

6. Rasheed, J. Kamile; Kitchel, Brandon; Zhu, Wenming; Anderson, Karen F.; Clark, Nancye C.; Ferraro, Mary Jane; Savard, Patrice; Humphries, Romney M.; Kallen, Alexander J.; Limbago, Brandi M. New Delhi metallo-β-lactamase-producing *Enterobacteriaceae*, United States. *Emerging Infectious Diseases*, **2013**. 19(6).

7. Kim, Robbert Q.; Offen, Wendy A.; Davies, Gideon J.; Stubbs, Keith A. Structural enzymology of *Helicobacter pylori* methylthioadenosine nucleosidase in the futalosine pathway. *Acta Crystalographica*, **2014**. D70; 177-185.

8. Gutierrez, Jemy A.; Crowder, Tamara; Rinaldo-Matthis, Agnes; Ho, Meng-Chiao; Almo, Steven C.; Schramm, Vern L. Transition state analogues of 5'-methylthioadenosine nucleosidase disrupt quorum sensing. *Nature Chemical Biology*, **2009**. 5(4); 251-257.

9. Gao, Qiang; Zheng, Dasheng; Yuan, Zhiming. Substrate preference of 5'-methylthioadenosine/S-adenosylhomocysteine nucleosidase in *Burkholderia thialandensis*. *FEMS Microbiology Letters*, **2013**. 339; 110-116.

10. Li, Xu; Apel, Dmitry; Gaynor, Erin C.; Tanner, Martin E. 5'-Methylthioadenosine nucleosidase is implicated in playing a key role in a modified futalosine pathway for menaquinone biosynthesis in *Campylobacter jejuni*. *Journal of Biological Chemistry*, **2011**. 286; 19392-19398.

11. Balestrino, Damien; Haagensen, Janus A.J.; Rich, Chantal; Forestier, Christiane. Characterization of Type 2 quorum sensing in *Klebsiella pneumoniae* and relationship with biofilm formation. *Journal of Bacteriology*, **2005**. 187(8); 2870-2880.

12. Singh, Vipender; Evans, Gary B.; Lenz, Dirk H.; Mason, Jennifer M.; Clinch, Keith; Mee, Simon; Painter, Gavin F.; Tyler, Peter C.; Furneaux, Richard H.; Lee, Jeffrey E.; Howell, P. Lynne; Schramm, Vern L. Femtomolar transition state analogue inhibitors of 5'-methylthioadenosine/S-adenosylhomocysteine nucleosidase from *Escherichia coli*. *Journal of Biological Chemistry*, **2005**. 280(18); 18265-18273.

13. Tedder, Martina E.; Nie, Zhe; Margosiak, Stephen; Chu, Shaosong; Feher, Victoria A.; Almassy, Robert; Appelt, Krzysztof; Yager, Kraig M. Structure-based design, synthesis, and antimicrobial activity of purine derived SAH/MTA nucleosidase inhibitors. *Bioorganic & Medicinal Chemistry Letters*, **2004**. 14; 3165-3168.

14. Wang, Shangzhi; Lim, Jihyeon; Thomas, Keisha; Yan, Funing; Angeletti, Ruth H.; Schramm, Vern L. Complex of methylthioadenosine/S-adenosylhomocysteine nucleosidase, transition state analogue, and nucleophilic water identified by mass spectrometry. *Journal of the American Chemical Society*, **2012**. 134; 1468-1470.

15. Cornell, Kenneth A.; Primus, Shekerah; Martinez, Jorge A.; Parveen, Nikhat. Assessment of methylthioadenosine/S-adenosylhomocysteine nucleosidases of *Borrelia burgdorferi* as targets for novel antimicrobials using a novel high-throughput method. *Journal of Antimicrobial Chemotherapy*, **2009**. 63; 1163-1172.

16. Heurlier, Karin; Vendeville, Agnes; Halliday, Nigel; Green, Andrew; Winzer, Klaus; Tang, Christoph M.; Hardie, Kim R. Growth deficiencies of *Neisseria meningitidis* pfs and luxS mutants are not due to inactivation of quorum sensing. *Journal of Bacteriology*, **2009**. 191(4) 1293-1392.

17. Cornell, Kenneth A.; Winter, R.W.; Tower, Paula A.; Riscoe, Michael K. Affinity purification of 5-methylthioribose kinase and 5'-methylthioadenosine/S-adenosylhomocysteine nucleosidase from *Klebsiella pneumoniae*. *Biochemical Journal*, **1996**. 317(1); 285-290.

18. Schlenk, Fritz. Methylthioadenosine. *Advances in Enzymology and Related Areas of Molecular Biology*, **1983**. 54; 195-265.

19. Gutierrez, Jemy A.; Luo, Minkui; Singh, Vipender; Li, Lei; Brown, Rosemary L.; Norris, Gillian E.; Evans, Gary B.; Furneaux, Richard H.; Tyler, Peter C.; Painter, Gavin F.; Lenz, Dirk H.; Schramm, Vern L. Picomolar inhibitors as transition-state probes of 5'-methylthioadenosine Nucleosidases. *ACS Chemical Biology*, **2007**. 2(11); 725-734.

20. Knippel, Reece. Effects of MTN enzyme deficiency on *E. coli* O157:H7 growth and virulence (Masters thesis). (**2013**).

21. Lee, Jeffrey E.; Cornell, Kenneth A.; Riscoe, Michael K.; Howell, P. Lynne. Structure of *E. coli* 5'-methylthioadenosine/S-adenosylhomocysteine nucleosidase reveals similarity to the purine nucleoside phosphorylases. *Structure*, **2001**. 9(10); 941-953.

22. Della Ragione, Fulvio; Porcelli, Marina; Carteni-Farina, Maria; Zappia, Vincenzo. *Escherichia coli* S-adenosylhomocysteine/5'-methylthioadenosine nucleosidase. *The Biochemical Journal*, **1985**. 232; 335-341.

23. Wecksler, Stephen R.; Stoll, Stefan; Iavarone, Anthony T.; Imsand, Erin M.; Tran, Ha; Britt, R. David; Klinman, Judith P. Interaction of PqqE and PqqD in the pyrroloquinoline quinone (PQQ) biosynthetic pathway links PqqD to the radical SAM superfamily. *Chemical Communications*, **2010**. 46; 7031-7033.

24. Sekowska, Agnieszka; Kung, Hsiang-Fu; Danchin, Antoine. Sulfur metabolism in *Escherichia coli* and related bacteria: facts and fiction. *Journal of Molecular and Microbiological Biotechnology*, **2000**. 2(2); 145-177.

25. Singh, Vipender; Shi, Wuxian; Almo, Steven C.; Evans, Gary B.; Furneaux, Richard H.; Tyler, Peter C.; Zheng, Renjian; Schramm, Vern L. Structure and inhibition of a quorum sensing target from *Streptococcus pneumoniae*. *Biochemistry*, **2006**. 45(43); 12929-12941.

26. Nordmann, Patrice; Cuzon, Gaelle; Naas, Thierry. The real threat of *Klebsiella pneumoniae* carbapenemase-producing bacteria. *The Lancet Infectious Diseases*, **2009**. 9(4); 228-236.

27. Wang, Shanzhi; Cameron, Scott A.; Clinch, Keith; Evans, Gary B.; Wu, Zhimeng; Schramm, Vern L.; Tyler, Peter C. New antibiotic candidates against *Helicobacter pylori*. *Journal of the American Chemical Society*, **2015**. 137(45); 14275-14280.

28. Li, Xiaoming; Chu, Sam; Feher, Victoria A.; Khalili, Mitra; Nie, Zhe; Margosiak, Stephen; Nikulin, Victor; Levin, James; Sprankle, Kelly G.; Tedder, Martina E.;. Almassy, Robert; Appelt, Krzysztof; Yager, Kraig M. Structure-based design, synthesis, and antimicrobial activity of indazole-derived SAH/MTA nucleosidase inhibitors. *Journal of Medicinal Chemistry*, **2003**. 46(26); 5663-5673.

29. Gasteiger, E.; Hoogland, C.; Gattiker, A.; Duvaud, S.; Wilkins, M.R.; Appel, R.D.; Bairoch, A. Protein identification and analysis tools on the ExPASy server. John M. Walker (ed): The Proteomics Protocols Handbook, Humana Press (2005). Pp. 571-607.

CHAPTER 4: PAPER #3 – INFLUENCE OF MTA/SAH NUCLEOSIDASE ACTIVITY ON BACTERIAL GROWTH AND VIRULENCE FACTOR GENE EXPRESSION

Abstract

The enzyme 5'methylthioadenosine/S-adenosylhomocysteine nucleosidase (MTN) is widely utilized among bacterial species and is involved in a diverse set of metabolic pathways. Investigations of drugs targeting this enzyme have identified strong enzymatic inhibitors that have shown disproportionately weak effects when used as therapeutics against most bacterial organisms. We present here an examination of the effects of transition state analog and novel non-nucleoside MTN inhibitors against the pathogenic bacteria *Klebsiella pneumoniae*. These inhibitors showed pleiotropic effects on cell growth, with members of both inhibitors types capable of inducing either growth deficiencies or enhanced growth rates. Neither of the two classes of MTN inhibitors were able to cause significant alterations in biofilm formation. Lysates of cells treated with TSA inhibitors had no observed alterations in MTN activity, but appear to display an increase in intracellular MTN concentration. *K. pneumoniae* treated with a TSA inhibitor showed upregulation of two siderophore genes and downregulation of a matrix binding protein. A supplemental examination of gene expression in an MTN gene knock-out in enteropathogenic *E. coli* O157:H7 showed significantly decreased expression in both Shiga-like toxins, hemolysin, and a component of type 3 secretory system relative to the wildtype strain. The results of these studies suggest antibiotics targeting MTN are

capable of producing effects on cellular proliferation and the expression of different virulence-associated genes in *Klebsiella*.

Introduction

Klebsiella pneumoniae is Gram-negative bacterium best known for its role as a nosocomial pathogen. *K. pneumoniae* is currently recognized as one of the eight most severe hospital-associated infectious agents [1]. As a pathogen, *K. pneumoniae* is notable for the breadth of antibiotic resistance genes found in clinically isolated strains. *K. pneumoniae* is the most common Carbapenem-resistant *Enterobactericeae* (CRE), and was the origin for both *Klebsiella pneumoniae* carbapenemase (KPC) and New-Delhi metallo-β-lactamase resistance genes [2][3]. Infectious strains of this organism typically carry multiple extended-spectrum β-lactamases and carbapenemases, providing a significant challenge for effective treatment [4]. This combination of drug resistances has resulted in outbreaks with mortality rates that exceed 50% [5].

The 5'methylthioadenosine/S-adenosylhomocysteine nucleosidase (MTN) enzyme is responsible for the hydrolytic breakdown of three distinct products of SAM-dependent metabolic pathways in many bacterial species. These substrates are: 5'-methylthioadenosine (MTA), S-adenosylhomocysteine (SAH), and 5'deoxyadenosine (5'dADO). Apart from the degradation of the toxic molecules MTA and SAH [6], MTN is additionally involved in the production of multiple metabolites important for cellular fitness. Metabolic processes expected to be impacted by the disruption of MTN activity include: methylations, polyamine synthesis, autoinducer production, purine and methionine salvage, and the synthesis of vitamins used in central carbon metabolism [7].

Transition state analog inhibitors of the MTN enzyme have displayed binding properties that are among the strongest non-covalent interactions observed in biological systems [8]. These inhibitors have shown potent bactericidal activity against the purine auxotrophs *Helicobacter pylori* and *Borrelia burgdorferi* [9][10]. However, applications of TSA inhibitors against *E. coli* and *V. cholerae* did not impact growth, and instead caused reductions in biofilms and autoinducer-2 production [11]. MTN gene knock-outs performed in *Staphyloccocus aureus, Neisseria miningitidis,* and *Escherichia coli* O157:H7 have implicated the enzyme to be involved more strongly with virulence-associated behavior than with cellular growth and fitness [12][13][14].

Materials and Methods

Strains and growth conditions – *K. pneumoniae* (ATCC strain 43816) was grown in minimal media [15] modified to substitute chloride salts for sulfates. Briefly, minimal media contains: 25 mM NH_4Cl, 35mM glucose, 1.5 mM KCl, 0.4 mM MgCl, 0.045 mM NaCl, 0.025 mM FeCl, 0.025 µg/mL thiamine, 66.6 mM sodium phosphate, $5x10^{-7}$ M $CaCl_2$, $5x10^{-8}$ M $CoCl_2$, 10^{-7} M $MnCl_2$, $5x10^{-7}$ M HBO_3, 10^{-8} M $ZnCl_2$, 10^{-8} M $CuCO_3$, $5x10^{-9}$ M $(NH_4)_6Mo_7O_{24}$, pH 7.4. The media was supplemented with 100µM MTA as a sulfur source. *E. coli* O157:H7 strains (ATCC 43894) were grown in Davis minimal media supplemented with 0.4% glucose, and either 25 µg/mL chloramphenicol (for MTN knock-out) or 50 µg/mL ampicillin + 25 µg/mL chloramphenicol (MTN knock-in).

Inhibitors - The transition state analogs **MTD** – (3R, 4S)-1-[(9-deazaadenin-9-yl)methyl]-3-hydroxy-4-(methylthiomethyl)pyrrolidine; **BCX** – (1S)-1-(9-deazaadenin-9-yl)-1,4-dideoxy-1,4-imino-5-methylthio-D-ribitol; **BCZ** - (1S)-1-(9-deazaadenin-9-yl)-1,4-dideoxy-1,4-imino-5-propyl-D-ribitol were kindly provided by Dr. Vern Schramm

(Albert Einstein Medical College, Bronx, NY). The non-nucleoside small molecule inhibitors **5A** - (N-(2-furylmethyl)-N'-(4-nitrophenyl)urea); **8A** - 1-(4-nitrophenyl)-3-[4-[4[(4-nitrophenyl) carbamoylamimino] phenoxy]phenyl]-urea; **15A** - 2-[2-(5,6-dimethyl-1H-benzoimidazol-2-yl)vinyl]-5,6-dimethyl-1H-benzoimidazole; **27A** - 3-(1,3-benzothiazol-2-yl) -1 -(5- {[(1,3-benzothiazol 2-yl) carbamoyl] amino}-2-methylphenyl)urea were obtained from the National Cancer Institute Developmental Therapeutics Program.

Growth assays – *K. pneumoniae* cells were grown overnight in MTA supplemented minimal media. Cells were then diluted 1:5000 into fresh minimal media and 20µL was used to inoculate 160µL of media in the wells of Thermo Scientific® polystyrene 96-well plates. A 20µL volume of dissolved drug (or solvent control) was added to each well to achieve 10µM total drug concentration. Solubility complications required the non-nucleoside drugs to be dissolved in DMSO, therefore the volume of drug used was limited to 1% of the total culture volume to minimize inherent toxic effects, and a corresponding DMSO control was performed. Growth was monitored by hourly OD_{600} readings using a BioTek SynergyHT multiwell plate reader. All trials were performed in triplicate using a minimum of three replicates per drug.

Biofilm assays – Biofilms were grown in 96-well plates that were inoculated in an identical fashion to the cell growth assays. The cells were allowed to grow without shaking at 30ºC over 72 hours. The cells were aspirated, and the wells washed three times with PBS before being fixed in 250µL 1% paraformaldehyde in PBS for 1 hour at 4°C. The wells were then washed twice with water, and stained with 250µL 0.1% crystal violet for 15 minutes at room temperature. Excess dye was removed with four washes

with water and the biofilm-bound crystal violet was solubilized using 250µL of a 20:80 mixture of acetone:ethanol for 10 minutes with gentle shaking. The absorbance of extracted crystal violet was measured at 595nm using a SynergyHT multiwell plate reader.

Intracellular MTN activity – *K. pneumoniae* cells were grown overnight in 10mL sulfate-free minimal media supplemented with 100µM MTA and BCZ (MTN inhibitor) at concentrations of 0, 5, 10, 20 and 50µM. The cells were collected by centrifugation (10,000 x g, 15 min) and the cell pellets washed three times with PBS. Cells were lysed in 3mL B-PER® lysis reagent (ThermoFisher) over 15 minutes at room temperature with frequent vortexing. The cell debris was removed by centrifugation (10,000 x g, 25 min) and the clarified supernatants were collected. The supernatant protein concentration was estimated by absorbance at 280 nm ($A_{0.1\%}$ = 1.0 mg/mL) and equivalent quantities of protein were assayed for MTN specific activity using a UV spectrophotometric assay as described by Singh, et al. [8].

Immunoblotting – Drug-treated cell lysates were electrophoresed on 15% SDS-polyacrylamide gels. Replicate gels were stained using Coomassie Blue dye and imaged, or electroblotted onto PVDF membranes at 120V for two hours. For immunoblot analysis the membrane was blocked overnight with 1% nonfat dry milk in PBS + 0.1% Tween 20 (PBST). The membrane was then washed three times with PBST and incubated for 30 minutes with of mouse α-MTN antibody (1:500 dilution in 1% nonfat dry milk in PBST). The membrane was washed twice with PBST, and the primary antibody detected by incubation for 30 minutes with goat α-mouse HRP (1:1000 dilution in PBST). The membrane was washed three more times with PBST and chemiluminescence was

detected using 1mL SuperSignal™ ELISA Femto Substrate (ThermoFisher) with a FluorChem™ E imager (Protein Simple).

Autoinducer Assays – *K. pneumoniae* cultures were grown in AB media [16] to early stationary phase (OD_{600} = 0.8) and the cells were harvested by centrifugation (10,000 x g, 20 min). The clarified supernatants were collected and filter sterilized using 0.22 micron syringe filters. AI-2 dependent bioluminescence was measured using opaque 96-well plates containing 180µL of a 1:5000 dilution of *V. harveyi* (BB 170) in AB media. Experiments were initiated by the addition of 20µL of *Klebsiella* culture supernatant and the plates were incubated at 30ºC. Luminescence readings were taken hourly using a BioTek SynergyHT multiwell plate reader over 24 hours. Relative bioluminescence was calculated at 12 hours post-inoculation as this time represented a maximal response for the positive control *V. harveyi* (BB120) strain supernatant, and luminescence values are presented as the ratio of luminescence to that of the BB120 strain.

qRT-PCR – Cellular RNA was extracted from either *K. pneumoniae* (ATCC 43816) or *E. coli* (ATCC 43894) cells grown to late log phase in minimal media (OD_{600} = 0.8) using the Qiagen RNEasy Miniprep Kit according to manufacturer's instructions, with the inclusion of the optional DNase incubation step. Purified RNA was quantified using a NanoDrop™ (ThermoFisher). The sample RNA concentrations were equalized to 100 ng/µL with RNase-free water. The primers used in the qRT-PCR assays are listed in Table 4.1 and Table 4.2. A 16S rRNA internal standard was used as a control. Primer amplification was confirmed against genomic DNA by visualization on 2% agarose gels stained with ethidium bromide. The qRT-PCR reactions were performed using a Verso 1-

Step qRT-PCR ROX Kit (ThermoFisher), 0.1µg template RNA, 50 pmol forward and reverse primers, and amplified with a Lightcycler® 96 (Roche). The thermocycler program consisted of a 15 minute preincubation at 95ºC followed by 40 cycles of 95ºC (15 seconds) 55ºC (20 seconds) and 72ºC (50 seconds). The experiment was conducted twice with all reactions performed in triplicate.

Table 4.1. *Klebsiella pneumoniae* virulence gene primers.

Gene	Protein	Sequence	Product size (bp)
K2	Capsule component	F: 5'-CAACCATGGTGGTCGATTAG -3' R: 5'- TGGTAGCCATATCCCTTTGG -3'	531
fimH-1	Type 1 pili	F: 5'- ATGAACGCCTGGTCTTTTGC -3' R: 5'- AGCTGAACGCCTATCCCCTG -3'	689
mrkD	Type 3 pili	F: 5'- ACACCACCAACTATTCCCTC -3' R: 5'- TGGAACCCACATCGACATTC -3'	243
ycfM	Fibronectin adhesin	F: 5'- ATCAGCAGTCGGGTCAGC -3' R: 5'- CTTCTCCAGCATTCAGCG -3'	160
Kfu	Iron channel	F: 5'- GGCCTTTGTCCAGAGCTACG -3' R: 5'- TCTGGCGCAGAGAATGCCAG -3'	632
entB	Siderophore	F: 5'- ATTTCCTCAACTTCTGGGGC -3' R: 5'- TATCGCGCATGAAAGCATCG -3'	384
rmpA	Capsule component	F: 5'- GGTCTAAAGCAGTTAACTGGAC -3' R: 5'- CCTTATGTACCCTTTACAGCC -3'	491
Irp-2	Siderophore	F: 5'- CTCAGGATTCGCTGTTACCGG -3' R: 5'- TTCGGTCATGTTCGGCCAGG -3'	304
ybtS	Siderophore	F: 5'- ACATCTGGCGTTACCAGAGG -3' R: 5'- AGTGGTGCGTTCTGCGTCG -3'	469
fyuA	Iron channel	F: 5'- ACATGATTAACCCCGCGACG -3' R: 5'- AATGCCAGGTCAGGTCACTG -3'	547
pfs	MTN	F: 5'- TCGTCGTCTCCGATGAAGCGC -3' R: 5'- GCGACCGCAAGGAACTCCTC -3'	359
16S rRNA	Internal control	F: 5'- TGGAGCATGTGGTTTAATTGGA -3' R: 5'- TGCGGGACTTAACCCAACA -3'	159

Table 4.2. *Escherichia coli* virulence gene primers.

Gene	Protein	Sequence	Product size (bp)
eaeA	Intimin	F: 5'- CGTCACCAGAGGAATCGGAG -3' R: 5'- TCAGTCGCGATCTCTGAACG -3'	628
Tir	Intimin receptor	F: 5'- TCAATGGCTTGCTGTTTGGC -3' R: 5'- CAAAAGGCGTTGGGGAGTTG -3'	415
Lpf1	Long-polar fimbriae	F: 5'- GGTCAATAGTCGTTTCCGTA -3' R: 5'- GGTCGTTGATTTAGGCAAAG -3'	410
espB	Type-3 secretion	F: 5'- CCGATTGCCCCATACGATTC -3' R: 5'- CTCTGGTCAAGGCTACGGAA -3'	474
fimA	Adhesin	F: 5'- GTCCCTCAGTTCTACAGCGG -3' R: 5'- CCGCATCAATCACCGTACCT -3'	269
ppD	Adhesin	F: 5'- GCGTCATCAAAGCGGAAGAC -3' R: 5'- GCACTCACCGACATGCTACA -3'	323
Stx1	Shiga-like toxin 1	F: 5'- ACACTGGATGATCTCAGTGG -3' R: 5'- CTGAATCCCCCTCCATTATG -3'	614
Stx2	Shiga-like toxin 2	F: 5'- CCATGACAACGGACAGCAGTT -3' R: 5'- CCTGTCAACTGAGCAGCACTTTG -3'	779
hlyA	Hemolysin A	F: 5'- ACGATGTGGTTTATTCTGGA -3' R: 5'- CTTCACGTGACCATACATAT -3'	165
pfs	MTN	F: 5'- TGGGCGATATCGTTGTCTCG -3' R: 5'- AGCCAGGAACTCATCGAAGC -3'	380
16S rRNA	Internal control	F: 5'- TGGAGCATGTGGTTTAATTGGA -3' R: 5'- TGCGGGACTTAACCCAACA -3'	159

Results and Discussion

Growth

The effects of TSAs and small molecule non-nucleoside inhibitors (see Figure 3.6 for structures) on *Klebsiella pneumoniae* growth were measured under multiple media conditions. *Klebsiella pneumoniae* growth in LB media and sulfate-containing minimal media was unaffected by TSA inhibitors at concentrations up to 20μM (data not shown). Similarly, the non-nucleoside inhibitors failed to impact growth in nutrient rich LB media. In order to improve the observed effects of inhibitor treatment, growth assays were performed in minimal media that contained the substrate MTA as the sole sulfur source. Among the transition state analog inhibitors, BCZ produced only moderate delays in reaching log-phase growth, with cultures reaching mid log-phase growth

approximately 4-5 hours after the untreated controls (Figure 4.1). BCX treatment accelerated growth relative to untreated cells, although the increased growth rate does not appear to be statistically significant. Potentially, the enhanced growth could be the result of transmethylthiolase activity that may degrade BCX and bolster the availability of

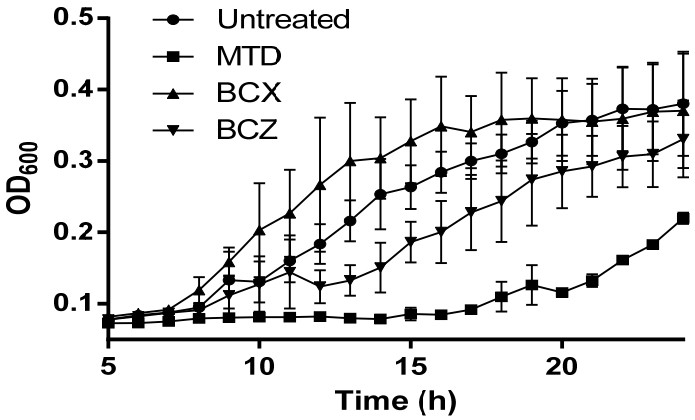

Figure 4.1. TSA inhibitor effects on *K. pneumoniae* growth. *K. pneumoniae* cultures were incubated with 10μM of inhibitor in minimal media containing MTA as the sulfur source. The data shows the average of three independent experiments performed in triplicate (±SEM, n=9).

sulfur. MTD treatment caused the most significant growth defects and delayed mid log-phase growth by approximately 11 hours compared to the control. MTD is a more potent inhibitor of the MTN enzyme than BCX or BCZ (Figure 3.6), which likely accounts for its greater effect towards cellular growth.

Among the non-nucleoside small molecule inhibitors, 8A and 15A treatments showed modest increases in cellular growth rates, while 5A treatment produced no observable effects (Figure 4.2). The inhibitor 27A successfully reduced the growth rate at mid-log and late-log phase growth, and resulted in an approximately 6 hour delay for the cultures to reach stationary phase.

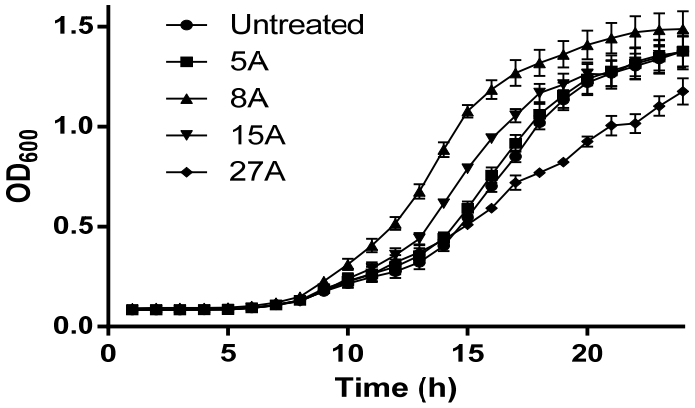

Figure 4.2. Non-nucleoside inhibitor effects on *K. pneumoniae* growth. *K. pneumoniae* cultures were incubated with 10μM of inhibitor in minimal media containing MTA as the sulfur source. The data shows the average of three independent experiments performed in triplicate (±SEM, n=9).

Biofilm Formation

Treatment with TSA inhibitors failed to cause a statistically significant impact on biofilm formation (Figure 4.3). Despite having lesser effects on planktonic growth, BCX and BCZ appear to cause a decreased biofilm accumulation while MTD did not.

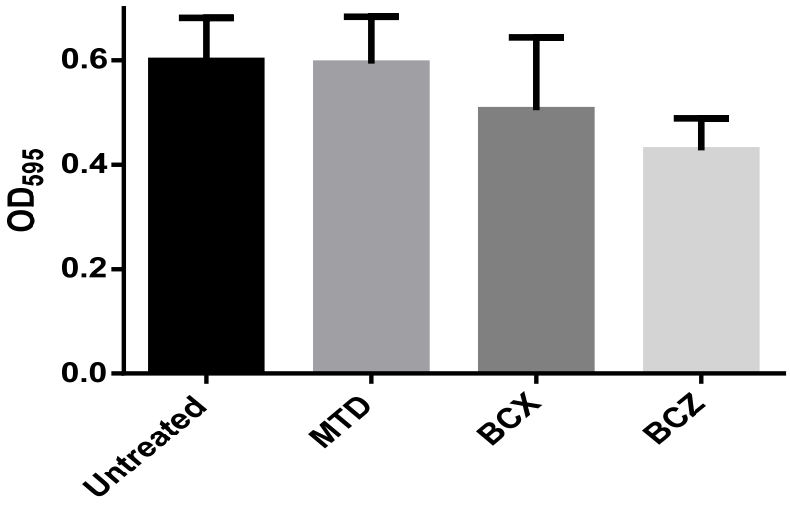

Figure 4.3. TSA inhibitor effects on biofilm formation. *K. pneumoniae* cultures were incubated for 72 hours with 10μM inhibitor, and biofilm accumulation was measured using crystal violet staining. The results are the average of three independent experiments with drug treatments performed in triplicate (±SEM, n=9).

Similarly, the non-nucleoside small molecule inhibitors failed to significantly reduce the formation of biofilms in *K. pneumoniae* cell cultures (Figure 4.4).

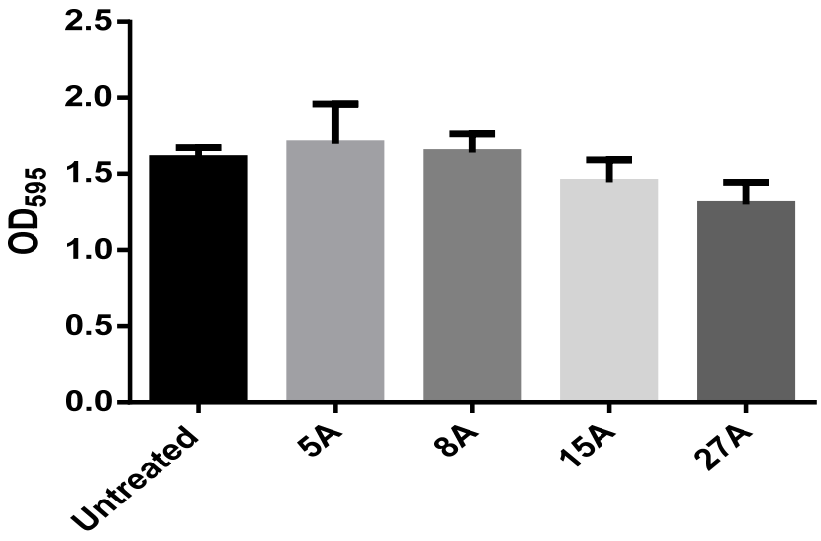

Figure 4.4. Non-nucleoside inhibitor effects on biofilm formation. *K. pneumoniae* cultures were incubated for 72 hours with 10μM inhibitor, and biofilm accumulation was measured using crystal violet staining. The results are the average of three independent experiments with drug treatments performed in triplicate (±SEM, n=9).

The weak effect of MTN inhibitors on biofilm accumulation was not entirely unexpected. Although biofilms deposition has been found to be under partial control by autoinducer-mediated quorum sensing in certain bacteria [17][18], a *luxS* mutant of *K. pneumoniae* incapable of autoinducer-2 production showed defects only in the structure of microcolonies during the initial stages of biofilm development (less than 40 hours) [19].

Intracellular MTN

Lysates of MTN inhibitor-treated *K. pneumoniae* did not exhibit differences in MTN specific activities relative to the untreated control (Table 4.3). Several factors could

Table 4.3. MTN activity in cell lysates following inhibition with BCZ

	Untreated	5 μM	10 μM	20 μM	50 μM
Specific Activity (nmol/min/mg)	5.464	5.594	5.465	5.306	5.516

account for this observation. First, the inhibitors may not be efficiently transported into the bacterial cells. However, the inhibition of planktonic cell growth by MTD and BCZ (Figure 4.1) does not support poor drug uptake as the cause for a lack of effect on specific activity. Alternatively, the inhibitors may be degraded or the production of enzyme upregulated to achieve a homeostatic intracellular specific activity. Western blot analysis of cell lysates using an MTN-specific antibody suggest an apparent increase in intracellular MTN in response to drug treatment, although the response does not appear to be clearly dose dependent (Figure 4.5). This would suggest a regulatory mechanism to compensate for the deficiency of nucleosidase activity in cells following drug inhibition. Potentially, the inability to process MTA as a sulfur source would lead to a decrease in SAM concentrations that would alleviate MetJ repression and stimulate MTN expression. However, previous research would suggest this is not the case, as no change in MTN specific activity under varied concentrations of exogenous methionine [20]. Indeed, an examination of the promoter sequence of the MTN gene reveals no strong matches for the consensus sequences associated with either methionine or purine regulatory elements (data not shown). However, MTN is also indirectly involved in the synthesis of many

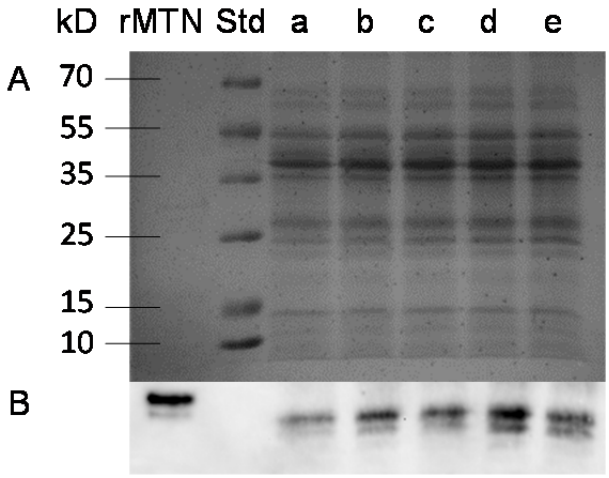

Figure 4.5. Effect of inhibitor treatment on MTN expression. A) Coomassie stained SDS-PAGE of cell lysates. Lane 1: 0.1 µg recombinant MTN, Lane 2: PageRuler Plus Prestained Protein Ladder, Lane 3-7: lysates (25 µg protein/lane) from cells grown minimal media with 0, 5, 10, 20, and 50 µM BCZ (a, b, c, d, e). **B)** Immunoblot of a replicate gel using an MTN-specific antibody.

additional metabolites and a further investigation into the regulatory mechanisms controlling the expression of MTN may elucidate the apparent genetic upregulation we have observed.

Autoinducer-2 Production

Treatment of *Klebsiella* cultures with the TSA inhibitor BCZ was predicted to result in MTN inhibition that would cause a decrease in Autoinducer-2 (AI-2) production, as has been shown in *E. coli* following treatment with TSAs [11]. AI-2 is typically assessed using a bioluminescent reporter strain of *Vibrio harveyi* that produces light in response to autoinducer detection. Unexpectedly, the BCZ-treated *K. pneumoniae* cell culture supernatants produced an enhanced *V. harveyi* bioluminescence response (Figure 4.6). A significant induction of AI-2 dependent bioluminescence was observed when 5µM or 10µM BCZ-treated culture supernatants were examined in the assay (relative to untreated control supernatants). The reason for this response is unclear. Potentially, this could be a result of the observed upregulation of MTN in treated cells that would

ultimately support a greater production of AI-2. Alternatively, it is possible that inhibitor-induced changes in *K. pneumoniae* metabolism, capsule formation, cellular growth, or secreted virulence factors resulted in alterations in unexamined molecules also being presented to *V. harveyi*. A reduction of harmful components in *K. pneumoniae* supernatants may have resulted in conditions that served to better facilitate the growth of *V. harveyi* and thereby further exaggerate the luminescence response.

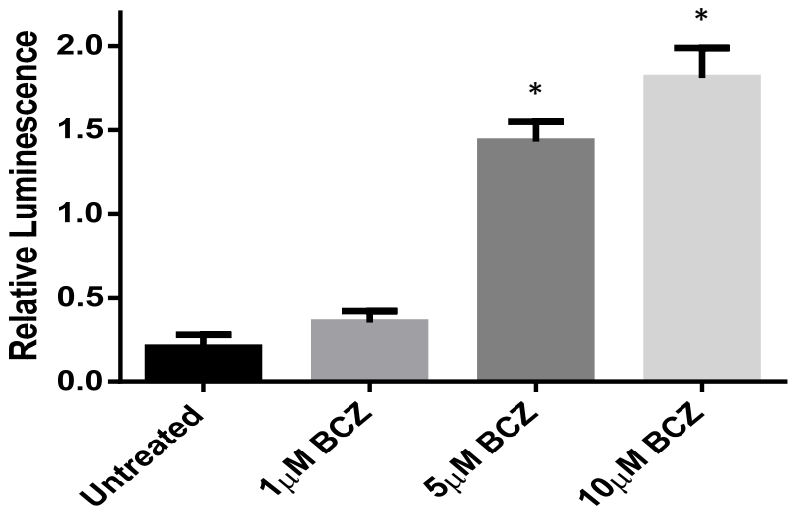

Figure 4.6. Bioluminescence assays. Average relative bioluminescence response, ± SEM, of *V. harveyi* BB170 scaled to values of *V. harveyi* BB120 supernatant positive control. * denotes $p < 0.05$ by student's T-test against untreated group, n=4.

Gene Expression

Since drug treatment produced effects on cellular behavior, we examined the potential effects of MTN inhibitor treatment on the transcriptional expression of genes involved in virulence for *K. pneumoniae*. The genes examined included those involved in mucoviscosity (K2, rmpA), cellular adhesion (fimH, mrkD, ycfM), siderophores (kfu, entB, irp2, ybtS, fyuA) and MTN. Transcription of most *K. pneumoniae* virulence genes were not strongly impacted by treatment with BCZ (Figure 4.7), though two genes related

to iron-scavenging (entB and irp2) showed a significant upregulation in transcript levels (1.2-fold and 3.4-fold increase, respectively). These genes are involved in the synthetic pathways for the siderophores enterobactin (entB) and yersiniabactin (irp2). This most probably represent a means of response to an exacerbated degree of metabolic starvation in minimal media that the previous growth assays indicate BCZ can induce. A reduction in transcriptional expression of the fibronectin-binding element ycfM was also observed,

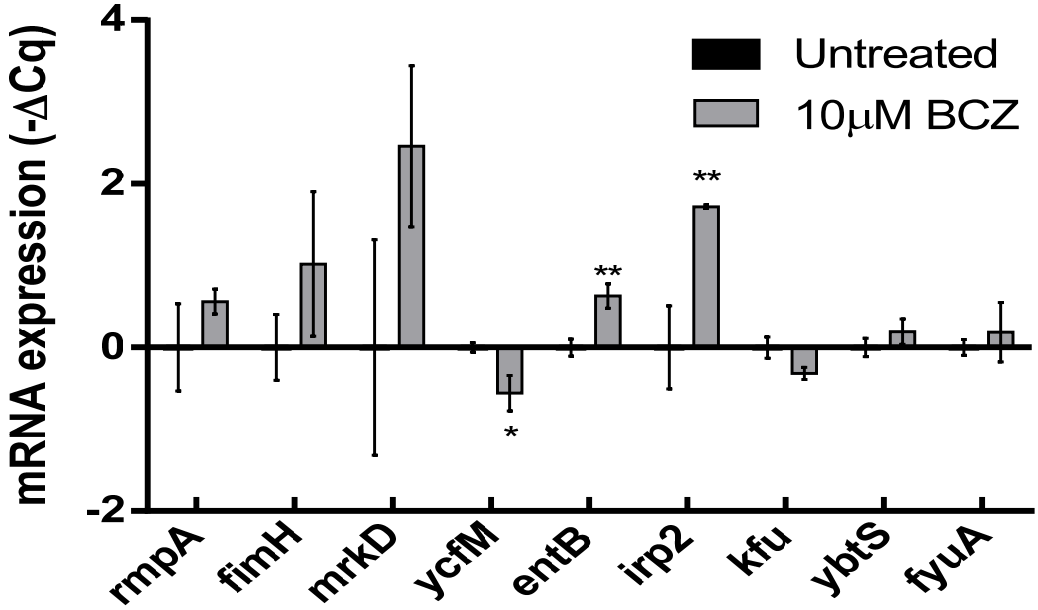

Figure 4.7. BCZ-induced alterations in *K. pneumoniae* gene expression. Average virulence factor expression (± SEM) represented as the change in threshold cycle relative to untreated cells (-ΔCq). * denotes p <0.1, and ** denotes p <0.05 by 1way ANOVA, n=6.

though with less confidence than for entB or irp2. Data for K2 and MTN were omitted, since their transcript levels in treated and untreated cells were not significantly greater than the negative controls. This is possibly a result of the downregulation of MTN expression that occurs following mid-log phase [21], as the transcriptomes were

harvested from cells during early-stationary growth. Since western-blot evidence suggests that MTN protein expression is upregulated in drug-treated cells (Figure 4.5), we expect the transcript levels for MTN would corroborate this observation, but the transcript levels appear to be too low to be detected by this assay. It will be necessary to assess the comparative gene expression from cells harvested at an earlier phase of growth in order to better determine whether a change in MTN transcription has truly occurred.

In order to assess a stronger direct causal relationship between MTN activity and the expression of virulence factors, three *E. coli* O157:H7 strains representing wildtype (WT), MTN knock-out (KO) and MTN knock-in (KI) were also compared for the expression of genes contributing to adhesion (lpf, eaeA, tir, ppD, fimA, espB), and for secreted virulence factors (stx1, stx2, hlyA). Statistically significant variations in gene expression were observed for both Shiga-like toxins (stx1, stx2), hemolysin (hly), and the type-3 secretory system component, espB (Figure 4.7). Shiga-like 1 was 3.6-fold decreased, and Shiga-like 2 was 2.2-fold decreased in the KO strain relative to WT. The other secreted virulence factor, hemolysin, also displayed a 2.8-fold transcript reduction from the WT, though with a lesser degree of confidence. Expression of espB was 2.4-fold decreased in the KO strain. The espB protein is a vital member of the secretory structure that enables cellular adhesion to mammalian cells. It functions by inserting the intimin receptor (tir) into the cell membranes of target cells to allow bacterial effacement through the intimin protein (eaeA) [22]. Through the expression of intimin and its receptor were not affected in the KO strain relative to WT, the reduction in espB transcription would act

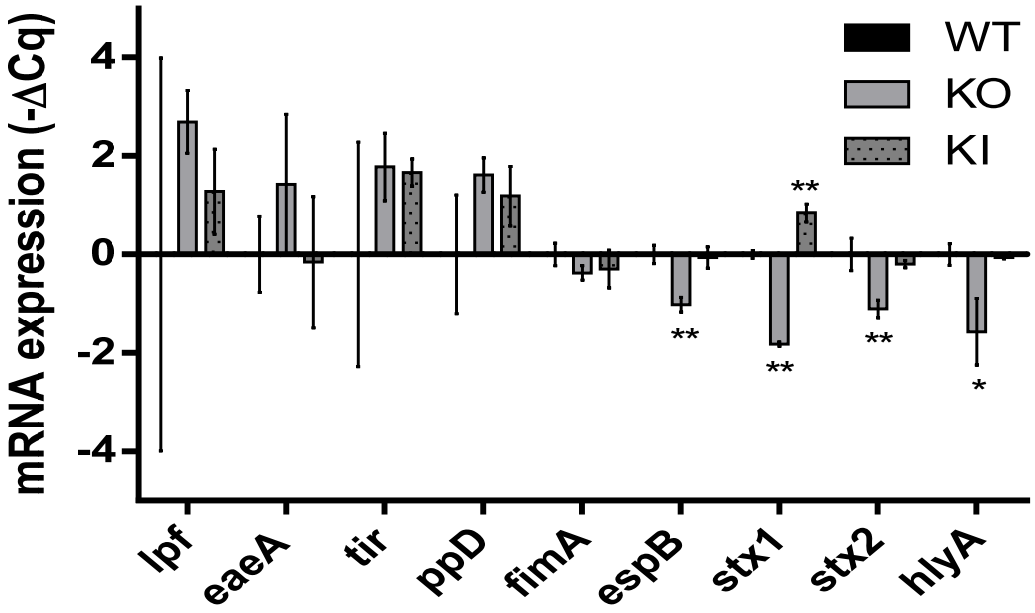

Figure 4.8. Comparative gene expression in *E. coli* O157:H7 WT, MTN KO and MTN KI strains. Average virulence factor expression (± SEM) represented as the change in threshold cycle relative to untreated cells (-ΔCq). * denotes p <0.1, and ** denotes p <0.05 by 1way ANOVA, n=6.

to subvert the activity of the binding mechanism as a whole. The observed decrease in transcriptional expression of these four genes serves to independently support the reported deficiencies in mammalian cell binding, hemolysin activity, and Shiga-toxin dependent Vero-cell cytotoxicity in the *E. coli* MTN KO strain [23]. Interestingly, the overexpression of MTN in the KI strain appears to have caused a significant change in the expression of Shiga-like toxin 1, and was increased 1.7-fold over the WT strain. This would suggest that Shiga-like 1 but not Shiga-like 2 is under positive regulatory control of MTN-dependent metabolism. This confirms the hypothesis that MTN activity plays an important role in supporting virulence phenotypes in *E. coli* and is therefore a valuable target in the search for a class of non-lethal antimicrobial agents that function by attenuating virulence.

Conclusion

This work serves as a partial assessment of the potency of MTN inhibitors against *Klebsiella pneumoniae* growth and virulence. Cultures in modified minimal media were susceptible to drug treatments and showed changes in proliferation without affecting biofilm formation. Treatment with TSA inhibitors caused an apparent accumulation of MTN in cell lysates while maintaining equal enzyme specific activities. In addition, supernatants from cells treated with TSA inhibitors showed an increase in AI-2 dependent luminescence response compared to untreated cells, though the reason for this is not yet understood. Drug treatments resulted in a transcriptional upregulation of two siderophore genes and a downregulation of an adhesion protein in *K. pneumoniae*. As a point of reference, *E. coli* O157:H7 MTN WT, KO and KI strains were also assessed for the expression of virulence genes. Relative to WT, the KO strain showed significant reductions in transcript levels for both Shiga-like toxins, hemolysin, and a secretory protein that contributes to cell adhesion. MTN inhibitors have largely shown poor results when used as antimicrobials, but our research demonstrates their potential application as drugs that act primarily through the debilitation of virulence and not through direct bactericidal activity.

Works Cited

1. Podschun, Rainer; Ullmann, U. *Klebsiella* spp. As nosocomial pathogens: epidemiology, taxonomy, typing methods, and pathogenicity factors. *Clinical Microbiology Reviews*, **1998**. 11(4); 589-603.
2. Nordmann, Patrice; Cuzon, Gaelle; Naas, Thierry. The real threat of *Klebsiella pneumoniae* carbapenemase-producing bacteria. *The Lancet Infectious Diseases*, **2009**. 9(4); 228-236.
3. Yong, Dongeun; Toleman, Mark A.; Giske, Christian G.; Cho, Hyun S.; Sundman, Kristina; Lee, Kyungwon; Walsh, Timothy R. Characterization of a new metallo-beta-lactamase gene, bla(NDM-1), and a novel erythromycin esterase gene carried on

a unique genetic structure in *Klebsiella pneumoniae* sequence type 14 from India. *Antimicrobial agents and chemotherapy*, **2009**. 53(12); 5046-5054.

4. Arnold, Ryan S; et al. Emergence of *Klebsiella pneumoniae* carbapenemase (KPC)-producing bacteria. *Southern Medical Journal*, **2011**. 104(1); 40-45.
5. Borer, Abraham; Saidel-Odes, Lisa; Riesenberg, Klaris; Eskira, Seada; Peled, Nejama; Nativ, Ronit; Schlaeffer, Fracise; Sherf, Michael. Attributable mortality rate for carbapenem-resistant *Klebsiella pneumoniae* bacteremia. *Infection Control & Hospital Epidemiology*, **2009**. 30(10); 972-976.
6. Christa, Laurence; Kersual, Joelle; Auge, Joelle; Perignon, Jean-Louis. Methylthioadenosine toxicity and metabolism to methionine in mammalian cells. *Biochemical Journal*, **1988**. 255(1); 145-152.
7. Parveen, Nikhat; Cornell, Kenneth A. Methylthioadenosine/S-adenosylhomocysteine nucleosidase, a critical enzyme for bacterial metabolism. *Molecular Microbiology*, **2011**. 79(1); 7-20.
8. Singh, Vipender; et al. Femtomolar transition state analogue inhibitors of 5'-methylthioadenosine/S-adenosylhomocysteine nucleosidase from *Escherichia coli*. *Journal of Biological Chemistry*, **2005**. 280(18); 18265-18273.
9. Wang, Shanzhi; et al. New antibiotic candidates against *Helicobacter pylori*. *Journal of the American Chemical Society*, **2015**. 137(45); 14275-15280.
10. Cornell, Kenneth A.; Primus, Shekerah; Martinez, Jorge A.; Parveen, Nikhat. Assessment of methylthioadenosine/S-adenosylhomocysteine nucleosidases of Borrelia burgdorferi as targets for novel antimicrobials using a novel high-throughput method. Journal of Antimicrobial Chemotherapy, 2009. 63; 1163-1172.
11. Gutierrez, Jemy A.; Crowder, Tamara; Rinaldo-Matthis, Agnes; Ho, Meng-Chiao; Almo, Steven C.; Schramm, Vern L. Transition state analogues of 5'-methylthioadenosine nucleosidase disrupt quorum sensing. *Nature Chemical Biology*, **2009**. 5(4); 251-257.
12. Bao, Yan; Li, Yajuan; Jiang, Qiu; Zhao, Liping; Xue, Ting; Hu, Bing; Sun, Baolin. Methylthioadenosine/S-adenosylhomocysteine nucleosidase (pfs) of *Staphylococcus aureus* is essential for the virulence independent of LuxS-AI-2 system. *International Journal of Medical Microbiology*, **2013**. 303; 190-200.
13. Knippel, Reece. Effects of MTN enzyme deficiency on *E. coli* O157:H7 growth and virulence (Masters thesis). (2013).
14. Heurlier, Karin; Vendeville, Agnes; Halliday, Nigel; Green, Andrew; Winzer, Klaus; Tang, Christoph M.; Hardie, Kim R. Growth deficiencies of Neisseria meningitidis pfs and luxS mutants are not due to inactivation of quorum sensing. Journal of Bacteriology, 2009. 191(4) 1293-1392.

15. Gianotti, Alan J.; Tower, Paula A.; Sheley, John H.; Conte, Paul A.; Spiro, Craig; Ferro, Adolph J.; Fitchen, John H.; Riscoe, Michael K. Selective Killing of Klebsiella pneumoniae by 5-Trifluoromethylthioribose: chemotherapeutic exploitation of the enzyme 5-methylthioribose kinase. *Journal of Biological Chemistry*, **1990**. 265, 831-837.

16. Greenberg, E.P.; Hastings, J.W.; Ulitzur, S. Induction of luciferase synthesis inBeneckea harveyi by other marine bacteria. *Archives of Microbiology*, **1979**. 120(2); 87-91.

17. Blehert, D.S.; Palmer, R.J.; Xavier, J.B.; Almeida, J.S.; Kotenbrander, P.E. Autoinducer 2 production by *Streptococcus gordonii* DL1 and the biofilm phenotype of a *luxS* mutant are influenced by nutritional conditions. *Journal of Bacteriology*, **2003**. 185(16); 4851-4860.

18. Miller, Melissa B.; Bassler, Bonnie L. Quorum sensing in bacteria. *Annual Review of Microbiology*, **2001**. 55; 165-199.

19. Balestrino, Damien; Haagensen, Janus A.J.; Rich, Chantal; Forestier, Christiane. Characterization of type 2 quorum sensing in *Klebsiella pneumoniae* and relationship with biofilm formation. *Journal of Bacteriology*, **2005**. 187(8); 2870-2880.

20. Tower, Paula A.; Alexander, David B.; Johnson, Linda L.; Riscoe, Michael K. Regulation of methylthioribose kinase by methionine in *Klebsiella pneumoniae*. *Journal of General Microbiology*, **1993**. 139, 1027-1031.

21. Beeston, Anne L.; Surette, Michael G. Pfs-dependent regulation of autoinducer 2 production in *Salmonella enterica serovar typhimurium*. *Journal of Bacteriology*, **2002**. 184(13); 3450-3456.

22. Ross, Nathan T.; Miller, Benjamin L. Characterization of the binding surface of the translocated intimin receptor, an essential protein for EPEC and EHEC cell adhesion. *Protein Science*, **2007**. 16(12); 2677-1683.

23. Knippel, Reece. Effects of MTN enzyme deficiency on *E. coli* O157:H7 growth and virulence (Masters thesis). (**2013**).

CHAPTER 5: CONCLUSION

The emergence and continual escalation of antibiotic resistances among pathogenic bacteria poses a danger to human health that must be addressed. The two bacterial enzymes MTN and MTRK provide unique opportunities for the development of unexploited classes of chemotherapeutic agents against a diverse array of infectious pathogens, including the important nosocomial agent *Klebsiella pneumoniae*.

The variety of 5-alkylthio substituted substrate analogs that were found to be recognized by MTRK has enabled the identification of drugs that either selectively inhibit the methionine salvage pathway or are processed into toxic intermediates (Gianotti, et al., 1990; Tower, et al., 1991). Substrate binding and product release of the enzyme were found to be consistent with an ordered sequential mechanism, with ATP binding first and MTR-1P released first. An analysis of MTR analogs showed that in general, compounds with bulky and polar 5-alkylthio substitutions were poorer substrates compared to shorter, hydrophobic substitutions. It is also likely that the sulfur atom plays a role in substrate acceptance, as 5'dRIB was not able to be utilized as a substrate.

MTN represents a broad-functioning enzyme that has been heavily explored as a therapeutic target. However, the well characterized transition-state analog inhibitors of MTN have shown highly inconsistent effects on cellular behavior and cytotoxicity. A comparison between TSA inhibitors and an assortment of novel inhibitors derived from *in silico* screening against bacterial MTN established weaker binding affinities of the newly identified inhibitors compared to the transition-state analogs. All of the inhibitors

examined showed lesser binding affinities towards *K. pneumoniae* MTN than against the *E. coli* enzyme. The impact of MTN inhibitors on *Klebsiella* cell growth was only measurable when the organism was cultured in minimal media that required MTN activity to salvage sulfur. Of the four small molecule MTN inhibitors only inhibitor 27A was potent enough to cause a decrease proliferation, which was most apparent during mid-log and late-log phase growth. None of the small molecule inhibitors caused significant effects on biofilm formation. Similarly, TSA inhibitors had variable impacts towards cellular growth, biofilms, autoinducer secretion, and the transcriptional regulation of important virulence factors. BCZ and MTD caused growth defects, but no discernable deficiency in biofilms. Treatment with BCZ also resulted in what appeared to be an increase in autoinducer-2 production and an upregulation in the transcription of two siderophore genes. *K. pneumoniae* appears to evade strong effects from MTN inhibitors by compensatory expression of MTN to combat enzymatic inactivation and by upregulation of iron-scavenging molecules that may ameliorate metabolic starvation.

Although the MTN inhibitors showed strong inhibitory power against the enzyme, more work must be done to improve their ability to exert antimicrobial effects towards pathogens like *K. pneumoniae*. Using the structures of the four novel non-nucleoside small molecule inhibitors characterized here as a jumping-off point, work is already being undertaken to make structural modifications to improve their inhibitory strengths.

We hope that this research presented here will serve to benefit the ongoing efforts to develop both MTRK and MTN inhibitors as a novel antibiotic agents.

BIBLIOGRAPHY

Deaths by cause, sex and mortality stratum in WHO Regions, estimates for 2001. *World Health Organization* (WHO). World Health Report -2002 Statistical Annex. Geneva: WHO; **2004**.

The World Health Report: 2004 statistical annex. *World Health Organization* (WHO), **2004**.

The World Health Report: 2014 selected infectious diseases. *World Health Organization* (WHO), **2014**.

Antimicrobial Resistance. *World Health Organization* (WHO). Updated **2015**. Fact Sheet No 194. Accessed 10-29-2015.

Al-Salihi, Siham; Mahmood, Yusra AR.; Al-Jubouri, Ali S. Pathogenicity of *Klebsiella pneumoniae* isolated from diarrheal cases among children in Kirkuk city. *Tikrit Journal of Pure Science*, **2012**. 17(4); 2012.

Albers, Eva. Metabolic characteristics and importance of the universal methionine salvage pathway recycling methionine from 5'-methylthioadenosine. *IUBMB Life*, **2009**. 61(12); 1132-1142.

Arakawa, Yoshichika; et al. Genomic organization of the *Klebsiella pneumoniae* cps region responsible for serotype K2 capsular polysaccharide synthesis in the virulent strain Chedid. *Journal of Bacteriology*, **1995**. 177(7); 1788-1796.

Araujo, Cecilia De; Balestrino, Damien; Roth, Lucile; Charbonnel, Nicolas; Forestier, Christiane. Quorum sensing affects biofilm formation through lipopolysaccharide synthesis in *Klebsiella pneumoniae*. *Research in Microbiology*, **2010**. 161(7); 595-603.

Arnold, Ryan S; et al. Emergence of *Klebsiella pneumoniae* carbapenemase (KPC)-producing bacteria. *Southern Medical Journal*, **2011**. 104(1); 40-45.

Bachman, Michael; Lenio, Steven; Schmidt, Lindsay; Oyler, Jennifer E.; Weiser, Jeffrey N. Interaction of lipocalin 2, transferrin, and siderophores determines the replicative niche of *Klebsiella pneumoniae* during pneumonia. *American Society for Microbiology*, **2012**. 3(6); 00224-11.

Balestrino, Damien; Haagensen, Janus A.J.; Rich, Chantal; Forestier, Christiane. Characterization of type 2 quorum sensing in *Klebsiella pneumoniae* and relationship with biofilm formation. *Journal of Bacteriology*, **2005**. 187(8); 2870-2880.

Bao, Yan; Li, Yajuan; Jiang, Qiu; Zhao, Liping; Xue, Ting; Hu, Bing; Sun, Baolin. Methylthioadenosine/S-adenosylhomocysteine nucleosidase (pfs) of

Staphylococcus aureus is essential for the virulence independent of LuxS-AI-2 system. *International Journal of Medical Microbiology*, **2013**. 303; 190-200.

Bao, Yan; Zhang, Xu; Jiang, Qiu; Xue, Ting; Sun, Baolin. Pfs promotes autolysis-dependent release of eDNA and biofilm formation in *Staphylococcus aureus*. *Medical Microbiology and Immunology*, **2015**. 204; 215-226.

Bassler, Bonnie L.; Greenberg, E. Peter; Stevens, Ann M. Cross-species induction of luminescence in the quorum-sensing bacterium *Vibrio harveyi. Journal of Bacteriology*, **1997**. 179(12); 4043-4045.

Beeston, Anne L.; Surette, Michael G. Pfs-dependent regulation of autoinducer 2 production in *Salmonella enterica serovar typhimurium*. *Journal of Bacteriology*, **2002**. 184(13); 3450-3456.

Blehert, D.S.; Palmer, R.J.; Xavier, J.B.; Almeida, J.S.; Kotenbrander, P.E. Autoinducer 2 production by *Streptococcus gordonii* DL1 and the biofilm phenotype of a *luxS* mutant are influenced by nutritional conditions. *Journal of Bacteriology*, **2003**. 185(16); 4851-4860.

Bodelon, Gustavo; Palomino, Carmen; Fernandez, Luis A. Immunoglobulin domains in *Escherichia coli* and other enterobacteria: from pathogenesis to applications in antibody technologies. *FEMS Microbiology Reviews*, **2013**. 37(2); 204-250.

Borer, Abraham; et al. Attributable mortality rate for carbapenem-resistant *Klebsiella pneumoniae* bacteremia. *Infection control and hospital epidemiology*, **2009**. 30(10); 972-976.

Caudill, Marie A.; et al. Intracellular S-adenosylhomocysteine concentrations predict global DNA hypomethylation in tissues of methyl-deficient cystathionine beta-synthase heterozygous mice. *Journal of Nutrition*, **2001**. 131(11); 2811-2818.

Challand, Martin R.; et al. Product inhibition in the radical S-adenosylmethionine family. *FEBS Letters*, **2009**. 583(8); 1358-1362.

Cheng, H.Y.; et al. RmpA regulation of capsular polysaccharide biosynthesis in *Klebsiella pneumoniae* CG43. *Journal of Bacteriology*, **2010**. 192(12); 3144-3158.

Cheng, Xiaodong; Roberts, Richard J. AdoMet-dependent methylation, DNA methyltransferases and base flipping. *Nucleic Acids Research*, **2001**. 29(18); 3784-3795.

Chhibber, Sanjay; Aggarwal, S.; Yadav, V. Contribution of capsular and lipopolysaccharide antigens to the pathogenesis of *Klebsiella pneumoniae* respiratory tract infection. *Folia Microbiologia*, **2003**. 48(5); 699-702.

Chiang, Peter K.; et al. S-adenosylmethionine and methylation. *FASEB Journal*, **1996**. 10(4); 471-480.

Choi-Rhee, E. J.; Cronan, J. E. A nucleosidase required for in-vivo function of the S-adenosyl-L-methionine radical enzyme, biotin synthase. *Chemistry & Biology*, **2005**. 12(4): 461-468.

Christa, Laurence; Kersual, Joelle; Auge, Joelle; Perignon, Jean-Louis. Methylthioadenosine toxicity and metabolism to methionine in mammalian cells. *Biochemical Journal*, **1988**. 255(1); 145-152.

Clatworthy, Anne E.; Pierson, Emily; Hung, Deborah T. Targeting virulence: a new paradigm for antimicrobial therapy. *Nature Chemical Biology*, **2007**. 3; 541-548.

Cornell, Kenneth A.; Winter, R.W.; Tower, P.A.; Riscoe, Michael K. Affinity purification of 5'-methylthioribose kinase and 5'-methylthioadenosine/S-adenosylhomocysteine nucleosidase from *Klebsiella pneumoniae*. *Biochemical Journal*, **1996**. 317(1); 285-290.

Cornell, Kenneth A.; Swarts, William E.; Barry, Ronald D.; Riscoe, Michael K. Characterization of recombinant *Escherichia coli* 5'-methylthioadenosine/S-adenosylhomocysteine nucleosidase: analysis of enzymatic activity and substrate specificity. *Biochemical and Biophysical Research Communications*, **1996**. 228(3); 724-732.

Costerton, J.W.; et al. Microbial Biofilms. *Annual Review of Microbiology*, **1995**. 49; 711-745.

Costerton, J.W.; Stewart, Philip S; Greenberg, E.P. Bacterial biofilms: a common cause of persistent infections. *Science*, **1999**. 284(2418); 1318-1322.

Domenico, Philip; Salo, Richard J.; Cross, Alan S.; Cunha, Burke A. Polysaccharide capsule-mediated resistance to opsonophagocytosis in . *Infection and Immunity*, **1994**. 62(10); 4495-4499.

Evans, Gary B.; Furneaux, Richard H; Schramm, Vern L.; Singh, Vipender; Tyler, Peter C. Targeting the polyamine pathway with transition-state analogue inhibitors of 5'-methylthioadenosine phosphorylase. *Medicinal Chemistry*, **2004**. 47(12); 3275-3281.

Fabianowska-Majewska, Krystyna; Duley, John; Fairbanks, Lynette; Simmonds, Anne; Wasiak, Tadeusz. Substrate specificity of methylthioadenosine phosphorylase from human liver. *Acta Biochimica Polonica*, **1994**. 41(4); 391-395.

Fader, Robert C.; Avots-Avotins, Andrejs E.; Davis, Charles P. Evidence of pili-mediated adherence of *Klebsiella pneumoniae* to rat bladder epithelial cells in-vitro. *Infection and Immunity*, **1979**. 25(2); 729-37.

Fader, Robert C.; Gondesen, Kelli; Tolley, Brooks, Ritchie David G.; Moller, Peter. Evidence that in vitro adherence of *Klebsiella pneumoniae* to ciliated hamster tracheal cells is mediated by type 1 fimbriae. *Infection and Immunity*, **1988**. 56(11); 3011-3013.

Fang, Chi-Tai; Chuang, Yi-Ping; Shun, Chia-Tung; Chang, Shan-Chwen; Wang, Jin-Town. A novel virulence gene in *Klebsiella pneumoniae* strains causing primary liver abscess and septic metastatic complications. *Journal of Experimental Medicine*, **2004**. 199(5); 697-705.

Fertas-Aissani, R.; Messai, Y.; Alouache, S.; Bakour, R. Virulence profiles and antibiotic susceptibility patterns of *Klebsiella pneumoniae* strains isolated from different clinical specimens. *Pathologie-biologie* (Paris), **2013**. 61(5); 209-216.

Flemming, Hans-Curt; Wingender, Jost. The biofilm matrix. *Nature Reviews Microbiology*, **2010**. 8(9); 623-633.

Fong, Karen P.; Chung, Whasun O.; Lamont, Richard J.; Demuth, Donald R. Intra- and interspecies regulation of gene expression by *Actinobacillus actinomycetemcomitans* LuxS. *Infection and Immunity*, **2001**. 69(12); 7625-7634.

Fontecave, Marc; Atta, Mohamed; Mulliez, Etienne. S-adenosylmethionine: nothing goes to waste. *TRENDS in Biochemical Sciences*, **2004**. 29:5, 243-249.

Frey, Perry A.; Hegeman, Adrian D.; Ruzicka, Frank J. The radical SAM superfamily. *Critical Reviews in Biochemistry and Molecular Biology*, **2008**. 43(1); 63-88.

Gianotti, Alan J.; Tower, Paula A.; Sheley, John H.; Conte, Paul A.; Spiro, Craig; Ferro, Adolph J.; Fitchen, John H.; Riscoe, Michael K. Selective Killing of *Klebsiella pneumoniae* by 5-Trifluoromethylthioribose: chemotherapeutic exploitation of the enzyme 5-methylthioribose kinase. *Journal of Biological Chemistry*, **1990**. 265, 831-837.

Gigliobianco, Tiziana; Lakaye, Bernard; Wins, Pierre; Moualij, Benaissa; Zorzi, Willy; Bettendorff, Lucien. Adenosine thiamine triphosphate accumulates in *Escherichia coli* cells in response to specific conditions of metabolic stress. BMC Microbiology, 2010. 10: 148.

Greenberg, E.P.; Hastings, J.W.; Ulitzur, S. Induction of luciferase synthesis inBeneckea harveyi by other marine bacteria. *Archives of Microbiology*, **1979**. 120(2); 87-91.

Gupta, Neil; Limbago, Brandi M.; Patel, Jean B.; Kallen, Alexander J. Carbapenem-resistant Enterobacteriaceae: epidemiology and prevention. *Clinical Infectious Diseases*, **2011**. 53(1); 60-67.

Gutierrez, Jemy A.; Crowder, Tamara; Rinaldo-Matthis, Agnes; Ho, Meng-Chiao; Almo, Steven C.; Schramm, Vern L. Transition state analogues of 5'-methylthioadenosine nucleosidase disrupt quorum sensing. *Nature Chemical Biology*, **2009**. 5(4); 251-257.

Hanna, Andrea; Berg, Michael; Stout, Valerie, Tazatos, Anneta. Role of capsular colonic acid in adhesion of uropathogenic *Escherichia coli*. *Applied and Environmental Microbiology*, **2003**. 69(8); 4474-4481.

Harmsen, Morten; Yang, Liang; Pamp, Sunje J.; Tolker-Nielsen, Tim. An update on *Pseudomonas aeruginosa* biofilm formation, tolerance, and dispersal. *FEMS Immunology & Medical Microbiology*, **2010**. 59(3) 253-268.

Harrigan, George G.; Maguire, Greg; Boros, Laszlo. Metabolomics in alcohol research and drug development. *Alcohol Research & Health*, **2008**. 31(1); 27-35.

Hennequin, Claire; Forestier, Christiane. Influence of capsule and extended-spectrum beta-lactamases encoding plasmids upon *Klebsiella pneumoniae* adhesion. *Research in Microbiology*, **2007**. 158(4); 339-347.

Heurlier, Karin; Vendeville, Agnes; Halliday, Nigel; Green, Andrew; Winzer, Klaus; Tang, Christoph M.; Hardie, Kim R. Growth deficiencies of *Neisseria meningitides pfs* and *luxS* mutants are not due to inactivation of quorum sensing. *Journal of Bacteriology*, **2009**. 191(4); 1293-1302.

Hirsch, Elizabeth B.; Tam, Vincent H. Detection and treatment options for *Klebsiella pneumoniae* carbapenemases (KPCs): an emerging cause of multidrug-resistant infection. *Journal of Antimicrobial Chemotherapy*, **2010**. 65(6); 1119-1125.

Hornick, Douglas; Allen, Bradley L.; Horn, Mark A.; Clegg, Steven. Adherence to respiratory epithelia by recombinant *Escherichia coli* expressing *Klebsiella pneumoniae* fimbrial gene product. *Infection and Immunity*, **1992**. 60(4); 1577-1588.

Hsieh, Pei-Fang; Lin, Tzu-Lung; Lee, Cha-Ze; Tsai, Shih-Feng; Wang, Jin-Town. Serum-induced iron-acquisition systems and TonB contribute to virulence in *Klebsiella pneumoniae* causing primary pyogenic liver abscess. *Journal of Infectious Diseases*, **2008**. 197(12); 1717-1727.

Jagnow, Jennifer; Clegg, Steven. *Klebsiella pneumoniae* MrkD-mediated biofilm formation on extracellular matrix and collagen coated surfaces. *Microbiology*, **2003**. 149(9); 2397-2405.

Jesaitis, Algirdas J.; Franklin, Michael J.; Berglund, Deborah; Sasaki, Maiko; Lord, Connie I.; Bleazard, Justin B.; Duffy, James E.; Beyenal, Haluk; Lewandowski, Zbigniew. Compromised host defense on *Pseudomonas aeruginosa* biofilms: characterization of neutrophil and biofilm interactions. *Journal of Immunology*, **2003**. 171(8); 4329-4339.

Kaplan, Heidi B.; Greenberg, E. P. Diffusion of autoinducer is involved in regulation of the *Vibrio fisheri* luminescence system. *Journal of Bacteriology*, **1985**. 163(3); 1210-1214.

Kievit, Teresa R.; Iglewski, Barbara H. Bacterial quorum sensing in pathogenic relationships. *Infection and Immunity*, **2000**. 68(9); 4839-4849.

Knippel, Reece. Effects of MTN enzyme deficiency on *E. coli* O157:H7 growth and virulence (Masters thesis). (2013).

Kostakioti, Maria; Hadjifrangiskou, Maria; Hultgren, Scott J. Bacterial biofilms: development, dispersal, and therapeutic strategies in the dawn of the postantibiotic era. *Cold Spring Harbor Perspectives in Medicine*, **2013**. 3(4).

Kusano, T.; Berberich, T.; Tateda, C.; Takahashi, Y. Polyamines: essential factors for growth and survival. *Planta*, **2008**. 228(3); 367-381.

Kushad, Mosbah M.; Richardson, Daryl G; Ferro, A.J. 5'-methylthioadenosine nucleosidase and 5'-methylthioribose kinase activities and ethylene production during tomato fruit development and ripening. *Plant Physiology*, **1985**. 79(2); 525-529.

Larson, Eric T.; Mudeppa, Devaraja G.; et al. The crystal structure and activity of a putative trypanosomal nucleoside phosphorylase reveal it to be a homodimeric uridine phosphorylase. *Journal of Molecular Biology*, **2010**. 396(5); 1244-1259.

Lawlor, Matthew S.; O'Connor, Christopher; Miller, Virginia L. Yersiniabactin is a virulence factor for *Klebsiella pneumoniae* during pulmonary infection. *Infection and Immunity*, **2007**. 75(3); 1463-1472.

Lee, Jeffrey E.; Cornell, Kenneth A.; Riscoe, Michael K.; Howell, P. Lynne. Structure of *E. coli* 5'-methylthioadenosine/S-adenosylhomocysteine nucleosidase reveals similar purine nucleoside phosphorylases. *Structure*, **2001**. 9(10); 941-953.

Lee, Jeffrey E.; Cornell, Kenneth A.; Riscoe, Michael K.; Howell, P. Lynne. Structure of *Escherichia coli* 5'-methylthioadenosine/S-adenosylhomocysteine nucleosidase inhibitor complexes provide insight into the conformational changes required for substrate binding and catalysis. *Journal of Biological Chemistry*, **2003**. 278; 8761-8770.

Lee, Jeffrey E.; et al. Structural comparison of MTA phosphorylase and MTA/AdoHcy nucleosidase explains substrate preferences and identifies regions exploitable for inhibitor design. *Biochemistry*, **2004**. 43; 5159-5169.

Lee, Jeongmi; et al. An alternative polyamine biosynthetic pathway is widespread in bacteria and essential for biofilm formation in *Vibrio cholerae*. *Journal of Biological Chemistry*, **2009**. 284(15); 9899-9907.

Lewis, Kim. Persister cells and the riddle of biofilm survival. *Nature Reviews. Microbiology*, **2007**. 5(1); 48-56.

Longshaw, Alistair I.; et al. Design and synthesis of potent "sulfur-free" transition state analogue inhibitors of 5'-methylthioadenosine nucleosidase and 5'-methylthioadenosine phosphorylase. *Journal of Medicinal Chemistry*, **2010**. 53(18); 6730-6746.

Machalek, Alisa Z. Making a microscopic metropolis. *National Institute of General Medical Sciences*, Dec. 22, **2008**. Accessed 10/20/2015. http://publications.nigms.nih.gov/computinglife/metropolis.htm

Magill, Shelley S; et al. Multistate point-prevalence survey of health care-associated infections. *New England Journal of Medicine*, **2014**. 370(3); 1198-1208.

Mah, Thien-Fah; O'Toole, George A. Mechanisms of biofilm resistance to antimicrobial agents. *Trends in Microbiology*, **2001**. 9(1); 34-39.

Martino, Patrick D.; et al. Molecular characterization and adhesive properties of CF29K, an adhesion of *Klebsiella pneumoniae* strains involved in nosocomial infections. *Infection and Immunity*, **1995**. 63(11); 4336-4344.

Mato, Jose M.; Alemany, Susana. What is the function of phospholipid N-methylation? *Biochemical Journal*, **1983**. 213; 1-10.

Messenger, Ann; Barclay, Raymond. Bacteria, iron and pathogenicity. *Biochemical Education*, **1983**. 11(2); 54-63.

Miethke, Marcus; Marahiel, Mohamed. Siderophore-based iron acquisition and pathogen control. *Microbiology and Molecular Biology Reviews*, **2007**. 71(3); 413-451.

Miller, Melissa B.; Bassler, Bonnie L. Quorum sensing in bacteria. *Annual Review of Microbiology*, **2001**. 55; 165-199.

Monroe, Don. Looking for chinks in the armor of bacterial biofilms. *PLoS Biology*, **2007**. 5(11); e307.

Murphy, Caitlin; Clegg, Steven. *Klebsiella pneumoniae* and type 3 fimbriae: nosocomial infection, regulation and biofilm formation. *Future Microbiology*, **2012**. 7(8); 991-1002.

Myers, Robert W.; Abeles, Robert H. Conversion of 5-S-ethyl-5-thio-D-ribose to ethionine in *Klebsiella pneumoniae*. Basis for the selective toxicity of 5-S-ethyl-5-thio-D-ribose. *Journal of Biological Chemistry*, **1989**. 264(18); 10547-10551.

Neilands, J. B. Siderophores: structure and function of microbial iron transport compounds. *Journal of Biological Chemistry*, **1995**. 270(45); 26723-26726.

Nordmann, Patrice; Cuzon, Gaelle; Naas, Thierry. The real threat of *Klebsiella pneumoniae* carbapenemase-producing bacteria. *The Lancet Infectious Diseases*, **2009**. 9(4); 228-236.

Pajula, R.L.; Raina, A. Methylthioadenosine, a potent inhibitor of spermine synthase from bovine brain. *FEBS Letters*, **1979**. 99(2); 343-345.

Parveen, Nikhat; Cornell, Kenneth A. Methylthioadenosine/S-adenosylhomocysteine nucleosidase, a critical enzyme for bacterial metabolism. *Molecular Microbiology*, **2011**. 79(1); 7-20.

Parveen, Nikhat; et al. Bgp, a secreted GAG-binding protein of *B. burgdorferi* strain N40, displays nucleosidase activity and is not essential for infection of immunodeficient mice. *Infection and Immunity*, **2006**. 74(5); 3016-3020.

Passador, Luciano O.; Cook, James M.; Gambello, Michael J.; Rust, Lynn; Iglewski, Barbara H. Expression of *Pseudomonas aeruginosa* virulence genes requires cell-to-cell communication. *Science*, **1993**. 260(5111); 1127-1130.

Payne, Shelley; Finkelstein, Richard. The critical role of iron in host-bacterial interactions. *Journal of Clinical Investigation*, **1978**. 61(6); 1428-1440.

Podschun, Rainer; Fischer, Arno; Ullmann, Uwe. Siderophores production of *Klebsiella* species isolated from different sources. Zentralblatt fur Bakteriologie: *International Journal of Medical Microbiology*, **1992**. 276(4); 481-486.

Podschun, Rainer; Ullmann, U. *Klebsiella* spp. As nosocomial pathogens: epidemiology, taxonomy, typing methods, and pathogenicity factors. *Clinical Microbiology Reviews*, **1998**. 11(4); 589-603.

Pratt, Leslie; Kolter, Roberto. Genetic analysis of *Escherichia coli* biofilm formation: roles of flagella motility, chemotaxis, and type 1 pili. *Molecular Microbiology*, **1998**. 30(2); 285-293.

Proft, T.; Baker, E.N. Pili in gram-negative and gram-positive bacteria – structure, assembly and their role in disease. Cellular and Molecular Life Sciences, **2009**. 66(4); 613-635.

Qureshi, Zubair A.; et al. Clinical characteristics of bacteraemia caused by extended-spectrum β –lactamase-producing Enterobacteriaceae in the era of CTX-M-type and KPC-type β–lactamases. *Clinical Microbiology and Infection*, **2012**. 18(9); 887-893.

Ragione, Della; et al. *Escherichia coli* S-adenosylhomocysteine/5'-methylthioadenosine nucleosidase. Purification, substrate specificity and mechanism of action. *Biochemical Journal*, **1985**. 232(2); 335-341.

Rasheed, Kamile; et al. New Delhi metallo-β-lactamase-producing Enterobacteriaceae, United States. *Emerging Infectious Diseases*, **2013**. 19(6).

Riscoe, Michael K.; Ferro, Adolph J.; Fitchen, John H. Analogs of 5-methylthioribose, a novel class of antiprotozoal agents. *Antimicrobial Agents and Chemotherapy*, **1988**. 1904-1906.

Russo, Thomas; Olson, Ruth; MacDonald, Ulrike; Beanan, Janet; Davidson, Bruce A. Aerobactin, but not yersiniabactin, salmochelin, or enterobactin, enables the growth/survival of hypervirulent (hypermucoviscous) *Klebsiella pneumoniae* ex vivo and in vivo. *Infection and Immunity*, **2015**. 83(8); 3325-3333.

Rutherford, Steven T.; Bassler, Bonnie L. Bacterial quorum sensing: its role in virulence and possibilities for its control. *Cold Spring Harbor Perspectives in Medicine*, **2012**. 2(11); a012427.

Schembri, Mark A.; Kjaergaard, Kristian; Klemm, Per. Global gene expression in *Escherichia coli* biofilms. *Molecular Microbiology*, **2003**. 48(1); 253-267.

Schembri, Mark A.; Blom, Jens; Krogfelt, Karen A.; Klemm, Per. Capsule and fimbria interaction in *Klebsiella pneumoniae*. *Infection and Immunity*, **2005**. 73(8); 4626-4633.

Schramm, Vern L.; et al. Transition state analogues in quorum sensing and SAM recycling. *Nucleic Symposium Series*, **2008**. (52); 75-76.

Schroll, Casper; Barken, Kim B.; Krogfelt, Karen A.; Struve, Carsten. Role of type 1 and type 3 fimbriae in *Klebsiella pneumoniae* biofilm formation. *BMC Microbiology*, **2010**. 10; 179.

Seiler, Nikolaus; Raul, Francis. Polyamines and apoptosis. *Journal of Cellular and Molecular Medicine*, **2005**. 9(3); 623-642.

Shah, Pratik; Swiatlo, Edwin. Polyamines and bacterial pathogenesis. *Molecular Microbiology*, **2008**. 68(1); 4-16.

Shon, Alyssa S.; Bajwa, Rajinder P.S.; Russo, Thomas A. Hypervirulent (hypermucoviscous) *Klebsiella pneumoniae*. *Virulence*, **2013**. 4(2); 107-118.

Singh, Vipender; et al. Femtomolar transition state analogue inhibitors of 5'-methylthioadenosine/S-adenosylhomocysteine nucleosidase from *Escherichia coli*. *Journal of Biological Chemistry*, **2005**. 280(18); 18265-18273.

Spellberg, Brad; et al. Trends in antimicrobial drug development: implications for the future. *Clinical Infectious Diseases*, **2004**. 38(9); 1279-1286.

Steiner, Kerstin; et al. Molecular basis of S-layer glycoprotein glycan biosynthesis in *Geobacillus staerothermophilus*. *Journal of Biological Chemistry*, **2008**. 283(30); 21120-21133.

Storey, Douglas G.; Ujack, Eva E.; Rabin, Harvey R.; Mitchell, Ian. *Pseudomonas aeruginosa* lasR transcription correlates with the transcription of iasA, iasB, and toxA in chronic lung infections associated with cystic fibrosis. *Infection and Immunity*, **1998**. 66(6); 2521-2528.

Struck, Anna-Winona; Thompson, Mark L.; Wong, Lu S.; Micklefield, Jason. S-adenosyl-methionine-dependent methyltransferases: highly versatile enzymes in biocatalysis, biosynthesis and other biotechnological applications. *Chembiochem*, **2012**. 13(18); 2642-2655.

Tabor, Celia W.; Tabor, Herbert. Polyamines in microorganisms. *Microbiological Reviews*, **1985**. 49(1); 81-99.

Tower, Paula A.; Johnson, Linda L.; Ferro, Adolph J.; Fitchen, John H.; Riscoe, Michael J. Synergistic activity of 5-trifluoromethylthioribose and inhibition of methionine synthesis against *Klebsiella pneumoniae*. *Antimicrobial Agents and Chemotherapy*, **1991**. 35(8); 1557-1561.

Tower, Paula A.; Alexander, David B.; Johnson, Linda L.; Riscoe, Michael K. Regulation of methylthioribose kinase by methionine in *Klebsiella pneumoniae*. *Journal of General Microbiology*, **1993**. 139, 1027-1031.

Trautner, Barbara W.; Darouiche, Rabih O. Role of biofilm in catheter-associated urinary tract infection. *American Journal of Infection Control*, **2004**. 32(3); 177-183.

Turner, Mary A.; et al. Structure and function of S-adenosylhomocysteine hydrolase. *Cell Biochemistry and Biophysics*, **2000**. 33(2); 101-125.

Urbonavicius, Jaunius; Skouloubris, Stephane; Myllykallio, Hannu; Grosjean, Henri. Identification of a novel gene encoding a Flavin-dependent tRNA:m5U methyltransferase in bacteria-evolutionary implications. *Nucleic Acids Research*, **2005**. 33(13); 3955-3964.

Vartivarian, Shahe E.; Anaissie, Elias J.; Cowart, Richard E.; Sprigg, Helen A.; Tingler, Mary J.; Jacobson, Eric S. Regulation of *Cryptococcal* capsular polysaccharide by iron. *The Journal of Infectious Disease*, **1993**. 167(1); 186-190.

Vasil, Michael L.; Ochsner, Urs A. The response of *Pseudomonas aeruginosa* to iron: genetics, biochemistry and virulence. *Molecular Microbiology*, **1999**. 34(3); 399-413.

Vester, Birte; Long, Katherine S. Antibiotic resistance in bacteria caused by modified nucleosides in 23S ribosomal RNA. DNA and RNA modification enzymes: structure, mechanism, function and evolution. *Landes Bioscience*, **2009**. 682.

Wang, Ching C.; Aldritt, Susan. Purine salvage networks in *Giardia lamblia*. *Journal of Experimental Medicine*, **1983**. 158(5); 1703-1712.

Wang, Shanzhi; et al. New antibiotic candidates against *Helicobacter pylori*. *Journal of the American Chemical Society*, **2015**. 137(45); 14275-15280.

Winter, R.W.; Cornell, Kenneth A.; Johnson, Linda L.; Riscoe, Michael J. Synthesis and testing of substituted phenylthioribose analogs against *Klebsiella pneumoniae*. *Bioorganic & Medicinal Chemistry Letters*, **1993**. 3(10); 2079-2082.

Wolfenden, Richard; Snider, Mark J. The depth of chemical time and the power of enzymes as catalysts. *Accounts of Chemical Research*, **2001**. 34(12); 938-945.

Wu, Keh-Ming; et al. Genome sequencing and comparative analysis of *Klebsiella pneumoniae* NTUH-K2044, a strain causing liver abscess and meningitis. *Journal of Bacteriology*, **2009**. 191(14); 4492-4501.

Yong, Dongeun; Toleman, Mark A.; Giske, Christian G.; Cho, Hyun S.; Sundman, Kristina; Lee, Kyungwon; Walsh, Timothy R. Characterization of a new metallo-beta-lactamase gene, bla(NDM-1), and a novel erythromycin esterase gene carried on a unique genetic structure in *Klebsiella pneumoniae* sequence type 14 from India. *Antimicrobial agents and chemotherapy*, **2009**. 53(12); 5046-5054.

APPENDIX

MTN Inhibitor Fits to the Equation for Competitive Inhibition

The section contains the complete set of data pertaining to the MTN inhibitors examined in Chapter 3. The four transition state analog inhibitors (MTD, BTD, BCX, BCZ) have two discrete inhibition values. The unmarked K_i values for the TSAs represent activity derived from initial enzyme velocities. Ki values labelled with "*" represent activities following delayed-onset increases in the binding affinity of the enzyme-substrate complex. The four examined non-nucleoside small molecule inhibitors (5A, 8A, 15A, 27A) displayed no delayed-onset inhibitory activity and possess a single K_i value. Velocities were related as a proportion of the untreated activity using a modified form of the Michaelis-Menten equation for competitive inhibition, where:

$$v_o'/v_o = (K_m + [S])/[(K_m + [S]) + (K_m[I]/K_i)]$$

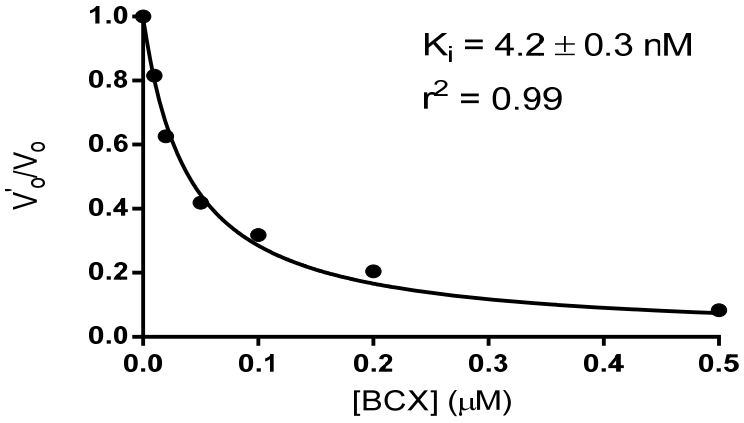

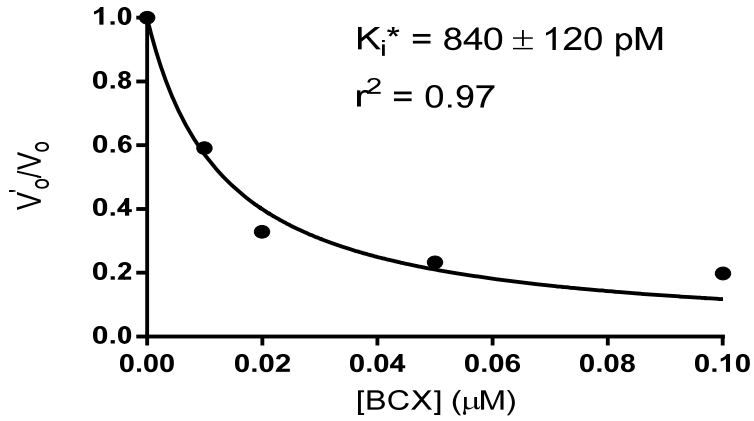
K_i^* = 840 ± 120 pM
r^2 = 0.97
V_o'/V_o
1.0
0.8
0.6
0.4
0.2
0.0
0.00
0.02
0.04
0.06
0.08
0.10
[BCX] (μM)

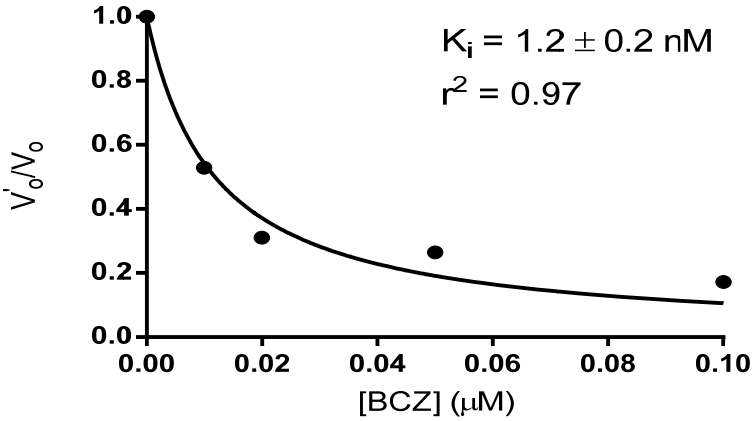
K_i = 1.2 ± 0.2 nM
r^2 = 0.97
V_o'/V_o
1.0
0.8
0.6
0.4
0.2
0.0
0.00
0.02
0.04
0.06
0.08
0.10
[BCZ] (μM)

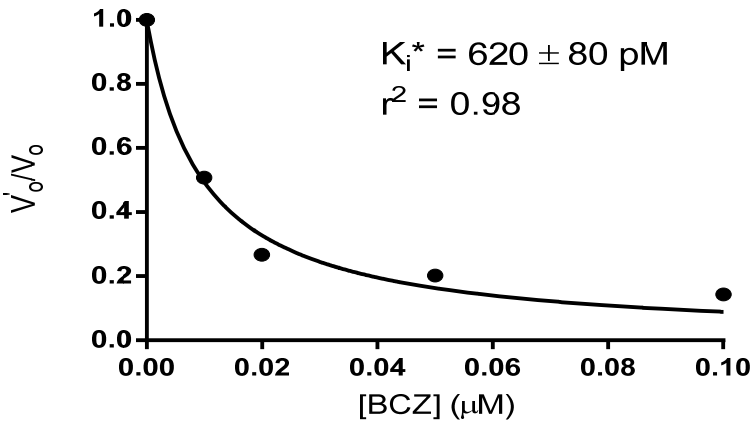
K_i^* = 620 ± 80 pM
r^2 = 0.98
V_o'/V_o
1.0
0.8
0.6
0.4
0.2
0.0
0.00
0.02
0.04
0.06
0.08
0.10
[BCZ] (μM)

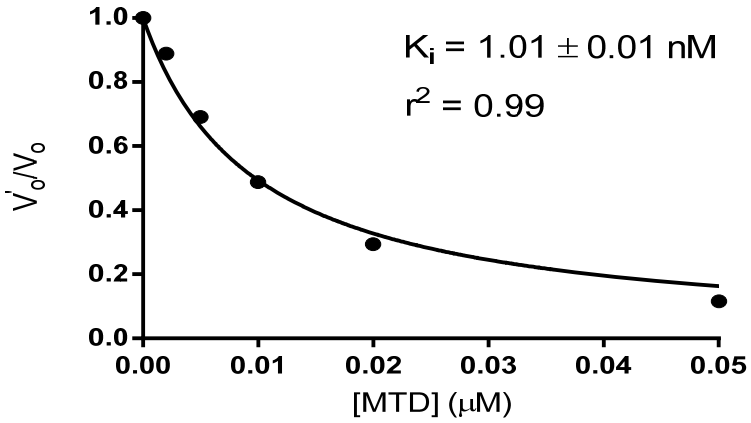
$K_i = 1.01 \pm 0.01$ nM
$r^2 = 0.99$
V_o'/V_o
1.0
0.8
0.6
0.4
0.2
0.0
0.00
0.01
0.02
0.03
0.04
0.05
[MTD] (μM)

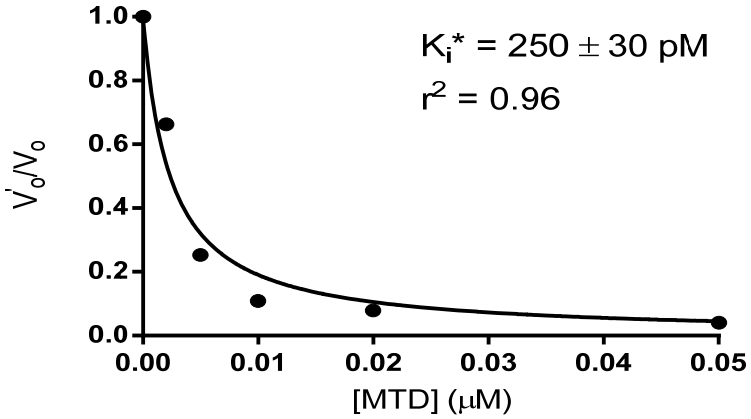
$K_i^* = 250 \pm 30$ pM
$r^2 = 0.96$
V_o'/V_o
1.0
0.8
0.6
0.4
0.2
0.0
0.00
0.01
0.02
0.03
0.04
0.05
[MTD] (μM)

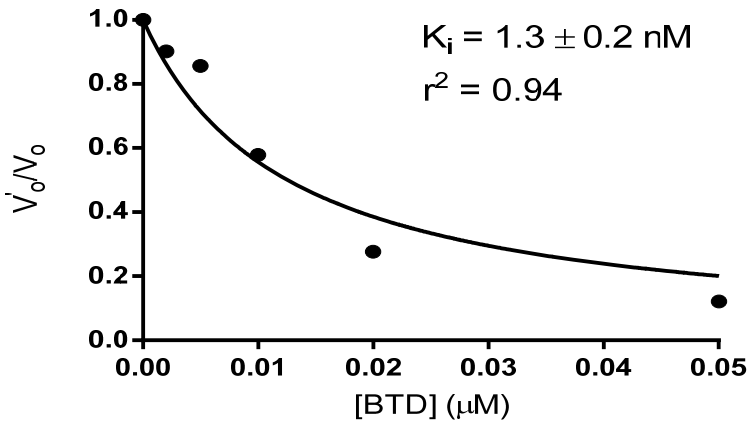
$K_i = 1.3 \pm 0.2$ nM
$r^2 = 0.94$
V_o'/V_o
1.0
0.8
0.6
0.4
0.2
0.0
0.00
0.01
0.02
0.03
0.04
0.05
[BTD] (μM)

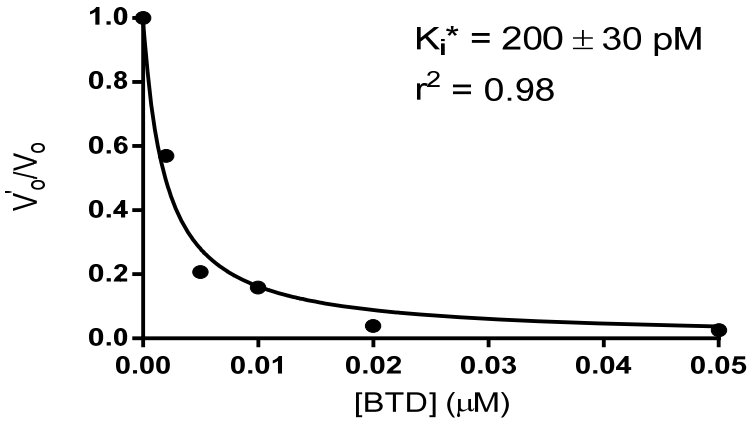
K_i^* = 200 ± 30 pM
r^2 = 0.98
V_o'/V_o
1.0
0.8
0.6
0.4
0.2
0.0
0.00
0.01
0.02
0.03
0.04
0.05
[BTD] (μM)

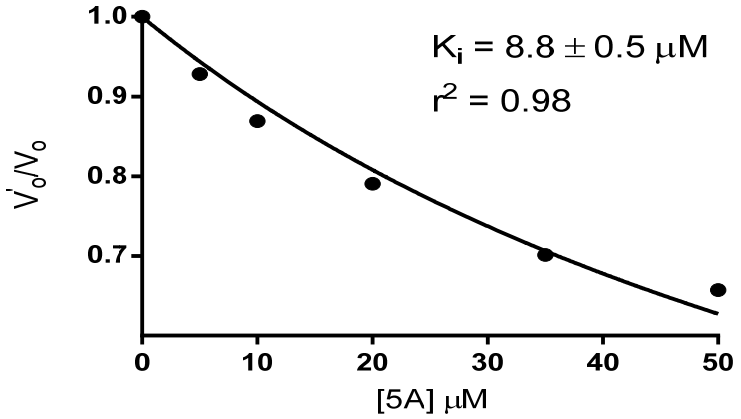
K_i = 8.8 ± 0.5 μM
r^2 = 0.98
V_o'/V_o
1.0
0.9
0.8
0.7
0
10
20
30
40
50
[5A] μM

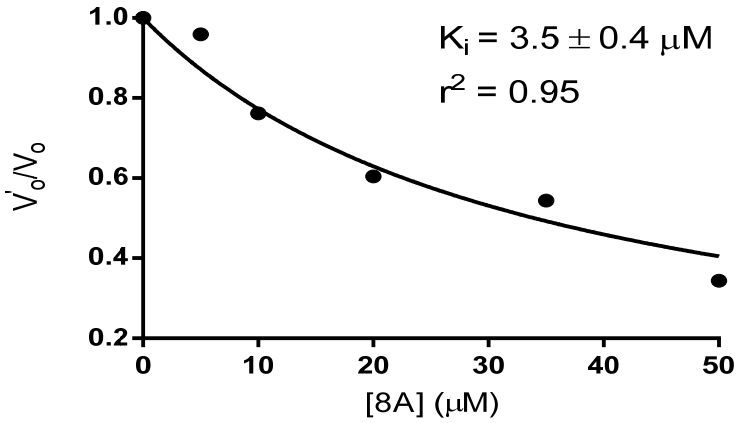
K_i = 3.5 ± 0.4 μM
r^2 = 0.95
V_o'/V_o
1.0
0.8
0.6
0.4
0.2
0
10
20
30
40
50
[8A] (μM)

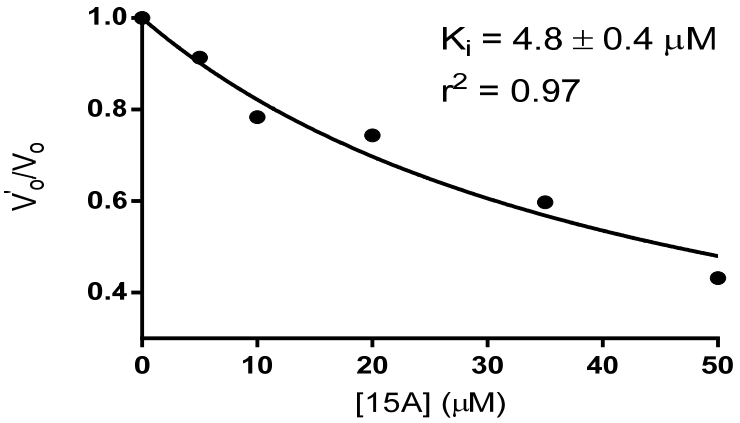
$K_i = 4.8 \pm 0.4\ \mu M$
$r^2 = 0.97$
V_o'/V_o
1.0
0.8
0.6
0.4
0
10
20
30
40
50
[15A] (μM)

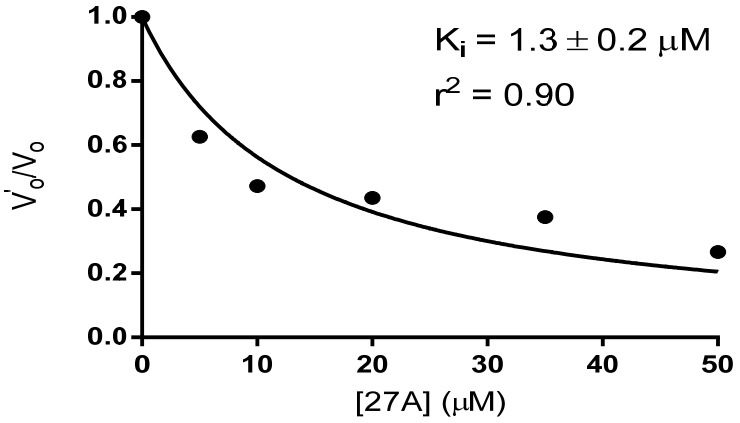
$K_i = 1.3 \pm 0.2\ \mu M$
$r^2 = 0.90$
V_o'/V_o
1.0
0.8
0.6
0.4
0.2
0.0
0
10
20
30
40
50
[27A] (μM)